C h a p t e r O n e

COMPARISON OF ARCHAEAL AND BACTERIAL DIVERSITY IN METHANE SEEP CARBONATE NODULES AND HOST SEDIMENTS, EEL RIVER BASIN AND HYDRATE RIDGE, USA

David H. Case[1,†]

in collaboration with,

Olivia U. Mason[1,2,†], Thomas H. Naehr[3], Raymond W. Lee[4], Randal B. Thomas[5], Jake V. Bailey[6], and Victoria J. Orphan[1]

[1]Division of Geological and Planetary Sciences, California Institute of Technology, Pasadena, CA 91125, USA

[2]Department of Earth, Ocean, and Atmospheric Science, Florida State University, Tallahassee, FL 32306, USA

[3]Department of Physical and Environmental Sciences, Texas A&M University-Corpus Christi, Corpus Christi, TX 78412, USA

[4]School of Biological Sciences, Washington State University, Pullman, WA 99164, USA

[5]US Geological Survey, Menlo Park, CA, 94025, USA

[6]Department of Earth Sciences, University of Minnesota, Minneapolis, MN 55455, USA

[†]In the publication of this article, first authorship is shared by D.H.C. and O.U.M. D.H.C. was the coordinating and principle author of the manuscript, performed iTAG preparation and analyses, and calculated and interpreted beta diversity analyses.

*****Published in Mason & Case et al., 2015. Comparison of Archaeal and Bacterial Diversity in Methane Seep Carbonate Nodules and Host Sediments, Eel River Basin and Hydrate Ridge, USA. Microbial Ecology 70 (3), 766-784.

1.0 ABSTRACT

Anaerobic oxidation of methane (AOM) impacts carbon cycling by acting as a methane sink and by sequestering inorganic carbon via AOM-induced carbonate precipitation. These precipitates commonly take the form of carbonate nodules that form within methane seep sediments. The timing and sequence of nodule formation within methane seep sediments are not well understood. Further, the microbial diversity associated with sediment-hosted nodules has not been well characterized and the degree to which nodules reflect the microbial assemblage in surrounding sediments is unknown. Here, we conducted a comparative study of microbial assemblages in methane-derived authigenic carbonate nodules and their host sediments using molecular, mineralogical, and geochemical methods. Analysis of 16S rRNA gene diversity from paired carbonate nodules and sediments revealed that both sample types contained methanotrophic archaea (ANME-1 and ANME-2) and syntrophic sulfate-reducing bacteria (Desulfobacteraceae and Desulfobulbaceae), as well as other microbial community members. The combination of geochemical and molecular data from Eel River Basin and Hydrate Ridge suggested that some nodules formed *in situ* and captured the local sediment-hosted microbial community, while other nodules may have been translocated or may represent a record of conditions prior to the contemporary environment. Taken together, this comparative analysis offers clues to the formation regimes and mechanisms of sediment-hosted carbonate nodules.

1.1 INTRODUCTION

Sulfate-coupled anaerobic oxidation of methane (AOM) is a significant biogeochemical process in continental margin settings and in areas of advective seafloor methane seepage, consuming a large fraction of methane in marine sediments prior to its release to the hydrosphere (Hoehler et al. 1994; Boetius et al. 2000; Reeburgh 2007). Within the seep environment, AOM is mediated by a symbiotic partnership between uncultured anaerobic methanotrophic archaea (ANME) and sulfate-reducing deltaproteobacteria (SRB). Sulfate-driven AOM increases the saturation state of sedimentary pore waters with respect to calcium carbonate by producing two units of alkalinity (Alk) per one unit of dissolved inorganic carbon (DIC), and has therefore been hypothesized to promote the precipitation of authigenic carbonate according to the general reactions (Luff and Wallmann 2003; Lein 2004; Luff et al. 2004):

$$CH_4 + SO_4^{2-} \leftrightarrow HCO_3^- + HS^- + H_2O;\ \Delta Alk = +2;\ \Delta DIC = +1 \quad \text{(Eq. 1)}$$

$$2HCO_3^- + Ca^{2+} \leftrightarrow CaCO_{3(s)} + CO_{2(aq)} + H_2O;\ \Delta Alk = -2;\ \Delta DIC = -1 \quad \text{(Eq. 2)}$$

Indeed, authigenic carbonates are often found in association with seep environments and AOM, and vary in morphology, size, and mineralogy. Observations have included cements (Hovland et al. 1987; Jørgensen 1989; 1992), nodules (sometimes termed "concretions"; Chen et al. 2006; Ussler and Paull 2008; Watanabe et al. 2008), massive chemoherm structures extending into the water column (Griffiths et al. 1982; Michaelis et al. 2002; Gulin et al. 2003; Teichert et al. 2005), and pavements that can cover hundreds of square meters (Paull et al. 1992; Boetius and Suess 2004). Most often, authigenic carbonates and nodules are observed within the sediment column or at the sediment/water interface (Greinert et al. 2001; Gieskes et al. 2005; Naehr et al. 2007; Haas et al. 2010).

Pore water geochemical profiles of Ca^{2+} and Alk, $\delta^{13}C_{DIC}$, $\delta^{13}C_{carb}$, ^{14}C labeling experiments, and lipid and DNA biomarkers provide strong evidence to substantiate the

hypothesized link between microbially-mediated AOM activity and the precipitation of authigenic carbonates (Michaelis et al. 2002; Peckmann and Thiel 2004; Boetius and Suess 2004; Naehr et al. 2009). It was recently shown that authigenic carbonates and nodules not only entrap microbial assemblages but furthermore host metabolically active methanotrophic populations, contributing substantially to methane oxidation in seep regions (Marlow et al. 2014a). Diagnostic lipids of methanotrophic archaea and their bacterial syntrophs, often showing characteristic depletion of ^{13}C, have been recovered in carbonate slabs from extant seep habitats and paleo-methane seeps dating as far back as the Pennsylvanian (Peckmann et al. 1999; Thiel et al. 2001; Peckmann and Thiel 2004; Stadnitskaia et al. 2005; Birgel et al. 2008b; a; Stadnitskaia et al. 2008; Naehr et al. 2009). A limited number of studies have also successfully recovered AOM-associated ANME and SRB 16S rRNA gene sequences associated with exhumed carbonate slabs and chemoherms within areas of methane seepage (Aloisi et al. 2002; Heijs et al. 2006; Stadnitskaia et al. 2008; Guan et al. 2013; Marlow et al. 2014b). These lipid and DNA biomarkers indicate a persistent relationship between relatives of AOM-associated archaea and deltaproteobacteria, and carbonate precipitation.

The discovery in 2002 of massive ANME-1 dominated deep-sea carbonate "reefs" extending tens of meters above active methane vents in the euxinic waters of the Black Sea further indicates that anaerobic methanotrophs do not merely colonize preformed carbonates but are capable of inducing and shaping their formation (Michaelis et al. 2002). Accordingly, the distribution of archaeal molecular signatures recorded in modern carbonates has been used to infer past environmental conditions and/or point to zones of previous AOM activity, as well as the ecological physiology of AOM-associated archaea. For example, archaeal ANME-2 16S rRNA gene sequences recovered from the upper part of a Gulf of Cadiz carbonate slab were interpreted to reflect carbonate precipitation in sediments containing elevated methane partial pressures, while the occurrence of ANME-1 sequences in the underlying crust were assumed to be

associated with a phase of precipitation under conditions of reduced methane flux (Stadnitskaia et al. 2008).

The majority of studies to date have focused on massive authigenic carbonates, which in many cases represent tens to hundreds of thousands of years of seep activity (Teichert et al. 2003; Luff and Wallmann 2003; Kutterolf et al. 2008; Ussler and Paull 2008; Watanabe et al. 2008; Liebetrau et al. 2010; Bayon et al. 2013). However, seep sediments themselves often harbor numerous millimeter-scale carbonate nodules representing diverse shapes, mineralogies, and formation histories (Chen et al. 2006; Ussler and Paull 2008; Watanabe et al. 2008). Due to their small size, nodules may capture a shorter time interval of *in situ* carbonate precipitation, and may be more relevant than massive carbonate pavements to understanding the immediate link between sediment- and carbonate-hosted microbial assemblages. Previous comparisons of sediment-, nodule-, and carbonate-associated microbial assemblages have suggested that archaeal community structures are dependent on methane seepage flux and not physical substrate type, while bacteria appeared to be more differentiated by substrate type than seep activity (Marlow et al. 2014b). Furthermore, endolithic microbial assemblages were found to be metabolically active, suggesting the possibility that 16S rRNA signatures recovered from nodules and carbonates might be different from the surrounding sediment-based assemblages (Marlow et al. 2014a). This implied that assemblages associated with nodules and carbonates might not be passive recorders of surrounding sediment communites but rather represent an extant, active, endolithic microbial community (Marlow et al. 2014a; b).

Comparative characterization of paired nodules and host sediments would provide insight into the degree to which early stages of carbonate formation passively record the sediment assemblage during lithification, or alternatively capture (or exclude) specific microorganisms directly mediating AOM and alkalinity production. Here, we examined microbial communities within sediments and their associated carbonate nodules (hereafter "nodules") from methane seeps located on the southern summit of Hydrate Ridge, OR, USA (HR; 44° 34.20351'N, 125°

8.8409'W; 800 meters below sea level (Boetius and Suess 2004)) and the northern ridge of Eel River Basin offshore of Eureka, CA, USA (ERB; 40° 48.7024'N, 124° 36.6754'W, 517 meters below sea level; Orphan et al. 2004). The microbial communities in 18 sediment and nodule samples (i.e., nine sediment/nodule pairs) from methane-seep environments of HR (n_{pairs} = 5) and ERB (n_{pairs} = 4) were characterized using iTAG sequencing of partial-length 16S rRNA genes to characterize relationships across geography ($HR_{n=10}$ *vs* $ERB_{n=8}$) and substratum ($sediment_{n=9}$ *vs* $nodule_{n=9}$). Depth (measured in centimeters below seafloor; cmbsf) was examined as an additional variable. Terminal restriction fragment length polymorphism (TRFLP) analysis using archaeal- and bacterial-specific 16S rRNA primers was also employed to complement diversity patterns observed using iTAG sequencing, in which universal primers were used. Additionally, four paired sediment and nodule samples from HR and ERB were selected for full-length archaeal and bacterial 16S rRNA gene cloning and sequencing. Pore water and solid phase geochemical, mineralogical, and isotopic analyses were conducted to provide physicochemical context for the interpretation of observed microbiological trends.

The goals of this comparative study were twofold: first, to determine whether the nodules reflect passive capture of the local sedimentary microbial community or host a unique microbial assemblage, and second, to examine the relationship between observed seep-associated microbial assemblages and physicochemical variables.

1.2 METHODS

1.2.1 SITE DESCRIPTION AND SAMPLE COLLECTION

Sediments and carbonates were recovered in September 2006 from active methane seep areas at HR and at ERB. All push cores (PC) were collected with *DSV Alvin* during dives AD4249 (HR: PC8) and AD4256 (ERB: PC29, PC23, PC20). Sampling locations were chosen based on the presence of benthic chemosynthetic communities (sulfide-oxidizing bacterial mats and

Calyptogena clam beds) – visual seabed indicators of localized seepage with high advective flux of sulfide, itself coupled via AOM to high subsurface methane fluxes (Sahling et al. 2002; Torres et al. 2002; Treude et al. 2003; Levin 2005).

Eel River Basin lies at the southern end of the Cascadia accretionary prism where organic-rich source rocks have led to the production and sequestration of abundant methane and other hydrocarbons (Orphan et al. 2004 and references therein). Variations in advective methane flux and pore water geochemistry occur frequently within methane seep habitats associated with sulfide-oxidizing microbial mats and chemosynthetic clam beds, and are sometimes organized in "bulls eye" structures at the seafloor (Barry et al. 1997; Treude et al. 2003; Orphan et al. 2004). Three push cores at ERB were collected along a lateral seep transect, from the center to the perimeter of a "bulls eye" consisting of a white sulfide-oxidizing microbial mat radially surrounded by *Calyptogena* clams. Two cores were collected from active seep zones (PC29, under a white microbial mat, hereafter "mat core"; PC23, under *Calyptogena* clams, hereafter "clam core"), and one core was collected on the edge of the "bulls eye" to capture low seep activity (PC20; hereafter "peripheral core"). Extensive sulfide-oxidizing microbial mats tend to exclusively overlie sulfidic seep sediments with a high methane flux (Boetius and Suess 2004). Chemosynthetic clams, which also rely on reduced fluids, cause substantial bioturbation, transporting seawater sulfate and oxygen to the underlying sediment layers and deepening the sulfate-methane transition zone (Orphan et al. 2004; Gieskes et al. 2005; Fischer et al. 2012). The periphery of these chemosynthetic clam and mat communities is typically defined by lower methane flux and correspondingly deeper sulfate penetration, slower rates of AOM, and lower concentrations of sulfide (Sahling et al. 2002; Treude et al. 2003; Orphan et al. 2004; Lloyd et al. 2010).

Nodules were recovered in only a few of the sectioned depth horizons along this ERB seep transect (Table 1), including two mid-depth sections in the mat core (6–9 cmbsf and 9–12 cmbsf; Pernthaler et al. 2008), one section in the clam core (0–3 cmbsf), and a deep section of the

peripheral core (9–12 cmbsf). Geochemistry and cell counts from this seep transect have previously been reported (Green-Saxena et al. 2014).

Hydrate Ridge lies approximately 250 miles north of Eel River Basin and is well known for extensive reduced fluid seepage, gas expulsion, and the presence of methane hydrates near the seafloor (Bohrmann et al. 1998; Suess et al. 2001; Boetius and Suess 2004). The site is associated with an accretionary complex located on the Cascadia Margin approximately 50 miles offshore Newport, OR, USA, and carbonate pavements are pervasive over much of the ridge (Bohrmann et al. 1998; Gieskes et al. 2005). At this site, the focus was on a single push core, PC8, which had carbonate nodules throughout its 0–15 cmbsf penetration depth (sectioned in 3-cm increments). PC8 was collected from the southern summit of Hydrate Ridge within a thick white microbial mat and processed shipboard according to previously published protocols (Orphan et al. 2001a). Samples were immediately frozen at -80ºC for subsequent DNA extraction.

1.2.2 X-RAY DIFFRACTION AND PETROGRAPHY

Bulk mineralogy and the relative abundance of carbonate minerals in each nodule sample were determined by X-ray diffraction (XRD) at the XRD Laboratory in the Department of Chemistry at Texas A&M University using a BRUKER D8 X-ray powder diffractometer. Samples for XRD analyses were prepared following standard procedures using an internal corundum standard (cf. Naehr et al. 2000). Scans were run from 2° to 60° 2θ at a scanning speed of 0.01°2θ/s. The relative proportions of different carbonate minerals were estimated on the basis of the (104) peak heights of calcite, Mg-calcite and dolomite, and the (111) peak height of aragonite (Table 1). Thin sections of carbonate nodules were examined using a Nikon Optiphot-pol polarizing microscope equipped with a Nikon DXM1200F digital imaging system.

1.2.3 METHANE AND SULFATE MEASUREMENTS

Methane was captured by immediately collecting 3–5 g sediment plugs into 1 M NaOH at a 1:1 g:mL ratio in gas-tight 20 mL serum vials. Methane concentrations in the headspace of the vials were determined with a Shimadzu mini-2 gas chromatograph equipped with a flame ion detector and magnesium perchlorate trap, with a 2 mL injection loop. A 9.93 ppm methane standard was used for calibration as described previously (Goffredi et al. 2008).

To collect pore waters for sulfate measurements, sediment samples were centrifuged (1380*g* for 15 min) in cut-off, stoppered 10 mL syringes without a headspace (Barry et al. 1996). Separated pore fluids were collected with a gas-tight syringe by puncturing the sidewall of the 10 mL syringe with a needle. Samples were preserved immediately in 0.5 M barium chloride (1:1::mL:mL). Sulfate in the pore fluids was determined by turbidimetry using a spectrophotometer (Gieskes et al. 1991). The turbidity was measured at 420 nm.

1.2.4 CARBON ISOTOPE AND CONCENTRATION ANALYSES

Carbon stable isotope measurements were performed on four sample types: total organic carbon ($\delta^{13}C_{org}$), nodule inorganic carbon ($\delta^{13}C_{nod}$), sedimentary inorganic carbon ($\delta^{13}C_{sed}$), and, in the case of samples from ERB, pore water dissolved inorganic carbon ($\delta^{13}C_{pw}$).

Isotopic composition of total organic carbon was measured on HR and ERB sediment samples, but not nodules, due to limited nodule material (Table 1). For the $\delta^{13}C_{org}$ analysis, sedimentary solid-phase inorganic carbon was removed by repeated application of 2 N phosphoric acid. Ten mg of dry material was placed into tin capsules and combusted in a Costech elemental analyzer (Valencia, CA). The resulting gases were separated by gas chromatography and admitted to the inlet of a GV Instruments (Manchester, UK) Isoprime isotope ratio mass spectrometer (IRMS). Typical $\delta^{13}C$ precision was ±0.2‰.

The solid-phase inorganic $\delta^{13}C$ was measured for nodules (HR & ERB; $\delta^{13}C_{nod}$) and sediments (HR; $\delta^{13}C_{sed}$; Table 1). All samples were dried at 60°C for 12 h, then milled to a fine powder. Powdered sediment or carbonate (0.4–1.0 mg) was placed in a labco vial, flushed with helium, then acidified with 100% phosphoric acid at 90°C. The CO_2 gas released was sampled and admitted to an Isoprime IRMS via a GV Multiflow preparatory system. Sodium bicarbonate was used as a consistency standard.

To analyze pore water isotopic composition (ERB; $\delta^{13}C_{pw}$; Table 1), N_2-pre-flushed 20-mL stoppered serum vials were amended with 0.1 mL of saturated ammoniacal $SrCl_2$. Squeezed pore water (1.8 mL) was added via syringe to the vial and stored as a basic solution until on-shore analysis. Prior to analysis, each sample vial was acidified with phosphoric acid and briefly vented to 1 atm to relieve slight positive pressure. Subsequently, a gas-tight syringe was used to remove and compress a sample to known volume. The sample was then injected into a continuous flow irm-GCMS instrument (Finnegan MAT 252) with a carbon-PLOT column (J&W Scientific) and splitless on-column injection. Due to sample limitation, DIC was not collected from Hydrate Ridge.

1.2.5 NODULE PREPARATION AND DNA EXTRACTION

Nodules analyzed in this study were recovered directly from clay-rich sediment. Thus, exterior portions of these samples were presumed to be contaminated with sediment-associated microorganisms. To minimize sedimentary contamination, a series of tests were performed to optimize the removal of external sediment microorganisms prior to DNA extraction from carbonate nodules (Supplemental Material). Ultimately, the most effective protocol for removal of loosely associated microorganisms from carbonate nodules was used for processing samples in this study. Specifically this entailed rinsing with 0.2 µm filtered 1X PBS, followed by sonication of the intact nodule at 8 W for 45 s in fresh, sterile, 1X PBS, and finally centrifugation at 4,000*g* for 5

min. This 3-step process was repeated 3*x* for each nodule. If any sediment-associated microorganisms were entrapped within the interior of nodules, and thus not removed by our techniques, they were considered endolithic for the purposes of this study. Nodules were powdered in sterile mortar and pestle prior to DNA extraction. Genomic DNA was extracted from sediments and nodules using a modified version of the MoBio UltraSoil DNA Isolation Kit (Orphan et al. 2001a).

1.2.6 16S rRNA GENE DEEP SEQUENCING (iTAG)

Initial PCR amplification was performed based on the specifications of the Earth Microbiome Project (EMP; Gilbert et al. 2011; Caporaso et al. 2011; 2012), with two exceptions: first, the single PCR step was split into two PCR steps, in which barcode indices were added at the second step in order to minimize PCR bias by employing long primers over many cycles (Berry et al. 2011). Thus, our first PCR followed the EMP protocol for 30 cycles with primers lacking adapter, barcode, pad, or linker (515f: GTGCCAGCMGCCGCGGTAA; 806r: GGACTACHVGGGTWTCTAAT). For the second PCR step, 5 µL of the amplicon product from PCR#1 was used as template in a 5 cycle, 25 µL reconditioning reaction with the same EMP-recommended conditions and the full EMP primers (515f_barcode: AATGATACGGCGACCACCGAGATCTACACTATGGTAATTGTGTGCCAGCMGCCGCGGTAA; 806r_barcode: CAAGCAGAAGACGGCATACGAGATXXXXXXXXXXXXAGTCAGTCAGCCGGACTACHVGGGTWTCTAAT). The second modification to the EMP protocol was to perform all PCR reactions in duplicate rather than triplicate. Internal lab tests showed that sequencing results were not significantly affected by including a third, triplicate, PCR product during preparation. After all PCR reactions were completed, duplicate barcoded products were pooled and quantified. Samples were mixed together in equimolar amounts and purified in bulk through a

Qiagen PCR Purification kit (Valencia, CA). At all PCR steps, amplification success and purity was checked by gel electrophoresis.

Paired-end sequences (2*x* 250 bp) were generated from barcoded amplicon products at Laragen, Inc (Los Angeles, CA) on an Illumina MiSeq platform. At Laragen the raw data was passed through a barcode filter which demultiplexed the library into individual samples and removed any sequences which had >1 basepair (bp) mismatch on the 12-bp barcode sequence (Golay barcodes were chosen with Levenshtein Distance ≥ 3; Caporaso et al. 2012). The resulting data were passed through MiSeq Recorder software (Illumina Inc, San Diego, CA), which assigned quality scores to each basepair call on every sequence. At the same time, adapter, barcode, and primer sequences were removed. The sequence data reported are available in the Sequence Read Archive under BioProject number PRJNA265122.

The sequences were then processed in-house with QIIME1.8.0 (Caporaso et al. 2010). The paired ends were first assembled into single contigs (join_paired_ends.py; $min_{overlap}$ = 50bp, $max_{bp\_mismatch}$ = 8%; Aronesty 2011). The contigs were then quality trimmed according to the q-scores, sequences with ambiguous 'N' base calls were removed from the dataset, sample names were added to each individual sequence, and the files were converted to fasta format (split_libraries_fastq.py; $q_{max\_unacceptable}$ = 29; max_N = 0). Chimeras were removed using the UCHIME_ref algorithm in USEARCH v7.0.1090 (minh = 0.28, xn = 8.0, dn = 1.4, mindiffs = 3, mindiv = 0.8; Edgar et al. 2011). The remaining sequences were used to pick *de novo* operational taxonomic units (OTUs) at 99% similarity (pick_otus.py; s = 0.99; Edgar 2010). Next, the default algorithm in QIIME1.8.0 was used for taxonomic assignments against representative sequences from each OTU (pick_rep_set.py; m = most_abundant; Wang et al. 2007). Taxa were assigned against the Silva 115 database clustered at 99% similarity (SSURef_NR99_115_SILVA_20_07_13_opt.arb; Quast et al. 2012), which was filtered to include only sequences with pintail value >75, and appended with 1,197 high-quality, full-length, seep-related bacterial and archaeal clones from Orphan lab clone libraries (assign_taxonomy.py; -

-uclust_max_accepts = 10; --uclust_min_consensus_fraction = 0.90; --uclust_similarity = 0.9; modified database is available upon request from the corresponding authors). The same appended database was used for the UCHIME_ref command described above. Singleton OTUs were removed from the dataset (remove_otus_from_otu_table.py; n = 2), as well as OTUs which were unassigned any taxonomy or assigned to Eukarya (filter_taxa_from_otu_table.py). Known contaminants in PCR reagents from sequencing of internal lab negative controls were removed by filtering out all sequences which clustered into Pseudomonadaceae, Enterbacteraceae, or Streptococcaceae, as well as extremely poorly defined Gammaproteobacteria observed in sequencing blanks (Gammaproteobacteria;Other;Other; Salter et al. 2014). In total these contaminant taxa accounted for an average of 2% of recovered sequences (range = 0–12%). Finally, tables of relative abundance were generated at the family level (summarize_taxa.py) and for each sample, families occurring at less than 0.01% relative abundance were removed in order to reduce the influence of spurious sequences. The full table of processed iTAG sequence data can be found in the Supplemental Material, while a summary of key taxa is included as Table 2.

Alpha (Shannon-Weiner) diversity was calculated in Microsoft Excel and beta (Bray-Curtis) diversity metrics were calculated in Primer-E (Clarke and Warwick 2001) from the family-level taxa abundance tables. For non-metric multidimensional scaling (NMDS) and analysis of similarity (ANOSIM) analyses, the taxa-abundance table was transformed with the square-root function prior to generation of the Bray-Curtis similarity matrix in Primer-E. Similarity Percentage (SIMPER) analysis, which deconvolves the whole-community differences between sample groups into quantitative contributions from each taxon, was also carried out in Primer-E (Clarke and Warwick 2001).

1.2.7 TERMINAL RESTRICTION FRAGMENT LENGTH POLYMORPHISM (TRFLP)

16S rRNA genes were amplified using archaeal primers 8F (fluorescently labeled with WellRED dye D4, Sigma-Proligo, St. Louis, MO) and 958R and bacterial primers 27F (fluorescently labeled with WellRED dye D3, Sigma-Proligo) and 1492R using the same PCR conditions as described in the Supplemental Material for clone libraries. PCR products were digested with *Hae*III overnight at 37°C, cleaned, and analyzed with a CEQ 8800 Genetic Analysis System from Beckman Coulter.

Prior to analysis, TRFLP peaks less than 70 bp were removed, thus avoiding spurious peaks that fall outside of the internal standards. Data were then converted to relative abundance, and peaks with relative abundance less than 1% were removed from further analysis. Further, peaks found in less than two samples were also removed from the dataset. Shannon-Weiner diversity indices were calculated using PC-ORD (Table 2; McCune et al. 2002). NMDS analysis was completed in Primer-E after square-root transforming the dataset and calculating Bray-Curtis similarities. NMDS coordinates were then transformed against reference iTAG NMDS coordinates in a procrustes analysis with QIIME 1.8.0 (transform_coordinate_matrices.py; r=1000, d=2). The purpose of this analysis was to test whether inter-sample similarity trends were supported between iTAG and TRFLP datasets. In both the archaeal and bacterial TRFLP beta diversity analyses, carbonate sample 2693 from ERB (clam core, 0–3 cmbsf, PC23) was determined to be an outlier (the outlier analysis in PC-ORD identifies samples whose community fingerprints are more than two standard deviations from the mean of the overall sample set (McCune et al. 2002) and was excluded from inclusion in procrustes analysis because it skewed the ordination plot beyond interpretation.

1.2.8 CLONE LIBRARIES AND FULL-LENGTH 16S rRNA GENE SEQUENCING

A subset of four samples were chosen for cloning and full-length 16S rRNA gene sequencing to gain greater taxonomic resolution of representative microbial taxa from HR and ERB (Table 1). Archaeal and bacterial libraries were prepared separately, resulting in eight clone libraries. A total of 384 bacterial and 384 archaeal clones were analyzed by restriction fragment length polymorphism (RFLP). Phylogenetic analysis and tree construction was carried out in ARB (Supplemental Material; Ludwig et al. 2004). The 16S rRNA gene sequences for the archaeal and bacterial clones were submitted to the GenBank database and are accessible under the following accession numbers: JQ036237–JQ036289. Clone library sequencing results for nodule 2518 at HR have been previously published in the Supplementary Material of Marlow et al. 2014a.

1.3 RESULTS

1.3.1 METHANE CONCENTRATIONS AND $\delta^{13}C$ OF ORGANIC AND INORGANIC CARBON

Recovered methane values were higher at HR than at ERB, and all values were consistent with previous descriptions of the HR and ERB methane seep regions (Table 1; Torres et al. 2002; Orphan et al. 2004). At HR, the recovered methane concentration was always >2 mmol CH_4 per g sediment and showed a minimum at 6–9 cmbsf (Figure 1a). Within the ERB horizons, recovered methane concentrations in the mat core were ~9-fold higher than in the clam and peripheral core horizons in which nodules were recovered, but all recovered methane concentrations were <1 mmol CH_4 per g sediment (Figure 1b). It is likely that some methane degassed during core recovery; therefore, the reported values should be taken as minimum methane concentrations.

At HR, the carbon isotopic composition of nodules from the PC8 mat core was always more ^{13}C-depleted than sedimentary inorganic carbon, which was in turn always more depleted than the organic carbon (Figure 1a). The depleted $\delta^{13}C_{nod}$ was indicative of a significant contribution of methane-derived bicarbonate to the sedimentary pore water DIC pool. The ERB nodule-bearing horizons across the seep transect demonstrated less consistent carbon isotopic results. In the two horizons with highest recovered methane concentrations (mat core, 6–9 cmbsf and 9–12 cmbsf), the nodules were more enriched in ^{13}C than either the pore water DIC or TOC (Figure 1b). The same relationship was true in the horizon from the peripheral core, in which <0.2 mmol CH_4 per g sediment was recovered. Although redox state was not determined, there was a notable change in sediment coloration in the ERB peripheral core relative to parallel cores collected beneath the microbial mat and clam bed, with shallow sediments having a brown-tan coloration transitioning to dark gray in the deepest sediment layers where the carbonate nodule was recovered. The nodule found in the ERB clam core was in the shallowest depth horizon (0–3 cmbsf), which demonstrated the lowest recovered methane concentration in this study (Table 1). The $\delta^{13}C_{pw}$ in this shallow horizon is relatively near the value of seawater (assumed ~0‰), consistent with bioturbation by *Calyptogena* clams. As observed in the HR samples, this nodule was also more depleted in ^{13}C than was the organic carbon (Figure 1b).

1.3.2 MINERALOGY AND PETROGRAPHY

X-ray diffraction (XRD) analyses revealed that nodules from both seep sites were at least partly composed of calcite (Table 1, Supplementary Figure 2). HR nodules were generally similar to one another, in that they were predominately composed of calcite with some (≤50%) aragonite and no measurable dolomite (Table 1). In contrast, the mineralogy of ERB nodules was more variable (Table 1, Supplementary Figure 2). Two of the ERB nodules (mat core 9–12 cmbsf; clam core 0–3 cmbsf) were composed entirely of calcite, while the other two (mat core 6–9 cmbsf;

peripheral core 9–12 cmbsf) contained a significant amount of dolomite (≥40%). None of the ERB nodules contained aragonite. The mineralogy of these sediment-hosted nodules was similar to previous descriptions of exhumed carbonates recovered from both the ERB and HR sites (Naehr et al. 2007).

Petrographic characterization of one representative nodule from HR (3–6 cmbsf) and ERB (PC29, 6–9 cmbsf) revealed distinct lithologies. For example, the HR nodule presented as a carbonate-cemented breccia, in which large angular carbonate clasts and bivalve fragments were cemented together by an aragonitic matrix (Figure 3c–d). Void-filling acicular aragonite cements were also abundant and internal fenestrate cavities in the nodule were surrounded by iron sulfide precipitates (Figure 3c). In comparison, thin section observations of the ERB nodule revealed a carbonate-cemented, quartz-dominated silt with low internal porosity (Figure 3a-b). Iron sulfide growth was observed to surround rare iron-rich lithic grains (Figure 3b). Discrete lithoclasts resembling the phyllosilicate glauconite were also observed, but are not visible in the field of view of the thin section images.

1.3.3 ARCHAEAL COMMUNITY COMPOSITION

Microbial community composition was estimated from recovered iTAG sequences from all 18 paired sediment/nodule samples in the study. Archaeal 16S rRNA clone libraries were additionally constructed from a subset of four samples, which were principally used to explore phylogenetic relationships between recovered HR and ERB clones and previously published 16S rRNA gene sequences. As a whole, the archaeal iTAG diversity data demonstrated consistent alpha diversity (Shannon-Weiner) across all samples (H'_{avg} = 1.7±0.3; Table 2). The greatest deviation from average appeared in the shallow (0–9 cmbsf) HR nodules, which exhibited lower alpha diversity than the majority of other archaeal iTAG data in this study. The deviation was not correlated with the number of recovered archaeal sequences. TRFLP data corroborated a

consistent level of archaeal alpha diversity across samples (H'_{avg} = 2.2±0.2), but without the deviation among shallow HR nodules (Table 2).

Euryarchaeotal ANME groups accounted for the majority of archaeal 16S rRNA iTAG sequences recovered from both sediment and nodule samples in most depth horizons of HR (PC8) and the ERB seep transect (PC29, PC23, PC20), comprising >35% of the recovered archaeal sequences in all samples (Table 2). Sequences associated with ANME-1 were more abundant in HR than in ERB samples across both nodule and sediment substratum types, by a factor of 2.3±1.6 (Table 2). ERB samples exhibited the highest observed ANME-2 abundances, but were also more variable than HR samples which had low-level ANME-2 presence that increased slightly with depth (Table 2). The observed variability of ANME-2 sequence abundance in ERB samples was not correlated to substratum or depth horizon.

Other commonly observed archaeal taxa in benthic marine settings were observed in iTAG data from both sediment and nodule samples. Sequences associated with DHVEG-6 were observed at higher relative enrichment in ERB samples than in HR samples by a factor of 4.6±4.2 (Table 2), and were also abundant in sediment samples from a Nankai Trough methane seep off Japan (Nunoura et al. 2012). Thermoplasmatales-associated sequences that clustered within the Marine Benthic Group D, which overlaps with the Deep Sea Hydrothermal Vent Group 1 (Takai and Horikoshi 1999; Teske and Sorensen 2008), were observed at consistent abundance in all samples, regardless of geographic location or substratum type (Table 2). Sequences associated with the Thaumarchaeotal Marine Benthic Group B were five-fold enriched in one sample relative to all others (ERB mat core nodule 9–12 cmbsf; Table 2).

Similarity rank ordering of the archaeal dataset was well-represented on a two dimensional NMDS plot, yielding a stress value of 0.07 when computed with the square root transformed archaeal iTAG data (Figure 2a). The samples were principally differentiated by geography (i.e., HR *vs* ERB), which an ANOSIM test revealed to be statistically robust ($p = 0.002$; $R = 0.63$; $n = 18$; Figure 2a). SIMPER analysis revealed that this geographical difference

was associated with observed abundances of ANME-1a and ANME-1b (more commonly observed in HR samples), and ANME-2ab and DHVEG-6 (more commonly observed in ERB samples).

At HR, the archaeal assemblages associated with sediments and nodules were all >70% similar (Figure 2a). Within the overall highly similar HR sample set, archaeal diversity was finely differentiated by substratum, with all sediments >80% similar to one another but less than 80% similar to the HR nodules ($p = 0.008$; $R = 0.51$, $n = 10$). This is in contrast to previous data, in which substrate type was not determined to be a factor differentiating seep archaeal communities (Marlow et al. 2014b). SIMPER analysis revealed that sequences associated with the subgroups ANME-1a and ANME-1b accounted for 20% of this substratum-based difference within HR samples. Relative abundances of recovered ANME-1a sequences were higher in nodules than sediments by a factor of 1.8±1.3, while ANME-1b sequences were observed at consistent relative abundance in HR sediments (0.43±0.03) and varied according to depth in the nodules (range 0.29-0.73, higher in shallow nodules; Table 2). Overall, shallow (0–9 cmbsf, $n = 3$) nodules were >80% similar to one another and deep (9–15 cmbsf, $n = 2$) nodules were also >80% similar to one another. Deeper samples were uniformly higher in MBGD relative abundance than shallow samples at HR. Shallow sediments were enriched in DHVEG-6. Sequences associated with the ANME-2c subgroup were observed at increasing relative abundance with depth for both nodules and sediments at HR, while ANME-2ab sequences were observed at consistent relative abundance in all HR samples (Table 2).

ERB archaeal sequences were <70% similar to HR samples. Furthermore, whereas HR samples were differentiated by substratum, the ERB samples appeared to be primarily differentiated by depth and were not significantly separated by substratum ($p=0.69$), in agreement with previously published data (Marlow et al. 2014b). Deep (9–12 cmbsf) ERB samples were >70% similar to one another but not to other ERB samples. The mid-depth ERB sediment-

nodule pair from the mat core (6–9 cmbsf) was >70% similar, and the shallowest pairing (clam core; 0–3 cmbsf) was <70% similar to one another and not similar to any other samples.

Full-length ANME 16S rRNA gene sequences grouped with phylotypes recovered from other methane seep sites within the Santa Barbara and Eel River Basins (Figure 4; Orphan et al. 2001a), Hydrate Ridge (Knittel et al. 2005), and other seep sites (e.g. Heijs et al. 2005). ANME-2a and ANME-2b phylotypes have also been reported from carbonate crust samples associated with submarine mud volcanoes (Heijs et al. 2005; Stadnitskaia et al. 2008). However, none of these phylotypes were closely related to the clone library archaeal sequences recovered from ERB and HR carbonate nodules. The majority of ANME-1b clones were most closely related to phylotypes from seep sites and other reducing sediment habitats (Knittel et al. 2005; Kendall et al. 2007). Sequence representatives associated with ANME-1a were not recovered. As with ANME-2a and -2b, the carbonate-associated ANME-1b phylotypes were distinct from those reported by Stadnitskaia et al. 2008 and Heijs et al. 2006.

1.3.4 BACTERIAL COMMUNITY COMPOSITION

Unlike the archaea, the Shannon-Weiner diversity of bacterial iTAG sequences in HR and ERB sediments samples decreased with increasing depth (R^2 = 0.41, HR and ERB; R^2 = 0.52, HR only), as has been observed in other deep-sea sedimentary environments (Lloyd et al. 2010). This depth trend was even more apparent in the TRFLP data (R^2 = 0.75, HR and ERB; R^2 = 0.82, HR only). As was observed in the archaeal dataset, alpha diversity was uncorrelated to number of recovered sequences and sediments at HR were slightly more diverse than nodules, especially in shallow (0–9 cmbsf) horizons (observed in both iTAG and TRFLP data; Table 2).

Deltaproteobacteria, dominated by members of Desulfobacteraceae and Desulfobulbaceae, were observed across all samples in the iTAG data set, regardless of geography or substratum type (Table 2). Recovered Desulfobulbaceae sequences decreased with depth in

both sediment and nodule samples from the ERB mat core (PC29; 6–9 cmbsf and 9–12 cmbsf), as has previously been observed in sediments by fluorescence *in situ* hybridization in a separate study on the same core (Green-Saxena et al. 2014). Numerous Desulfobacteraceae and Desulfobulbaceae full-length 16S rRNA gene clones were recovered from sediments and nodules at both methane seep sites (Figure 5). Related clones were reported from HR sediments (Knittel et al. 2005), Santa Barbara Basin and ERB sediments (Orphan et al. 2001a), and from the previously analyzed overlying 3–6 cm interval of the ERB mat core (PC29; Pernthaler et al. 2008).

Epsilonprotebacteria were often observed at higher relative abundance in sediments than in nodules at both HR and ERB sites, and were most often associated with the genus Sulfurovum in the Helicobacteraceae family. Related Epsilonproteobacteria have been previously observed in shallow cold seep sediments (Roalkvam et al. 2011; Nunoura et al. 2012; Niemann et al. 2013) and are related to known sulfur oxidizers (Inagaki et al. 2004). Epsilonproteobacterial clones were also recovered, and the closest cultured relatives were the sulfur-oxidizers *Sulfuricurvum kujiense* (Kodama and Watanabe 2003) and *Sulfurimonas autotrophica* (Inagaki et al. 2003), both members of the Helicobacteraceae family. In six of the nine sediment-nodule pairs in this study, the Epsilonproteobacterial iTAG relative abundance in the sediment was greater than a factor of five over the corresponding nodule (n_{HR} = 4; n_{ERB} = 2; Table 2). In one case where the nodule conversely had higher abundance than the sediment (PC29, 9–12 cmbsf), the difference was so small it may be insignificant.

At HR, relative abundances of sequences associated with Gammaproteobacteria were higher in sediments than nodules, whereas at ERB the nodules were elevated in Gammaproteobacteria relative abundance as compared to the sediments. ERB samples tended to have overall higher Gammaproteobacterial relative abundances than HR samples (Table 2). Additional bacterial diversity, observed in both iTAG and clone library data, included members of the Bacteroidetes (consistent across geography and substratum type), the Nitrospirae

(principally ERB nodules), the Chloroflexi (enriched at HR over ERB by a factor of 2.0±1.6), and Candidate Division JS1, all previously described from marine methane seeps.

Bacterial communities were represented on a two dimensional Non-Metric Multidimensional Scaling (NMDS) plot with a stress value of 0.05, and the overall separation was similar as observed with archaea, where bacterial assemblages were significantly differentiated by geography ($p < 0.001$; $R = 0.35$; $n = 18$; Figure 2b). SIMPER analysis revealed that the epsilonproteobacterial Helicobacteraceae (high in HR sediments), Candidate Division JS1 (high in HR sediments and nodules), and Desulfobacteraceae (high in ERB sediments and nodules) were associated with HR *vs* ERB differences.

Within the HR samples, as was observed in the archaea, the bacterial assemblages were separated by substratum ($p = 0.008$; $R = 0.67$; $n = 10$), consistent with previous observations of bacterial community structure (Marlow et al. 2014b). The taxa most strongly associated with this separation were the epsilonproteobacterial Helicobacteraceae (enriched in sediments over nodules) and deltaproteobacterial Desulfobacteraceae (enriched in nodules over sediments). The detailed breakdown by substratum- and depth-dependent factors was more complex with bacteria than with archaea (Figure 2b). Whereas all ten HR archaeal assemblages from the mat core (PC8) were highly similar to one another (with some fine-scale differences as presented above), three of the shallow bacterial HR sediment assemblages (PC8, 0–9 cmbsf) were <70% similar to the main bacterial HR cluster of five nodules (0–15 cm) and two deeper sediment horizons (9–15 cm). Those three HR sediment bacterial assemblages were >80% similar to one another and demonstrated the highest recovery of epsilonproteobacterial Helicobacteraceae sequences among all 18 bacterial community samples. Two ERB samples that clustered near the shallow HR sediments also contained a high abundance of Helicobacteraceae sequences.

Within the cluster of seven similar HR samples, as with archaea, the nodule-associated bacterial assemblages separated into shallow (0–9 cmbsf) and deep (9–15 cmbsf) groups. The two deep HR sediment samples were most similar to the shallow nodules (Figure 2b). There was

generally more variability in bacterial iTAG data from the ERB transect than from the single HR core. To some extent, ERB bacterial assemblages appeared to be differentiated by depth. Most deep samples were highly similar to one another, as was observed in the archaeal ERB data, and the shallow samples demonstrated high biological dissimilarity (Figure 2b).

1.4 DISCUSSION

In modern and ancient settings, authigenic carbonates that precipitate as a result of AOM may provide a geological record of anaerobic methanotrophy in marine sediments (Peckmann and Thiel 2004). However, the degree to which precipitation passively captures a biological record of sediment-hosted microorganisms, or represents a distinct carbonate-hosted microbiome predicated on unique physicochemical constraints, remains unclear (Marlow et al. 2014a; b). More fundamentally, the consistency of the relationship between the microbial diversity of host sediments and carbonate nodules across geochemical regimes remains unexplored. Through parallel molecular, geochemical, and isotopic analyses of seep sediments and the carbonate nodules they host, we addressed these outstanding questions.

At HR, nodules were uniformly depleted in ^{13}C ($\delta^{13}C_{nod}$ = -45.9±3.2‰) relative to other carbon phases, including sedimentary inorganic carbon and organic carbon (Figure 1). These isotopic values are consistent with the relatively high recovered methane concentrations at HR, which could enable high AOM rates, as well previous isotopic measurements of seafloor carbonates from this site (Greinert et al. 2001). Although the carbon isotopic composition of methane in the mat core (PC8) from HR was not measured, it can reasonably be predicted to be depleted in ^{13}C, as has been consistently reported from other studies at HR (Suess et al. 1999; Boetius and Suess 2004). A high rate of AOM lowers the $\delta^{13}C$ value of the DIC pool, a signal that is then incorporated into carbonate nodules (Ussler and Paull 2008). The consistent offset between $\delta^{13}C_{nod}$ and $\delta^{13}C_{sed}$ ($offset_{avg}$ = 9.6±1.2‰) also merits consideration. It is possible that the

inorganic carbon isolated from the sediment represents more recent precipitation than the nodules, or, perhaps, the bulk sediment includes some carbonate at circa 0‰ (e.g., planktonic foraminifera tests) that is not methane-derived. This could make the bulk sediment appear less ^{13}C depleted than the nodule that is composed of all or mostly methane-derived carbon. Based on the isotopic offset, one interpretation is that $\delta^{13}C_{sed}$ may represent a contemporary snapshot of AOM activity, while the $\delta^{13}C_{nod}$ may represent a longer, time-integrated history of AOM activity at HR. Indeed, other studies have found that carbonate nodules and concretions precipitate over 10^2 to 10^4 years, and therefore represent time-integrated records of seep activity (Luff et al. 2004; Ussler and Paull 2008). The $\delta^{13}C_{org}$ values at HR were only moderately depleted in ^{13}C (-30.5±2.5‰), suggesting other contributions besides AOM-associated organisms to the total sediment-associated organic carbon pool.

Regardless of the timing of nodule formation, the geochemical data at HR was consistent across depth and concordant with conditions favoring *in situ* carbonate formation within seep sediments: relatively high methane concentrations fueling AOM and thus an increase in alkalinity and carbonate saturation (Luff et al. 2004), followed by precipitation of nodules with depleted ^{13}C content. The archaeal iTAG data are in agreement with this interpretation: all HR samples (nodules and sediments) demonstrated similar Shannon-Weiner diversity and high community similarity to one another, especially when contrasted with the diversity in ERB molecular data (see discussion below). Moreover, the overall archaeal similarity at HR was linked in SIMPER analysis to the observed abundance of ANME-1 subgroups, taxa known to be involved in AOM (Hoehler et al. 1994; Boetius et al. 2000; Orphan et al. 2001b). Thus, it appears that in geochemical regimes favorable for AOM, nodules broadly mirror the archaeal communities found in surrounding sediment. This broad finding is consistent with previous findings that substrate type was not a major differentiator of archaeal populations (Marlow et al. 2014b).

However, close examination of the dataset reveals further structure to the molecular data, which reflects subtle differences in the nodule assemblage relative to the host sediment as a

function of depth. This is most likely ultimately due to depth-dependent differences in geochemistry affecting changes in microbial assemblage composition, as has been observed previously (Lloyd et al. 2010). Within the archaeal communities, shallow (0–9 cmbsf) nodules were distinct from deep (12–15 cmbsf) nodule-associated microbial communities (Figure 2a). This suggestion of a depth-dependent factor driving microbial communities was even stronger in the bacterial iTAG data, where all nodule-associated bacterial communities at HR were highly similar to deep (12–15 cmbsf) sediment communities, but different from shallow (0–9 cmbsf) sediment-hosted communities (Figure 2b). This molecular evidence thus suggests that nodules might be formed within the deep sediment horizons, entrap the adjacent microbial communities during formation, and may be subsequently transported upward, perhaps by local uplift and sediment erosion, bioturbation, or seismic activity.

That a depth-dependent trend, and inferred translocation, was strongest in bacterial molecular data at HR is intrinsic to the fundamental differences between the geochemical and archaeal *vs* the bacterial datasets: the geochemical characteristics and archaeal sediment diversity were largely homogenous with depth, and so did not provide a framework for observing strong differences across depth within the studied sediment core (PC8). Since the bacterial sediment-associated microbial communities were well-differentiated into deep and shallow groups, the effects of an origin at depth and vertical translocation of nodules, if true, was observable. TRFLP data generally supported the iTAG molecular observations (Supplemental Material). Nonetheless, it cannot be ruled out that rather than translocation, local geochemical conditions may have shifted over time, followed by a shift in the sediment-associated microbial community but unobserved in the DNA recorded within nodule precipitates. Alternatively, macrofaunal grazing pressures in shallower horizons could have influenced the selective enrichment of native sediment microbiota (Thurber et al. 2012).

Petrographic evidence was inconclusive regarding the origination of nodules at HR. The 3–6 cmbsf nodule, the only nodule from HR that was examined petrographically, exhibited

bivalve fragments contained within an aragonitic cement (Figure 3c). Although the bacterial mat site where the PC8 core was recovered did not exhibit clam beds at the seafloor, it is possible that bivalve shell hash present in the underlying sediment was historic. The petrographic fabric of the HR nodule is consistent with one or more phases or carbonate cementation and re-precipitation. This is evidenced by the incorporation of angular clasts of previous generations of authigenic carbonate cemented into an aragonitic matrix. The angular shape of the clasts suggests localized disruption, perhaps from hydrofracturing of carbonate mudstones, involving little or no immediate subsequent transport. The absence of clasts within intraclasts suggests only one disruption event followed by cementation. A disruption event may support the hypothesis that the HR nodules formed in a deep horizon and were subsequently exhumed. However, abundant un-oxidized sulfide precipitates suggest that the nodule has not been uplifted enough for exposure to oxygenated conditions sufficient to alter those phases. This is consistent with the mat-type habitat, which is not expected to greatly bioturbate the sediment. Overall, examination of the paired sediment/nodule depth profile (0–15 cmbsf) at HR suggested that, at active seeps, carbonate nodules precipitate within a few 10s of centimeters below seafloor. These nodules can and do capture the sediment-hosted microbial community, and multiple scenarios can be invoked to explain cases where biological deviation is observed between the nodules and adjacent sediments.

Examining the geochemical data from ERB, it is clear that sediment/nodule pairs across the seep transect exhibited more complex relationships than within the single PC8 core at HR. The 0–3 cmbsf horizon from PC23 (clam core) demonstrated geochemical characteristics that do not predict a favorable environment for carbonate precipitation, despite the recovery of a nodule. The very low recovered methane concentrations indicate little contemporary geochemical driving force for alkalinity generation via AOM, and the somewhat ^{13}C-enriched $\delta^{13}C_{pw}$ value (-7.4‰; Table 1) is likely a combination of low AOM rates and mixing of ~0‰ seawater due to bioturbation by *Calyptogena* clams. Molecular data further indicate the nodule did not precipitate *in situ* in these geochemical conditions, where both archaeal and bacterial diversity, recovered

both by iTAG and TRFLP, clearly shows that the nodule is distinct from the host sediment (Figure 2). Thus, two conclusions are drawn. First, that bioturbation of shallow sediment by overlying clams generates a distinct archaeal and bacterial sediment-associated microbial community, and second, that the recovered nodule either originated in a separate location and was subsequently moved by sediment winnowing or uplift to the shallow location from which it was recovered, or precipitated *in situ* at a time when sediment geochemistry and microbial populations were different than their modern states.

The PC29 mat core (6–9 and 9–12 cmbsf) was collected from beneath a sulfide-oxidizing bacterial mat at ERB, and is thus most parallel to the HR mat core (PC8) with respect to benthic habitat type. However, the samples exhibited geochemical and microbiological variability which exemplified the potential for inhomogeneity within seep ecosystems, compared to the relatively homogenous conditions in HR core PC8. Centimeter-scale vertical variability (both geochemical and biological) has previously been reported from methane seep sediments, including Hydrate Ridge (Treude et al. 2003), Eel River Basin (a separate study of the same cores we sampled for this study; Green-Saxena et al. 2014), and the Gulf of Mexico (Lloyd et al. 2010). The depleted $\delta^{13}C_{org}$ value (-40.7‰) from the shallower (6–9 cmbsf) horizon of the ERB mat core is indicative of significant methanotrophic biomass, along with depleted $\delta^{13}C_{pw}$ (-36.1‰) suggestive of active AOM. The deeper horizon's biomass ($\delta^{13}C_{org}$ = -31.0‰) and pore water inorganic carbon ($\delta^{13}C_{pw}$ = -32.9‰) values also suggest active AOM processes, although perhaps at a more moderate rate. The deeper nodule's carbon isotope enrichment over the pore water ($\delta^{13}C_{nod}$ = -27.2‰; $\Delta^{13}C_{nod\text{-}pw}$ = 5.7‰) also suggests at most moderate AOM rates. That the nodule is slightly enriched in ^{13}C relative to surrounding pore water could be the result of time-integrated precipitation of the nodule over varying or different historic conditions.

The shallower nodule more substantially deviated from the pore water carbon isotopic composition ($\delta^{13}C_{nod}$ = -23.1‰; $\Delta^{13}C_{nod\text{-}pw}$ = 13.0‰). However, mineralogical evidence revealed that the shallower nodule was composed of 40% dolomite, and nodules that include substantial

dolomite have been documented to have much more ^{13}C-enriched carbon isotopic signatures (Greinert et al. 2001; Naehr et al. 2007). Indeed, a ^{13}C-enriched value was also observed for the other dolomite-containing nodule recovered at ERB (PC20, 9–12 cmbsf, Table 1). Microbially-mediated methanogenesis enriches the DIC pool in ^{13}C; thus, ^{13}C-enriched dolomites are often interpreted to have formed in deeper, methanogenic horizons, often below the sulfate methane transition zone (SMTZ; Greinert et al. 2001; Naehr et al. 2007). Sulfate-reducing bacteria can also mediate dolomite precipitation (Vasconcelos et al. 1995; 2005; Krause et al. 2012), but with a depletion rather than enrichment in $\delta^{13}C$ as observed in our data (Vasconcelos et al. 1995). Previous geochemical characterization of PC29 suggested the local SMTZ peaks at 6–9 cmbsf (Green-Saxena et al. 2014), making it likely that the methanogenic zone, which may have originally hosted the nodule, was deeper in the sediment column. Thus, a possible interpretation of this study's geochemical data is that both the 6–9 cmbsf and 9–12 cmbsf sediments in the mat core host contemporary, active AOM, but the nodules record one or more intervals of environmental conditions that differed from current conditions, or record conditions from precipitation elsewhere than their recovery location.

The microbiological iTAG data are mostly consistent with this hypothesis. In the deeper sediment horizon, the archaeal and bacterial sequence data demonstrated close coupling between the sediment/nodule pair (Figure 2). Both the sediment and nodule exhibited high abundances of AOM-associated taxa, most notably ANME-1 subgroups and Desulfobacteraceae (Table 1). Thus, the nodule appeared to passively mirror the adjacent sediment-associated microbial assemblage as was the case at HR. In the shallower horizon, the sediment/nodule pair similarity was notably low within the bacterial data and consistent with either nodule translocation or a nodular signal of preserved, relic genetic material combined with signatures from extant endolithic microorganisms (Figure 2). Indeed, endolithic microbial activity in massive seep carbonates and nodules has been recorded recently (Marlow et al. 2014a).

Bacteria appear to be more sensitive to nodule provenance, translocation, and/or geochemical shift than archaea, as even in the generally homogenous HR core, the bacteria demonstrated variability – shallow sediments were relatively dissimilar from other HR samples. In the shallower ERB horizon, for which bacterial and geochemical data support translocation from and/or precipitation within a methanogenic zone, the archaeal iTAG data contrasts by suggesting a tightly coupled sediment/nodule pair and little evidence of conventional methanogens such as members of the family Methanosarcinaceae (Figure 2a; Supplemental Material). Close analysis reveals that this tight archaeal coupling is due to the highest observations of ANME-2ab-affiliated sequences in this study's entire sample set. Previous measurements have found carbonate nodules to contain 100-fold more methane than surrounding sediments due to adsorption processes (Ijiri et al. 2009). Therefore, methane-consuming taxa might have a strong driving force to colonize nodules. The mechanism behind such colonization remains unknown, as ANME are thought to have doubling times on the order of several months and are not know to be motile. However, transport and/or colonization could occur via seep metazoans, some of which have been demonstrated to feed on archaea as a food source (Thurber et al. 2012). It is possible metazoans could act as a transportation mechanism for undigested microorganisms.

Whether specific mineralogy plays a role in microbial colonization is undetermined, but could be a factor contributing to some of the decoupling between sediment and nodule assemblages. The ERB nodule which was petrographically examined, from the 6-9 cmbsf horizon of the mat core, was a carbonate-cemented siliclastic sediment – a lithology that is common at seep sites throughout the world (e.g. Peckmann et al. 2001; Campbell et al. 2010). The ERB nodule did not show evidence of multiple stages of carbonate precipitation, erosion, dissolution, or exposure at the sediment/water interface. Changes in the redox regime in seep-associated sediments can commonly result in the partial or complete oxidation of sulfide mineral phases, including in the Eel River Basin (Bailey et al. 2010). The presence of unoxidized sulfides in the ERB nodule suggest that the nodule has not encountered oxygenated conditions, consistent with

the overlying presence of a bacterial mat which would not bioturbate the underlying sediment. The undisturbed, un-oxidized condition of the nodule is not conclusive but suggests it may not have been translocated, which would be consistent with the closely coupled archaeal sediment/nodule data.

Interestingly, the peripheral ERB core (PC20) exhibited geochemical data most similar to the 6–9 cmbsf horizon from the ERB mat core (PC29). That is, the nodule contained a significant fraction of dolomite (50%; Table 1) and was more ^{13}C-enriched than either the pore water or organic carbon. The bacterial iTAG data suggests the nodule is not similar to the paired sediment (Figure 2b), which is corroborated by bacterial TRFLP data. The archaeal iTAG data suggests a closer coupling (Figure 2a), although it does not appear to be due to ANME subgroup similarities. Indeed, the nodule is depleted in ANME-1 subgroups and enriched in ANME-2 subgroups relative to the host sediment. The observation of a large number of ANME-2-affiliated sequences in the dolomite-containing nodule is consistent with ANME-2-affiliated sequences recovered from the 6–9 cmbsf nodule in the ERB mat core (PC29). Thus, the bulk of the geochemical and molecular evidence from the deep horizon of the peripheral ERB core leads to a similar conclusion as for the 6–9 cmbsf sediment/nodule pair from the mat core: the nodule exhibits signatures consistent with possible original precipitation elsewhere and/or within a different geochemical regime and subsequent translocation to the current site. This hypothesis is more strongly supported by the bacterial sequence data than the more ambiguous archaeal and petrographic signals.

1.5 CONCLUSIONS

The ^{13}C-depleted carbonates, organic lipid biomarkers, and associated 16S rRNA gene signatures previously documented from carbonate pavements and chemoherm structures provide evidence for the involvement of archaeal methanotrophs and their syntrophic sulfate-reducing

bacterial partners in carbonate precipitation (Heijs et al. 2006; Stadnitskaia et al. 2008; Marlow et al. 2014b). Previous microbiological data suggested that nodule-associated microbial assemblages might not be simply passive recorders of sediment-associated microorganisms, but could host distinctive, extant, active microbial populations (Marlow et al. 2014a; b). This study directly addressed that hypothesis and confirmed that in some cases divergence was observed between sediment- and nodule-associated assemblages, while in other cases nodules most likely precipitated *in situ* and entrapped the local microbial communities. This may be due to translocation laterally and/or vertically, or shifting local geochemical conditions. Sediment/nodule disconnect appears to be a more common phenomenon among nodules recovered from shallow sites, potentially indicating that nodules form within deeper AOM horizons of the sediment column (~9–15 cmbsf), where alkalinity generation is highest, and subsequently experience exhumation from sediment winnowing. Petrographic evidence from HR indicated post-depositional fracturing of mineral phases, potentially supporting translocation of the nodules. Alternatively, bioturbation from above may rapidly change shallow sediment geochemistry, to which sediment-associated microbial assemblages may respond more quickly than nodule-associated assemblages. Studies suggesting nodules and carbonate slabs grow over 10^2 to 10^4 years support the likelihood that translocation could occur, given the geologic activity at regions such as HR and ERB. If nodules form over prolonged timescales, then the tight sediment/nodule coupling observed in some of this study's samples implies that microbial assemblages can maintain a stable composition over extended periods. Alternatively, it may be that nodules can precipitate over timescales much less than 10^2 years. Further, in petrographic thin sections the presence of reduced minerals entrapped within carbonate nodules from HR and ERB indicate that subseafloor and/or intra-nodule conditions may remain reducing for periods of time at least as long as the lifetime of the nodules. The coupling between seep flux, microbial carbon cycling, and mineralogy can be further explored with a larger sample set. Furthermore, the degree to which microbial assemblage entrapment, as demonstrated in this manuscript for

nodules, extends to massive carbonate pavements, merits further exploration. In the future, comparative tracking of carbonates and host sediments will contribute information to further constrain the many factors influencing the timing, location, and diversity of organisms linked to authigenic carbonate precipitation during sulfate-coupled AOM.

1.6 ACKNOWLEDGMENTS

VO conceived of the study and collected the samples at sea. OM processed the samples and optimized DNA extraction, as well as TRFLP and clone library analyses. DC performed iTAG processing and analyses, as well as beta diversity analyses, and was the coordinating author of the manuscript. TN provided XRD data, RL performed the isotopic composition analyses, JB provided thin section images, and RT performed the pore water geochemical measurements. DC, OM, and VO principally contributed to writing the manuscript. Three anonymous reviews provided constructive suggestions to improve the manuscript.

Elizabeth Trembath-Reichert, Stephanie Connon, and Jeff Marlow helped with customization of the Silva115_NR99 database. Alexis Pasulka provided helpful discussion regarding ordination and statistical probing of microbial communities. Josh Steele also provided discussion on ecological statistics and aided with bench-top lab work. Benjamin Harrison helped with TRFLP data interpretation. Jeff Marlow provided useful feedback on the manuscript. The crew of the R/V *Atlantis* cruise AT-15-11, as well as the pilots of DSV *Alvin* dives AD4249 and 4256, aided in sample recovery at sea.

Funding for this work was provided by a National Science Foundation grant (BIO-OCE 0825791) to VO and an early career grant by the United States Department of Energy, Office of Biological and Environmental Research (DE-SC0003940) to VO. This research was also supported by a grant from the NASA Astrobiology Institute (Award #NNA13AA92A) to VO. This is NAI-Life Underground Publication 009. DC was funded by a National Science Foundation Graduate Research Fellowship.

1.7 TABLES

Table 1. Geochemical Observations. Blank cells indicate measurement was not applicable. Cells with "–" indicate measurement was applicable but not completed, generally due to a limitation from the amount of sample collected or available

		Sample number	Core	Benthic ecosystem	Depth (cmbsf)	Methane (mmol CH_4/g sediment)	Sulfate (mM)	$\delta^{13}C_{org}$ (‰)	$\delta^{13}C_{nod}$ (‰)	$\delta^{13}C_{sed}$ (‰)	$\delta^{13}C_{pw}$ (‰)	Mineralogy (%calc/%arag/%dolo)
Hydrate Ridge	Sediments	S2517	PC8	Mat	0–3	4.33	13.99	−29.7		−35.4	–	–
		S2518	PC8	Mat	3–6	2.74	0.00	−34.5		−38.6	–	–
		S2519	PC8	Mat	6–9	2.10	10.15	−31.2		−39.5	–	–
		S2520	PC8	Mat	9–12	4.16	8.28	−29.2		−37.3	–	–
		S2521	PC8	Mat	12–15	3.41	8.72	−27.9		−32.0	–	–
	Nodules	C2517	PC8	Mat	0–3	4.33	13.99	–	−45.9			90/10/0
		C2518	PC8	Mat	3–6	2.74	0.00	–	−49.0			60/40/0
		C2519	PC8	Mat	6–9	2.10	10.15	–	−47.3			50/50/0
		C2520	PC8	Mat	9–12	4.16	8.28	–	–			–
		C2521	PC8	Mat	12–15	3.41	8.72	–	−41.6			100/0/0
Eel River Basin	Sediments	S2688	PC29	Mat	6–9	0.95	19.24	−40.7		–	−36.1	–
		S2689	PC29	Mat	9–12	0.91	5.40	−31.0		–	−32.9	–
		S2693	PC23	Clam	0–3	0.06	15.28	−24.2		–	−7.4	–
		S2703	PC20	Peripheral	9–12	0.14	25.94	−25.0		–	−31.9	–
	Nodules	C2688	PC29	Mat	6–9	0.95	19.24	–	−23.1			60/0/40
		C2689	PC29	Mat	9–12	0.91	5.40	–	−27.2			100/0/0
		C2693	PC23	Clam	0–3	0.06	15.28	–	−34.1			100/0/0
		C2703	PC20	Peripheral	9–12	0.14	25.94	–	−18.0			50/0/50

Table 2. Microbiological Observations. All microbial relative abundance data shown is calculated from iTAG sequencing results. Heat scales are calculated separately for each column. As is always the case in PCR-based analyses, relative abundance between taxa (i.e., comparing across a row) should be interpreted cautiously. A safer interpretation is the relative abundance of one taxon across multiple samples (i.e., comparing down a column). Shannon–Weiner diversity (H′) is also given for Archaea and Bacteria, calculated from both the iTAG and TRFLP data. For a complete reporting of iTAG sequencing results, see Supplemental Tables 1 and 2.

		Sample number	Core	Benthic Ecosystem	Depth (cmbsf)	16S rRNA gene deep sequencing	Clone libraries	*Archaea*											*Bacteria*						
								H' (TRFLP)	H' (iTAG)	ANME (total)	ANME-1a	ANME-1b	ANME-1_{other}	ANME-2ab	ANME-2c	MBGB	MBGD	DHVEG-6	H' (TRFLP)	H' (iTAG)	*Delta-proteobacteria* (total)	*Desulfo-bulbaceae*	*Desulfo-bacteraceae*	*Epsilon-proteobacteria* (total)	*Gamma-proteobacteria* (total)
Hydrate Ridge	Sediments	S2517	PC8	Mat	0-3	✔	--	2.5	1.8	0.66	0.20	0.41	0.01	0.02	0.02	0.01	0.15	0.11	2.8	3.2	0.21	0.08	0.08	0.29	0.08
		S2518	PC8	Mat	3-6	✔	✔	2.4	1.8	0.71	0.24	0.41	0.02	0.02	0.02	0.01	0.11	0.10	2.8	3.4	0.23	0.08	0.10	0.21	0.07
		S2519	PC8	Mat	6-9	✔	--	2.5	1.6	0.78	0.22	0.48	0.04	0.02	0.02	0.01	0.11	0.05	2.2	3.2	0.31	0.10	0.15	0.18	0.04
		S2520	PC8	Mat	9-12	✔	--	2.1	1.9	0.67	0.12	0.39	0.04	0.04	0.07	0.01	0.19	0.07	2.4	3.0	0.33	0.09	0.19	0.11	0.01
		S2521	PC8	Mat	12-15	✔	--	2.2	1.8	0.72	0.16	0.44	0.04	0.02	0.05	0.01	0.17	0.05	1.7	3.0	0.37	0.12	0.20	0.10	0.01
	Nodules	C2517	PC8	Mat	0-3	✔	--	2.2	1.2	0.90	0.17	0.65	0.04	0.02	0.02	0.01	0.07	0.01	1.7	2.9	0.42	0.19	0.15	0.02	0.01
		C2518	PC8	Mat	3-6	✔	✔	2.2	1.1	0.91	0.08	0.73	0.07	0.01	0.02	0.01	0.06	0.01	1.9	2.8	0.45	0.14	0.23	0.03	0.00
		C2519	PC8	Mat	6-9	✔	--	2.4	1.4	0.87	0.18	0.58	0.04	0.03	0.03	0.01	0.07	0.02	2.0	2.8	0.38	0.10	0.23	0.07	0.00
		C2520	PC8	Mat	9-12	✔	--	2.3	1.8	0.68	0.04	0.44	0.08	0.04	0.08	0.01	0.22	0.05	1.8	2.7	0.40	0.06	0.28	0.01	0.00
		C2521	PC8	Mat	12-15	✔	--	1.7	1.8	0.62	0.04	0.29	0.11	0.03	0.15	0.01	0.31	0.02	1.9	2.7	0.47	0.08	0.34	0.01	0.00
Eel River Basin	Sediments	S2688	PC29	Mat	6-9	✔	✔	2.1	1.7	0.68	0.04	0.06	0.02	0.49	0.07	0.00	0.04	0.20	2.5	3.2	0.38	0.15	0.17	0.14	0.04
		S2689	PC29	Mat	9-12	✔	--	2.0	1.5	0.71	0.00	0.46	0.20	0.01	0.04	0.00	0.09	0.18	1.4	2.2	0.48	0.05	0.40	0.00	0.00
		S2693	PC23	Clam	0-3	✔	--	2.3	1.6	0.35	0.02	0.01	0.01	0.30	0.01	0.02	0.01	0.46	2.6	3.6	0.31	0.10	0.11	0.23	0.14
		S2703	PC20	Peripheral	9-12	✔	--	2.1	1.8	0.51	0.00	0.24	0.18	0.05	0.03	0.00	0.13	0.32	1.5	2.2	0.50	0.02	0.44	0.01	0.00
	Nodules	C2688	PC29	Mat	6-9	✔	✔	2.1	2.0	0.66	0.01	0.06	0.09	0.38	0.13	0.05	0.12	0.09	2.7	3.6	0.36	0.18	0.10	0.02	0.11
		C2689	PC29	Mat	9-12	✔	--	1.7	1.8	0.40	0.01	0.12	0.14	0.02	0.12	0.01	0.24	0.32	1.4	1.7	0.58	0.02	0.54	0.01	0.00
		C2693	PC23	Clam	0-3	✔	--	2.3	1.4	0.49	0.00	0.03	0.46	0.00	0.00	0.00	0.26	0.07	1.5	3.2	0.15	0.03	0.03	0.01	0.51
		C2703	PC20	Peripheral	9-12	✔	--	2.1	2.1	0.49	0.01	0.17	0.09	0.19	0.04	0.00	0.21	0.20	2.2	3.2	0.39	0.19	0.15	0.19	0.03

1.8 FIGURES

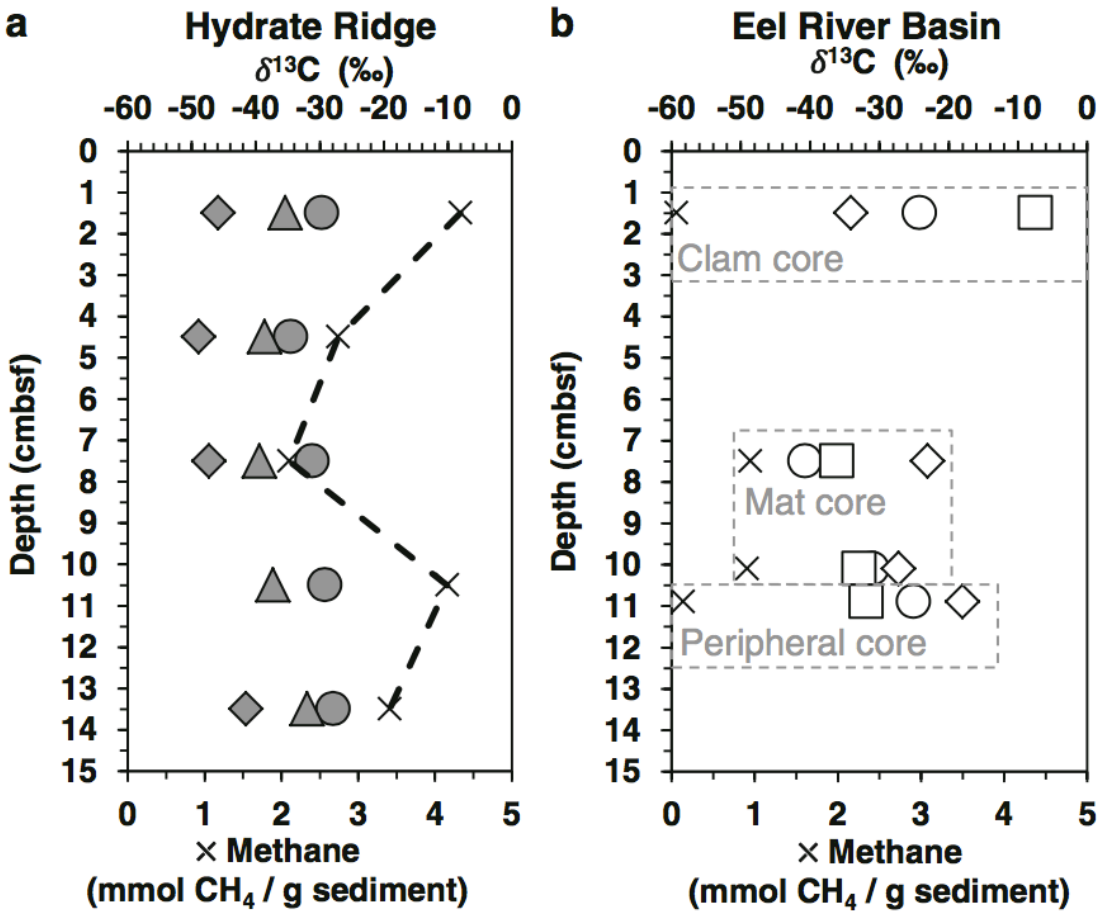

Figure 1. $\delta^{13}C$ variation at HR (a) and ERB (b), for four types of samples: nodule inorganic carbon ($\delta^{13}C_{nod}$; diamonds), organic carbon ($\delta^{13}C_{org}$; circles), sedimentary inorganic carbon ($\delta^{13}C_{sed}$; triangles), and porewater inorganic carbon ($\delta^{13}C_{pw}$; squares). Methane concentrations, shown by 'x', at HR are connected by a dashed line to emphasize that all samples originated from one core (PC8), while ERB samples were obtained from three separate cores (defined by dashed gray boxes). The deep (9–12 cmbsf) samples from the ERB mat core and ERB peripheral core were vertically offset in order to more clearly display the data

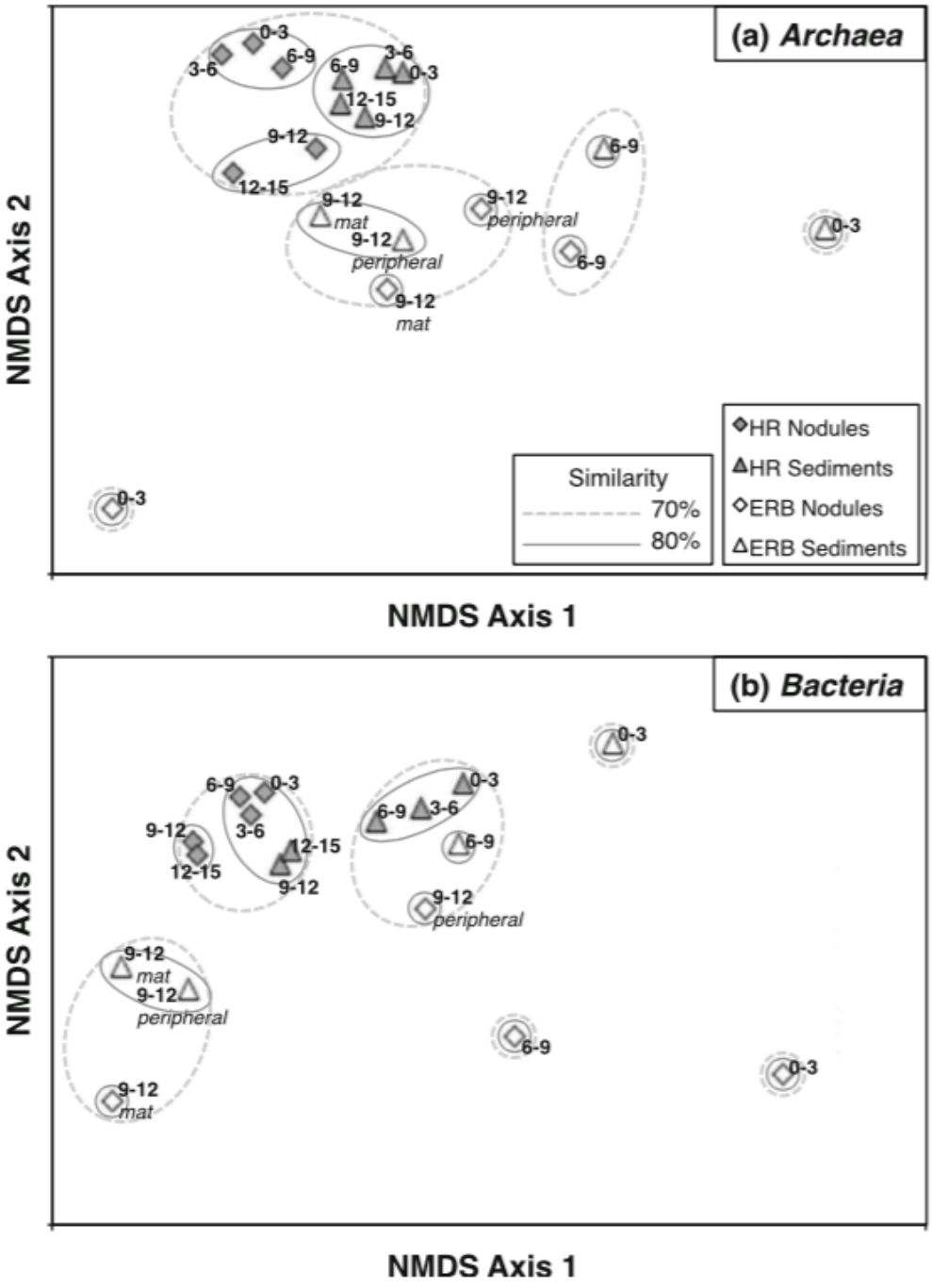

Figure 2. Nonmetric Multidimensional Scaling (NMDS) ordination of iTAG sample similarities for (a) Archaea and (b) Bacteria. Displayed data was square root transformed prior to ordination, which minimizes errors in the ordination due to PCR bias while also not sacrificing genuine differences between samples. Samples with similar microbial communities plot closer together. Archaeal plot stress is 0.07. Bacterial plot stress is 0.05. Legend in (a) applies to both panels. The depth in centimeters below seafloor is listed in bold text next to each sample point. The ERB dataset includes two sediment/nodule pairs from the 9- to 12-cmbsf horizon; for clarity, these are additionally labeled in italics with the relevant core name.

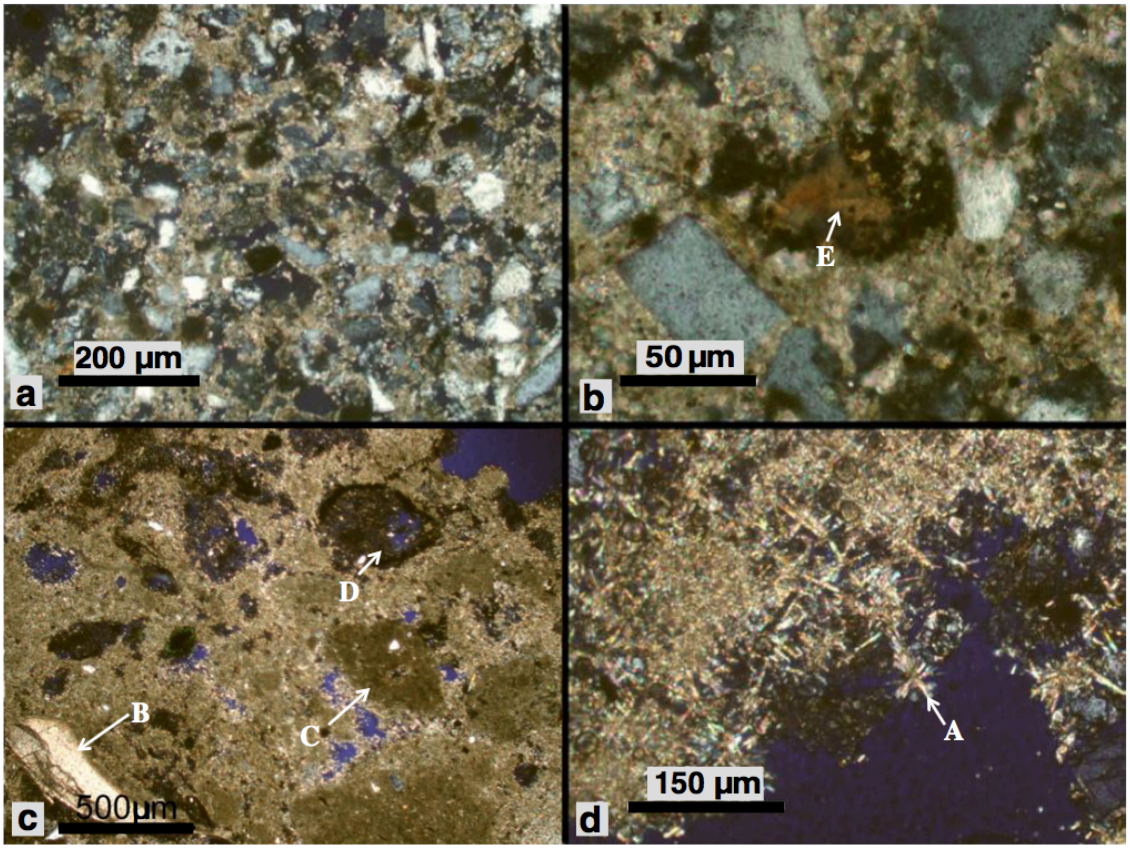

Figure 3. Petrographic thin sections of nodules from (a, b) the 6- to 9- cmbsf horizon on the ERB mat core (PC29), and (c, d) the 3- to 6- cmbsf horizon of the HR mat core (PC8). The ERB sample is quartz- dominated with low internal porosity. Carbonate phases are a mix of calcite, aragonite, and dolomite (see Table 1 in main text). Within an acicular aragonitic matrix (A), the HR sample exhibits cemented bivalve shells (B). Angular carbonate clasts are also observable in the HR sample (C), as well as iron sulfide precipitates (D). Sometimes iron sulfide precipitates surround iron-rich lithic grains (E).

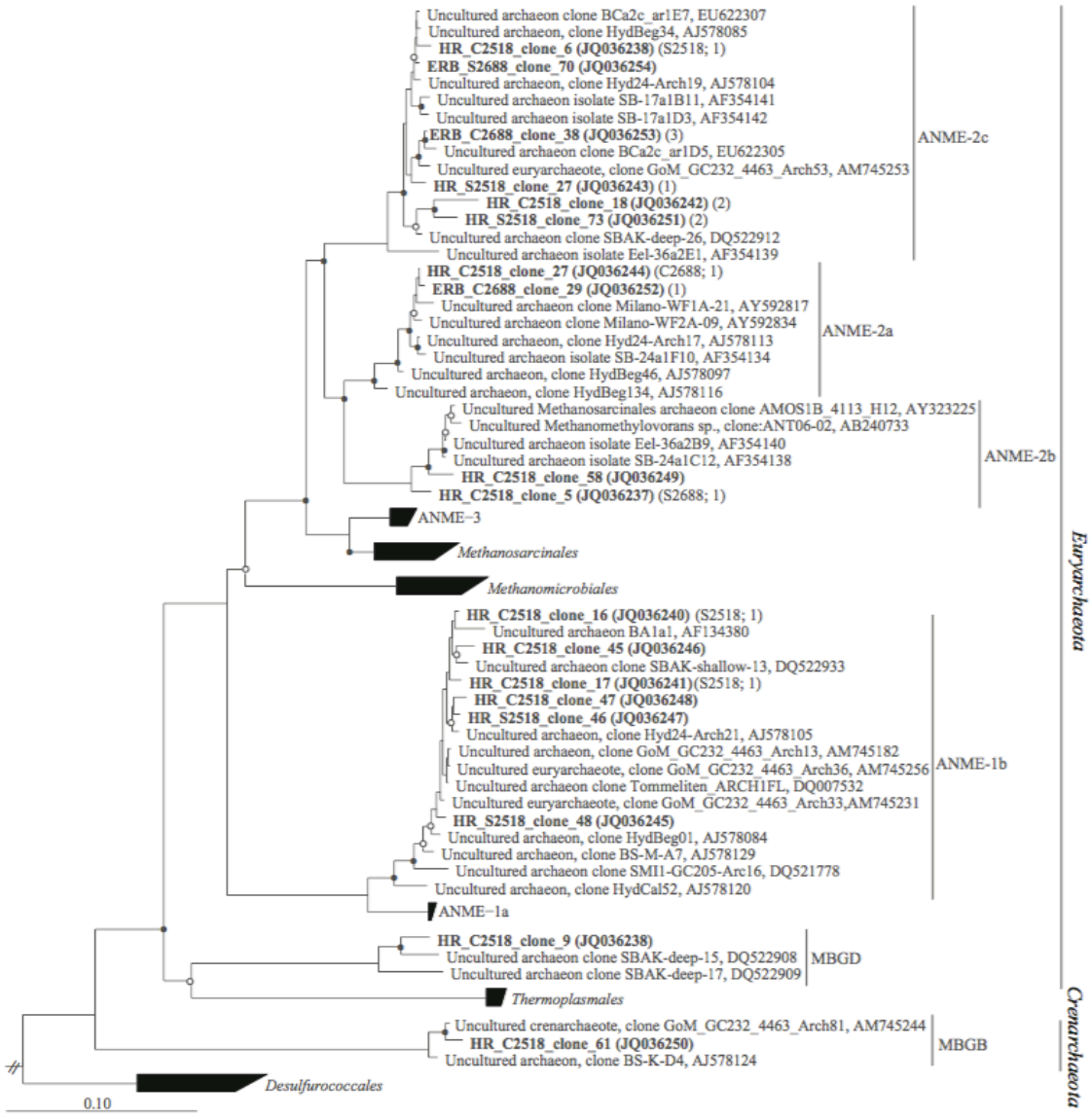

Figure 4. Phylogenetic analysis of archaeal clones. Clones were recovered representing ANME-1b, -2a, -2b, and -2c. ANME-1a clones were not recovered. Samples are named according to the following convention: *Site_Samplenumber_clone_number (accession number)*. Thus, "HR_C2518_clone_61 (JQ036250)" represents a full-length 16S sequence originating from a nodule in the 3- to 6-cmbsf horizon of the HR core.

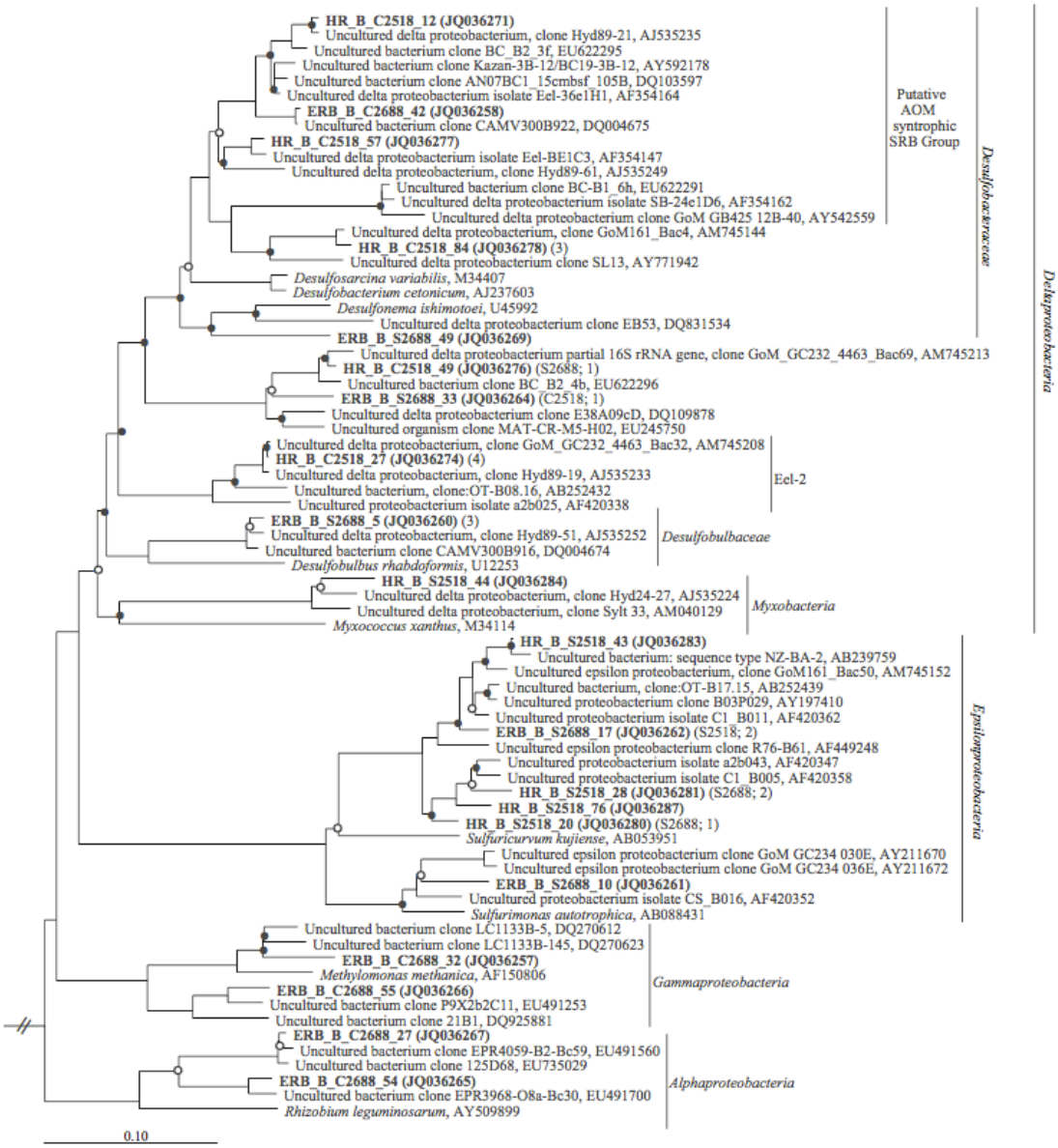

Figure 5. Phylogenetic analysis of bacterial clones. Clones were recovered representing the families *Desulfobulbaceae* and *Desulfobacteraceae*. In addition, alpha-, gamma-, and epsilonproteobacteria clones were recovered. Besides the *Proteobacteria*, clones were recovered representing the *Firmicutes*, *Nitrospirae*, *Bacteroidetes*, *Chloroflexi*, and Candidate Division JS1.

1.9 SUPPLEMENTAL MATERIAL: TEXT

1.9.1 OPTIMIZATION OF NODULE CLEANING TECHNIQUE

To optimize the removal of microbial contamination from carbonate nodules, a series of decontamination experiments were carried out using samples from a carbonate slab from the Eel River basin, broken into several ~10 cm^3 pieces and sterilized by autoclaving. For each experimental condition tested one carbonate section was aseptically maintained, while the second was placed in a 200-mL turbid *Escherichia coli* culture for several hours. Each pair of sterile and contaminated carbonate was then subjected to one of four conditions: 1) UV sterilization for 0.5 hr per side, 2) 70% ethanol rinsing and flaming, 3) rinsing with 1X PBS buffer, and 4) rinsing with 1X PBS and sonication (Branson sonifier 150, Danbury, CT). Each sample was then powdered with a mortar and pestle that was sterilized by baking overnight at 220 °C. Genomic DNA was extracted from 0.5 g of carbonate powder using an Ultraclean Soil DNA kit (MoBio Laboratories, Carlsbad, CA) following the manufacturer's protocol, with a few modifications. Specifically, following addition of the first solution, samples were incubated at 65°C for 5 min, vortexed briefly, and placed at 65°C for 5 min for a second time. After adding the MoBio IRS solution samples were placed at 4°C for 5 min. To determine which sterilization protocol removed exterior contamination, genomic DNA was amplified from both the sterile and *E. coli* contaminated carbonate following the PCR protocol discussed below.

A comparison of the four different treatment protocols indicated that the most effective treatment for removing external DNA and cell contamination (i.e. resulting in no 16S rRNA genes amplified from *E. coli* contaminated sample, or from aseptically maintained control) was to rinse the carbonates with 0.2 µm filtered 1X PBS, followed by sonication at 8 watts for 45 s in fresh, sterile 1X PBS. Samples were centrifuged at 4,000*g* for 5 min. Supernatant was removed and nodules were transferred into fresh 1X PBS between sonication treatments. A total of three

rinse and sonication steps were carried out. All subsequent carbonate nodule and sediment samples were treated according to the protocol discussed above. Genomic DNA was extracted from ERB and HR sediment and 'decontaminated' carbonate samples as described above.

1.9.2 CLONING AND SEQUENCING OF FOUR SELECTED SAMPLES

PCR mixtures (25 μl) contained 0.4 μM each of either archaeal specific primers 8F and 958R (DeLong, 1992), or the bacterial primer 27F with a general 1492R primer. Reactions also contained (final concentrations) 1X 5 Prime *HotMaster Taq Buffer* with 2.5 mM Mg^{2+} (Gaithersburg, MD), 0.2 mM each deoxynucleotide triphosphates, and 0.05 U of 5 Prime HotMaster Taq. PCR reactions were carried out according to the protocol: initial denaturation at 94°C for 3 min, followed by 35 cycles for 45 s at 94°C, 54°C, and 72°C, with a final extension of 72°C for 6 min.

PCR products of the correct length were cut out of a 1% agarose gel. Extracted bands were purified using Qiagen's QIAquick Gel Extraction Kit (Valencia, CA). Purified PCR products were then cloned into a Topo TA cloning kit (Invitrogen, Carlsbad, CA). Clones with the correct insert size were analyzed by restriction fragment length polymorphism (RFLP) using the *HaeIII* restriction enzyme. One representative from each of 35 unique archaeal OTUs was sequenced using a CEQ 8800 Genetic Analysis System from Beckman Coulter (Fullerton, CA). Of these sequenced clones a total of 18 unique, non-chimeric, near full-length archaeal 16S rRNA gene sequences were generated, all of which were 97% or less in similarity. For bacterial libraries, one clone from each of 101 unique OTUs identified by RFLP analysis was sequenced at Laragen, Inc (Los Angeles, CA). Of these sequenced near full-length clones, 35 unique, non-chimeric 16S rRNA phylotypes were recovered, all of which were 97% or less in similarity. For both archaea and bacteria, chimeric sequences were identified with Pintail (Ashelford et al. 2005) and Mallard (Ashelford et al. 2006). Non-chimeric, full-length sequences, including closely related sequences in Genbank and cultured representatives, were aligned using SINA from Silva and imported into ARB (Ludwig et al. 2004). Neighbor-joining trees were constructed using the Olsen distance correction, with 1000 replicates. Maximum likelihood trees were also generated in ARB.

1.10 SUPPLEMENTARY MATERIAL: TABLES

Supplementary Table 1. Archaeal iTAG sequence data. All data is post-processed according to the details given in the methods section.

	Core	Hydrate Ridge										Eel River Basin									
		Sediments				Nodules						Sediments				Nodules					
	Benthic Ecosystem	PC8 Mat	PC8 Rift	PC8 Rift	PC8 Mat	PC8 Mat	PC8 Mat	PC8 Rift	PC8 Rift	PC8 Mat	PC8 Mat	PC29 Mat	PC29 Rift	PC23 Clam	PC26 Peripheral	PC29 Mat	PC29 Rift	PC23 Clam	PC26 Peripheral
	Depth Cmbsf (m)	0.23	24.5	24.5	0.23	0.23	24.5	24.5	0.23	24.5	24.5	0.23	24.5	0.23	24.5	0.23	24.5	0.23	24.5
	Total Archaeal Sequences	4582	9053	8915	8817	12836	17503	9112	12449	7577	8361	7133	12059	756	12043	1829	3748	202	4446
Archaea;__Ancient_Archaeal_Group(AAG);__c;__o;__f		0.00	0.00	0.00	0.01	0.01	0.00	0.00	0.01	0.00	0.01	0.00	0.00	0.00	0.00	0.00	0.00	0.02	0.00
Archaea;__Euryarchaeota;__Halobacteria;__Halobacteriales;__Deep_Sea_Euryarchaeotic_Group(DSEG)		0.01	0.00	0.00	0.01	0.01	0.00	0.00	0.00	0.00	0.01	0.00	0.01	0.00	0.00	0.01	0.01	0.00	0.01
Archaea;__Euryarchaeota;__Halobacteria;__Halobacteriales;__Deep_Sea_Hydrothermal_Vent_Gp_6(DHVEG-6)		0.11	0.10	0.05	0.07	0.05	0.01	0.01	0.02	0.05	0.02	0.20	0.18	0.46	0.32	0.09	0.32	0.07	0.30
Archaea;__Euryarchaeota;__Halobacteria;__Halobacteriales;__Marine_Hydrothermal_Vent_Group(MHVG)		0.02	0.01	0.01	0.01	0.01	0.00	0.00	0.00	0.01	0.01	0.00	0.00	0.00	0.00	0.02	0.01	0.00	0.02
Archaea;__Euryarchaeota;__Halobacteria;__Halobacteriales;__Miscellaneous_Euryarchaeotic_Group(MEG)		0.01	0.00	0.00	0.00	0.01	0.00	0.00	0.00	0.00	0.00	0.00	0.00	0.00	0.00	0.00	0.00	0.00	0.00
Archaea;__Euryarchaeota;__Halobacteria;__Halobacteriales;__SM1K20		0.01	0.00	0.00	0.00	0.01	0.00	0.00	0.00	0.00	0.00	0.00	0.00	0.00	0.00	0.00	0.00	0.00	0.00
Archaea;__Euryarchaeota;__Methanomicrobia;__ANME-1;Other		0.01	0.02	0.04	0.04	0.04	0.07	0.04	0.08	0.11	0.02	0.20	0.01	0.18	0.09	0.14	0.46	0.09	0.09
Archaea;__Euryarchaeota;__Methanomicrobia;__ANME-1;__ANME-1a		0.20	0.24	0.22	0.12	0.16	0.17	0.08	0.18	0.04	0.04	0.04	0.00	0.02	0.00	0.01	0.01	0.01	0.01
Archaea;__Euryarchaeota;__Methanomicrobia;__ANME-1;__ANME-1b		0.41	0.41	0.48	0.39	0.44	0.65	0.73	0.58	0.44	0.28	0.06	0.46	0.01	0.24	0.06	0.12	0.03	0.17
Archaea;__Euryarchaeota;__Methanomicrobia;__Methanocellales;Other		0.00	0.00	0.00	0.00	0.00	0.00	0.00	0.00	0.00	0.00	0.00	0.00	0.00	0.00	0.00	0.00	0.00	0.00
Archaea;__Euryarchaeota;__Methanomicrobia;__Methanocellales;__RS-K-E8		0.00	0.00	0.00	0.00	0.00	0.00	0.00	0.00	0.00	0.00	0.00	0.00	0.00	0.00	0.00	0.00	0.00	0.00
Archaea;__Euryarchaeota;__Methanomicrobia;__Methanosarcinales;__ANME-2a-2b		0.02	0.02	0.02	0.07	0.04	0.02	0.02	0.03	0.08	0.15	0.07	0.04	0.01	0.03	0.13	0.12	0.00	0.04
Archaea;__Euryarchaeota;__Methanomicrobia;__Methanosarcinales;__ANME-2c		0.02	0.02	0.02	0.07	0.05	0.02	0.02	0.03	0.08	0.15	0.07	0.04	0.01	0.03	0.13	0.12	0.00	0.04
Archaea;__Euryarchaeota;__Methanomicrobia;__Methanosarcinales;__GOM_Arc_I		0.00	0.00	0.00	0.00	0.00	0.00	0.00	0.00	0.00	0.00	0.00	0.00	0.00	0.00	0.00	0.00	0.00	0.00
Archaea;__Euryarchaeota;__Methanomicrobia;__Methanosarcinales;__Methanosaetaceae		0.00	0.00	0.00	0.00	0.00	0.00	0.00	0.00	0.00	0.00	0.00	0.00	0.00	0.00	0.00	0.00	0.00	0.00
Archaea;__Euryarchaeota;__Methanomicrobia;__Methanosarcinales;__Methanosarcinaceae		0.00	0.00	0.00	0.00	0.00	0.00	0.00	0.00	0.01	0.00	0.00	0.00	0.01	0.00	0.00	0.00	0.00	0.01
Archaea;__Euryarchaeota;__Thermoplasmatales;__1dc-33;__f		0.00	0.00	0.00	0.00	0.00	0.00	0.00	0.00	0.00	0.00	0.00	0.00	0.00	0.00	0.00	0.00	0.00	0.00
Archaea;__Euryarchaeota;__Thermoplasmatales;__20a-8;__f		0.00	0.00	0.00	0.00	0.00	0.00	0.00	0.00	0.00	0.00	0.00	0.00	0.00	0.00	0.00	0.00	0.00	0.00
Archaea;__Euryarchaeota;__Thermoplasmatales;__Fe-Aa;__f		0.00	0.00	0.00	0.01	0.00	0.00	0.00	0.00	0.00	0.00	0.00	0.00	0.00	0.00	0.00	0.00	0.00	0.00
Archaea;__Euryarchaeota;__Thermoplasmatales;__Kazan-3A-21;__f		0.00	0.00	0.00	0.00	0.00	0.00	0.00	0.00	0.00	0.00	0.00	0.00	0.00	0.00	0.00	0.00	0.00	0.00
Archaea;__Euryarchaeota;__Thermoplasmatales;__South_African_Goldmine_Gp(SAGMEG);__f		0.00	0.00	0.00	0.00	0.00	0.00	0.00	0.00	0.00	0.00	0.00	0.00	0.00	0.00	0.00	0.00	0.00	0.00
Archaea;__Euryarchaeota;__Thermoplasmatales;__Thermoplasmatales;Other		0.00	0.00	0.00	0.00	0.00	0.00	0.00	0.00	0.00	0.00	0.00	0.00	0.01	0.00	0.00	0.00	0.00	0.00
Archaea;__Euryarchaeota;__Thermoplasmatales;__Thermoplasmatales;__20c-4		0.00	0.00	0.00	0.00	0.00	0.00	0.00	0.00	0.00	0.00	0.00	0.00	0.00	0.00	0.00	0.00	0.00	0.00
Archaea;__Euryarchaeota;__Thermoplasmatales;__Thermoplasmatales;__ANT61A-H113-D04		0.01	0.01	0.01	0.01	0.01	0.00	0.00	0.00	0.00	0.00	0.01	0.00	0.00	0.00	0.00	0.00	0.00	0.00
Archaea;__Euryarchaeota;__Thermoplasmatales;__ANT61H-05		0.00	0.00	0.00	0.00	0.00	0.00	0.00	0.00	0.00	0.00	0.00	0.00	0.00	0.00	0.00	0.00	0.00	0.00
Archaea;__Euryarchaeota;__Thermoplasmatales;__ASC21		0.00	0.00	0.00	0.00	0.00	0.00	0.00	0.00	0.00	0.00	0.00	0.00	0.03	0.00	0.00	0.00	0.00	0.00
Archaea;__Euryarchaeota;__Thermoplasmatales;__CCA47		0.02	0.02	0.00	0.01	0.00	0.00	0.00	0.00	0.00	0.02	0.00	0.00	0.04	0.00	0.01	0.01	0.00	0.02
Archaea;__Euryarchaeota;__Thermoplasmatales;__MKC5T43		0.00	0.00	0.00	0.00	0.00	0.00	0.00	0.00	0.00	0.00	0.00	0.00	0.00	0.00	0.00	0.00	0.00	0.00
Archaea;__Euryarchaeota;__Thermoplasmatales;__Marine_Benthic_Group_D_and_DHVEG-1		0.15	0.11	0.11	0.19	0.17	0.07	0.06	0.07	0.22	0.31	0.04	0.09	0.01	0.13	0.12	0.24	0.26	0.21
Archaea;__Euryarchaeota;__Thermoplasmatales;__Marine_Group_II		0.00	0.00	0.00	0.00	0.00	0.00	0.00	0.00	0.00	0.00	0.00	0.00	0.00	0.00	0.00	0.00	0.00	0.00
Archaea;__Euryarchaeota;__Thermoplasmatales;__Marine_Group_III		0.00	0.00	0.00	0.00	0.00	0.00	0.00	0.00	0.00	0.00	0.00	0.00	0.00	0.00	0.00	0.00	0.00	0.00
Archaea;__Euryarchaeota;__Thermoplasmatales;__Terrestrial_Miscellaneous_Gp(TMEG)		0.00	0.00	0.00	0.00	0.00	0.00	0.00	0.00	0.00	0.00	0.00	0.00	0.00	0.00	0.00	0.00	0.00	0.00
Archaea;__Euryarchaeota;__Thermoplasmatales;__Thermoplasmataceae		0.00	0.00	0.00	0.00	0.00	0.00	0.00	0.00	0.00	0.00	0.00	0.00	0.00	0.00	0.00	0.00	0.00	0.00
Archaea;__Euryarchaeota;__Thermoplasmatales;__VC21_Arc6		0.00	0.00	0.00	0.00	0.00	0.00	0.00	0.00	0.00	0.01	0.00	0.00	0.00	0.01	0.00	0.00	0.00	0.00
Archaea;__Thaumarchaeota;__Group_C3;__o;__f		0.00	0.00	0.00	0.00	0.00	0.00	0.00	0.00	0.00	0.00	0.00	0.00	0.00	0.00	0.00	0.00	0.00	0.00
Archaea;__Thaumarchaeota;__Marine_Benthic_Group_B;__o;__f		0.00	0.00	0.00	0.01	0.01	0.00	0.00	0.00	0.00	0.00	0.00	0.00	0.00	0.00	0.00	0.00	0.00	0.00
Archaea;__Thaumarchaeota;__Marine_Group_I;Other;Other		0.00	0.00	0.00	0.00	0.00	0.00	0.00	0.00	0.00	0.00	0.00	0.00	0.03	0.00	0.00	0.00	0.16	0.00
Archaea;__Thaumarchaeota;__Marine_Group_I;__Order_Incertae_Sedis;__Family_Incertae_Sedis		0.00	0.00	0.00	0.00	0.00	0.00	0.00	0.00	0.00	0.00	0.00	0.00	0.00	0.00	0.00	0.00	0.00	0.00
Archaea;__Thaumarchaeota;__Marine_Group_I;__o;__f		0.00	0.00	0.00	0.00	0.00	0.00	0.00	0.00	0.00	0.00	0.00	0.00	0.00	0.00	0.00	0.00	0.00	0.00
Archaea;__Thaumarchaeota;__Miscellaneous_Crenarchaeotic_Group;__o;__f		0.00	0.00	0.00	0.00	0.00	0.00	0.00	0.00	0.00	0.00	0.00	0.00	0.01	0.00	0.02	0.01	0.00	0.00
Archaea;__p;__c;__o;__f		0.00	0.00	0.00	0.00	0.00	0.00	0.00	0.00	0.00	0.00	0.00	0.00	0.00	0.00	0.00	0.00	0.00	0.00

Supplementary Table 2-1. Bacterial iTAG sequence data, page 1 of 4. All data is post-processed according to the details given in the methods section.

	Hydrate Ridge										Eel River Basin							
	Sediments					Nodules					Sediments				Nodules			
Core	PC8	PC8	PC8	PC8	PC8	PC8	PC8	PC8	PC8	PC8	PC29	PC29	PC23	PC20	PC29	PC29	PC23	PC20
Benthic Ecosystem	Mat	Mat	Mat	Mat	Mat	Mat	Mat	Mat	Mat	Mat	Mat	Mat	Clam	Peripheral	Mat	Mat	Clam	Peripheral
Depth (cmbsf)	0-3	3-6	6-9	9-12	12-15	0-3	3-6	6-9	9-12	12-15	6-9	9-12	0-3	12-15	6-9	9-12	0-3	12-15
Total Bacterial Sequences	32773	37437	29300	23504	34074	41208	20864	33306	22835	42582	34821	24117	38928	31590	33496	36917	34752	42684
Bacteria;Other;Other;Other;Other	0.00	0.00	0.00	0.00	0.00	0.00	0.00	0.00	0.00	0.00	0.00	0.00	0.00	0.00	0.00	0.00	0.00	0.00
Bacteria;__Acidobacteria;Other;Other;Other	0.00	0.00	0.00	0.00	0.00	0.00	0.00	0.00	0.00	0.00	0.00	0.00	0.00	0.00	0.00	0.00	0.00	0.00
Bacteria;__Acidobacteria;__Acidobacteria;Other;Other	0.00	0.00	0.00	0.00	0.00	0.00	0.00	0.00	0.00	0.00	0.00	0.00	0.00	0.00	0.00	0.00	0.00	0.00
Bacteria;__Acidobacteria;__Acidobacteria;__AT-23-28;__f	0.00	0.00	0.00	0.00	0.00	0.00	0.00	0.00	0.00	0.00	0.00	0.00	0.00	0.00	0.00	0.00	0.00	0.00
Bacteria;__Acidobacteria;__Acidobacteria;__Subgroup_13;__f	0.00	0.00	0.00	0.00	0.00	0.00	0.00	0.00	0.00	0.00	0.00	0.00	0.00	0.00	0.00	0.00	0.00	0.00
Bacteria;__Acidobacteria;__Acidobacteria;__Subgroup_17;__f	0.00	0.00	0.00	0.00	0.00	0.00	0.00	0.00	0.00	0.00	0.00	0.00	0.00	0.00	0.00	0.00	0.00	0.00
Bacteria;__Acidobacteria;__Acidobacteria;__Subgroup_21;__f	0.00	0.00	0.00	0.00	0.00	0.00	0.00	0.00	0.00	0.00	0.00	0.00	0.00	0.00	0.00	0.00	0.00	0.00
Bacteria;__Acidobacteria;__Acidobacteria;__Subgroup_25;__f	0.00	0.00	0.00	0.00	0.00	0.00	0.00	0.00	0.00	0.00	0.00	0.00	0.00	0.00	0.00	0.00	0.00	0.00
Bacteria;__Acidobacteria;__Acidobacteria;__Subgroup_3;Other	0.00	0.00	0.00	0.00	0.00	0.00	0.00	0.00	0.00	0.00	0.00	0.00	0.00	0.00	0.00	0.00	0.00	0.00
Bacteria;__Acidobacteria;__Acidobacteria;__Subgroup_3;__PAUC26f	0.00	0.00	0.00	0.00	0.00	0.00	0.00	0.00	0.00	0.00	0.00	0.00	0.00	0.00	0.00	0.00	0.00	0.00
Bacteria;__Acidobacteria;__Acidobacteria;__Subgroup_9;__f	0.00	0.00	0.00	0.00	0.00	0.00	0.00	0.00	0.00	0.00	0.00	0.00	0.00	0.00	0.00	0.00	0.00	0.00
Bacteria;__Acidobacteria;__Acidobacteria;__d142;__f	0.00	0.00	0.00	0.00	0.00	0.00	0.00	0.00	0.00	0.00	0.00	0.00	0.00	0.00	0.00	0.00	0.00	0.00
Bacteria;__Acidobacteria;__Holophagae;__Acanthopleuribacterales;__Acanthopleuribacteraceae	0.00	0.00	0.00	0.00	0.00	0.00	0.00	0.00	0.00	0.00	0.00	0.00	0.00	0.00	0.00	0.00	0.00	0.00
Bacteria;__Acidobacteria;__Holophagae;__Subgroup_10;Other	0.00	0.00	0.00	0.00	0.00	0.00	0.00	0.00	0.00	0.00	0.00	0.00	0.00	0.00	0.00	0.00	0.00	0.00
Bacteria;__Acidobacteria;__Holophagae;__Subgroup_10;__CA002	0.00	0.00	0.00	0.00	0.00	0.00	0.00	0.00	0.00	0.00	0.00	0.00	0.00	0.00	0.00	0.00	0.00	0.00
Bacteria;__Acidobacteria;__Holophagae;__Subgroup_10;__Sva0725	0.00	0.00	0.00	0.00	0.00	0.00	0.00	0.00	0.00	0.00	0.00	0.01	0.00	0.00	0.00	0.00	0.00	0.00
Bacteria;__Acidobacteria;__Holophagae;__Subgroup_23;__NKB17	0.01	0.01	0.00	0.00	0.00	0.00	0.00	0.00	0.00	0.00	0.02	0.00	0.01	0.00	0.02	0.00	0.00	0.00
Bacteria;__Acidobacteria;__Holophagae;__Subgroup_7;__f	0.00	0.00	0.00	0.00	0.00	0.00	0.00	0.00	0.00	0.00	0.00	0.00	0.00	0.00	0.00	0.00	0.00	0.00
Bacteria;__Acidobacteria;__Holophagae;__TPD-58;__f	0.00	0.00	0.00	0.00	0.00	0.00	0.00	0.00	0.00	0.00	0.00	0.00	0.00	0.00	0.00	0.00	0.00	0.00
Bacteria;__Acidobacteria;__Subgroup_22;__o;__f	0.00	0.00	0.00	0.00	0.00	0.00	0.00	0.00	0.00	0.00	0.00	0.00	0.01	0.00	0.00	0.00	0.00	0.00
Bacteria;__Acidobacteria;__Subgroup_26;__o;__f	0.00	0.00	0.00	0.00	0.00	0.00	0.00	0.00	0.00	0.00	0.00	0.00	0.00	0.00	0.00	0.00	0.00	0.00
Bacteria;__Actinobacteria;Other;Other;Other	0.00	0.00	0.00	0.00	0.00	0.00	0.00	0.00	0.00	0.00	0.00	0.00	0.00	0.00	0.00	0.00	0.00	0.00
Bacteria;__Actinobacteria;__Acidimicrobiia;__Acidimicrobiales;Other	0.00	0.00	0.00	0.00	0.00	0.00	0.00	0.00	0.00	0.00	0.00	0.00	0.00	0.00	0.00	0.00	0.00	0.00
Bacteria;__Actinobacteria;__Acidimicrobiia;__Acidimicrobiales;__Acidimicrobiaceae	0.00	0.00	0.00	0.00	0.00	0.00	0.00	0.00	0.00	0.00	0.00	0.00	0.00	0.00	0.00	0.00	0.00	0.00
Bacteria;__Actinobacteria;__Acidimicrobiia;__Acidimicrobiales;__Family_Incertae_Sedis	0.00	0.00	0.00	0.00	0.00	0.00	0.00	0.00	0.00	0.00	0.00	0.00	0.00	0.00	0.00	0.00	0.00	0.00
Bacteria;__Actinobacteria;__Acidimicrobiia;__Acidimicrobiales;__Iamiaceae	0.00	0.00	0.00	0.00	0.00	0.00	0.00	0.00	0.00	0.00	0.00	0.00	0.00	0.00	0.00	0.00	0.00	0.00
Bacteria;__Actinobacteria;__Acidimicrobiia;__Acidimicrobiales;__OCS155_marine_group	0.03	0.03	0.02	0.01	0.01	0.00	0.00	0.01	0.00	0.00	0.01	0.00	0.02	0.00	0.03	0.00	0.00	0.01
Bacteria;__Actinobacteria;__Acidimicrobiia;__Acidimicrobiales;__Sva0996_marine_group	0.00	0.00	0.00	0.00	0.00	0.00	0.00	0.00	0.00	0.00	0.00	0.00	0.00	0.00	0.00	0.00	0.00	0.00
Bacteria;__Actinobacteria;__Acidimicrobiia;__Acidimicrobiales;__uncultured	0.00	0.00	0.00	0.00	0.00	0.00	0.00	0.00	0.00	0.00	0.00	0.00	0.00	0.00	0.01	0.00	0.00	0.00
Bacteria;__Actinobacteria;__Actinobacteria;Other;Other	0.00	0.00	0.00	0.00	0.00	0.00	0.00	0.00	0.00	0.00	0.00	0.00	0.00	0.00	0.00	0.00	0.00	0.00
Bacteria;__Actinobacteria;__Actinobacteria;__Corynebacteriales;__Corynebacteriaceae	0.00	0.00	0.00	0.00	0.00	0.00	0.00	0.00	0.00	0.00	0.00	0.00	0.00	0.00	0.00	0.00	0.00	0.00
Bacteria;__Actinobacteria;__Actinobacteria;__Frankiales;__Geodermatophilaceae	0.00	0.00	0.00	0.00	0.00	0.00	0.00	0.00	0.00	0.00	0.00	0.00	0.00	0.00	0.00	0.00	0.00	0.00
Bacteria;__Actinobacteria;__Actinobacteria;__Micrococcales;__Micrococcaceae	0.00	0.00	0.00	0.00	0.00	0.00	0.00	0.00	0.00	0.00	0.00	0.00	0.00	0.00	0.00	0.00	0.00	0.00
Bacteria;__Actinobacteria;__Actinobacteria;__Streptomycetales;__Streptomycetaceae	0.00	0.00	0.00	0.00	0.00	0.00	0.00	0.00	0.00	0.00	0.00	0.00	0.00	0.00	0.00	0.00	0.00	0.00
Bacteria;__Actinobacteria;__Coriobacteriia;__Coriobacteriales;__Coriobacteriaceae	0.00	0.00	0.00	0.00	0.00	0.00	0.00	0.00	0.00	0.00	0.00	0.00	0.00	0.00	0.00	0.00	0.00	0.00
Bacteria;__Actinobacteria;__KB1-LJY01;__o;__f	0.00	0.00	0.00	0.00	0.00	0.00	0.00	0.00	0.00	0.00	0.00	0.00	0.00	0.00	0.00	0.00	0.00	0.00
Bacteria;__Actinobacteria;__OPB41;__o;__f	0.00	0.00	0.00	0.01	0.00	0.01	0.01	0.01	0.02	0.01	0.00	0.00	0.00	0.00	0.01	0.00	0.00	0.00
Bacteria;__Actinobacteria;__Thermoleophilia;__Gaiellales;__Gaiellaceae	0.00	0.00	0.00	0.00	0.00	0.00	0.00	0.00	0.00	0.00	0.00	0.00	0.00	0.00	0.00	0.00	0.00	0.00
Bacteria;__Actinobacteria;__Thermoleophilia;__Gaiellales;__uncultured	0.00	0.00	0.00	0.00	0.00	0.00	0.00	0.00	0.00	0.00	0.00	0.00	0.00	0.00	0.00	0.00	0.00	0.00
Bacteria;__Actinobacteria;__Thermoleophilia;__Solirubrobacterales;Other	0.00	0.00	0.00	0.00	0.00	0.00	0.00	0.00	0.00	0.00	0.00	0.00	0.00	0.00	0.00	0.00	0.00	0.00
Bacteria;__Actinobacteria;__Thermoleophilia;__Solirubrobacterales;__0319-6M6	0.00	0.00	0.00	0.00	0.00	0.00	0.00	0.00	0.00	0.00	0.00	0.00	0.00	0.00	0.00	0.00	0.00	0.00
Bacteria;__Actinobacteria;__Thermoleophilia;__Solirubrobacterales;__288-2	0.00	0.00	0.00	0.00	0.00	0.00	0.00	0.00	0.00	0.00	0.00	0.00	0.00	0.00	0.00	0.00	0.00	0.00
Bacteria;__Actinobacteria;__Thermoleophilia;__Solirubrobacterales;__480-2	0.00	0.00	0.00	0.00	0.00	0.00	0.00	0.00	0.00	0.00	0.00	0.00	0.00	0.00	0.00	0.00	0.00	0.00
Bacteria;__Armatimonadetes;__c;__o;__f	0.00	0.00	0.00	0.00	0.00	0.00	0.00	0.00	0.00	0.00	0.00	0.00	0.00	0.00	0.00	0.00	0.00	0.00
Bacteria;__BD1-5;__c;__o;__f	0.00	0.00	0.00	0.00	0.00	0.00	0.00	0.00	0.00	0.00	0.00	0.00	0.00	0.00	0.00	0.00	0.00	0.00
Bacteria;__BHI80-139;__c;__o;__f	0.00	0.00	0.00	0.00	0.00	0.00	0.00	0.00	0.01	0.00	0.00	0.00	0.00	0.00	0.00	0.00	0.00	0.00
Bacteria;__Bacteroidetes;Other;Other;Other	0.02	0.02	0.01	0.00	0.00	0.00	0.00	0.00	0.00	0.00	0.02	0.01	0.01	0.00	0.01	0.00	0.00	0.01
Bacteria;__Bacteroidetes;__BD2-2;__o;__f	0.02	0.02	0.02	0.02	0.02	0.03	0.02	0.03	0.04	0.03	0.05	0.03	0.02	0.02	0.02	0.01	0.00	0.02
Bacteria;__Bacteroidetes;__Bacteroidia;__Bacteroidales;__Bacteroidaceae	0.00	0.00	0.00	0.00	0.00	0.00	0.00	0.00	0.00	0.00	0.00	0.00	0.00	0.00	0.00	0.00	0.00	0.00
Bacteria;__Bacteroidetes;__Bacteroidia;__Bacteroidales;__Marinilabiaceae	0.00	0.00	0.00	0.00	0.00	0.00	0.00	0.00	0.00	0.00	0.00	0.00	0.00	0.00	0.00	0.00	0.00	0.00
Bacteria;__Bacteroidetes;__Bacteroidia;__Bacteroidales;__Prevotellaceae	0.00	0.00	0.00	0.00	0.00	0.00	0.00	0.00	0.00	0.00	0.00	0.00	0.00	0.00	0.00	0.00	0.00	0.00
Bacteria;__Bacteroidetes;__Cytophagia;__Cytophagales;__Flammeovirgaceae	0.00	0.00	0.00	0.00	0.00	0.00	0.00	0.00	0.00	0.00	0.00	0.00	0.00	0.00	0.00	0.00	0.00	0.00
Bacteria;__Bacteroidetes;__Cytophagia;__Order_II_Incertae_Sedis;__Rhodothermaceae	0.00	0.00	0.00	0.00	0.00	0.00	0.00	0.00	0.00	0.00	0.00	0.00	0.00	0.00	0.00	0.00	0.00	0.00
Bacteria;__Bacteroidetes;__Flavobacteriia;__Flavobacteriales;__Cryomorphaceae	0.00	0.00	0.00	0.00	0.00	0.00	0.00	0.00	0.00	0.00	0.00	0.00	0.00	0.00	0.00	0.00	0.00	0.00
Bacteria;__Bacteroidetes;__Flavobacteriia;__Flavobacteriales;__Flavobacteriaceae	0.00	0.00	0.00	0.00	0.00	0.00	0.00	0.00	0.00	0.00	0.01	0.00	0.01	0.00	0.00	0.00	0.00	0.01
Bacteria;__Bacteroidetes;__SB-1;__o;__f	0.00	0.00	0.00	0.00	0.00	0.00	0.00	0.00	0.00	0.00	0.00	0.00	0.00	0.00	0.00	0.00	0.00	0.00
Bacteria;__Bacteroidetes;__SB-5;__o;__f	0.00	0.00	0.00	0.00	0.00	0.00	0.00	0.00	0.00	0.00	0.00	0.00	0.00	0.00	0.00	0.00	0.00	0.00
Bacteria;__Bacteroidetes;__Sphingobacteriia;__Sphingobacteriales;Other	0.00	0.00	0.00	0.00	0.00	0.00	0.00	0.00	0.00	0.00	0.00	0.00	0.00	0.00	0.00	0.00	0.00	0.00
Bacteria;__Bacteroidetes;__Sphingobacteriia;__Sphingobacteriales;__Chitinophagaceae	0.00	0.00	0.00	0.00	0.00	0.00	0.00	0.00	0.00	0.00	0.00	0.00	0.00	0.00	0.00	0.00	0.00	0.00
Bacteria;__Bacteroidetes;__Sphingobacteriia;__Sphingobacteriales;__E6aC02	0.00	0.00	0.00	0.00	0.00	0.00	0.00	0.00	0.00	0.00	0.00	0.00	0.00	0.00	0.00	0.00	0.00	0.00
Bacteria;__Bacteroidetes;__Sphingobacteriia;__Sphingobacteriales;__NS11-12_marine_group	0.00	0.00	0.00	0.00	0.00	0.00	0.00	0.00	0.00	0.00	0.00	0.00	0.00	0.00	0.00	0.00	0.00	0.00
Bacteria;__Bacteroidetes;__Sphingobacteriia;__Sphingobacteriales;__PHOS-HE51	0.00	0.00	0.00	0.00	0.00	0.00	0.00	0.00	0.00	0.00	0.00	0.00	0.00	0.00	0.00	0.00	0.00	0.00
Bacteria;__Bacteroidetes;__Sphingobacteriia;__Sphingobacteriales;__ST-12K33	0.00	0.00	0.00	0.00	0.00	0.00	0.00	0.00	0.00	0.00	0.00	0.00	0.00	0.00	0.00	0.00	0.00	0.00
Bacteria;__Bacteroidetes;__Sphingobacteriia;__Sphingobacteriales;__Saprospiraceae	0.00	0.00	0.00	0.00	0.00	0.00	0.00	0.00	0.00	0.00	0.00	0.00	0.00	0.00	0.00	0.00	0.00	0.00
Bacteria;__Bacteroidetes;__Sphingobacteriia;__Sphingobacteriales;__Sphingobacteriaceae	0.00	0.00	0.00	0.00	0.00	0.00	0.00	0.00	0.00	0.00	0.00	0.00	0.00	0.00	0.00	0.00	0.00	0.00
Bacteria;__Bacteroidetes;__Sphingobacteriia;__Sphingobacteriales;__WCHB1-69	0.01	0.02	0.01	0.01	0.02	0.04	0.03	0.02	0.03	0.02	0.03	0.00	0.01	0.01	0.00	0.00	0.00	0.00
Bacteria;__Bacteroidetes;__VC2.1_Bac22;__o;__f	0.01	0.01	0.01	0.00	0.00	0.00	0.00	0.00	0.00	0.00	0.00	0.00	0.00	0.00	0.00	0.00	0.00	0.00
Bacteria;__Bacteroidetes;__vadinHA17;__o;__f	0.00	0.00	0.00	0.00	0.00	0.00	0.00	0.00	0.00	0.00	0.00	0.00	0.00	0.00	0.00	0.00	0.00	0.00
Bacteria;__Caldiserica;__Caldisericia;__Caldisericales;__Caldisericaceae	0.00	0.00	0.00	0.00	0.00	0.00	0.00	0.00	0.00	0.00	0.00	0.00	0.00	0.00	0.00	0.00	0.00	0.00
Bacteria;__Caldiserica;__Caldisericia;__Caldisericales;__LF045	0.00	0.00	0.00	0.00	0.00	0.00	0.00	0.00	0.00	0.00	0.00	0.00	0.00	0.00	0.00	0.00	0.00	0.00
Bacteria;__Candidate_division_BRC1;__c;__o;__f	0.00	0.00	0.00	0.00	0.00	0.00	0.00	0.00	0.00	0.00	0.00	0.00	0.00	0.00	0.00	0.00	0.00	0.00
Bacteria;__Candidate_division_JS1;__c;__o;__f	0.03	0.06	0.10	0.19	0.16	0.15	0.19	0.18	0.21	0.15	0.01	0.24	0.00	0.23	0.02	0.25	0.06	0.05
Bacteria;__Candidate_division_OD1;__c;__o;__f	0.00	0.01	0.01	0.01	0.01	0.00	0.00	0.00	0.01	0.01	0.01	0.02	0.00	0.03	0.00	0.01	0.00	0.01
Bacteria;__Candidate_division_OP11;__c;__o;__f	0.00	0.00	0.00	0.00	0.00	0.00	0.00	0.00	0.00	0.00	0.00	0.00	0.00	0.00	0.00	0.00	0.00	0.00
Bacteria;__Candidate_division_OP3;__c;__o;__f	0.01	0.02	0.02	0.02	0.02	0.00	0.00	0.00	0.01	0.00	0.01	0.07	0.00	0.05	0.00	0.03	0.00	0.01
Bacteria;__Candidate_division_OP8;__c;__o;__f	0.00	0.01	0.01	0.01	0.01	0.02	0.02	0.03	0.02	0.02	0.01	0.00	0.00	0.00	0.01	0.01	0.00	0.01
Bacteria;__Candidate_division_SR1;__c;__o;__f	0.00	0.00	0.00	0.00	0.00	0.00	0.00	0.00	0.00	0.00	0.00	0.00	0.00	0.00	0.00	0.00	0.00	0.00
Bacteria;__Candidate_division_WS3;__c;__o;__f	0.01	0.01	0.01	0.02	0.02	0.02	0.02	0.02	0.02	0.02	0.01	0.01	0.01	0.01	0.01	0.01	0.00	0.01
Bacteria;__Chlamydiae;__Chlamydiia;__Chlamydiales;Other	0.00	0.00	0.00	0.00	0.00	0.00	0.00	0.00	0.00	0.00	0.00	0.00	0.00	0.00	0.00	0.00	0.00	0.00
Bacteria;__Chlamydiae;__Chlamydiae;__Chlamydiales;__Chlamydiaceae	0.00	0.00	0.00	0.00	0.00	0.00	0.00	0.00	0.00	0.00	0.00	0.00	0.00	0.00	0.00	0.00	0.00	0.00
Bacteria;__Chlamydiae;__Chlamydiae;__Chlamydiales;__Family_Incertae_Sedis	0.00	0.00	0.00	0.00	0.00	0.00	0.00	0.00	0.00	0.00	0.00	0.00	0.00	0.00	0.00	0.00	0.00	0.00
Bacteria;__Chlamydiae;__Chlamydiae;__Chlamydiales;__Parachlamydiaceae	0.00	0.00	0.00	0.00	0.00	0.00	0.00	0.00	0.00	0.00	0.00	0.00	0.00	0.00	0.00	0.00	0.00	0.00
Bacteria;__Chlamydiae;__Chlamydiae;__Chlamydiales;__Simkaniaceae	0.00	0.00	0.00	0.00	0.00	0.00	0.00	0.00	0.00	0.00	0.00	0.00	0.00	0.00	0.00	0.00	0.00	0.00
Bacteria;__Chlamydiae;__Chlamydiae;__Chlamydiales;__cvE6	0.00	0.00	0.00	0.00	0.00	0.00	0.00	0.00	0.00	0.00	0.00	0.00	0.00	0.00	0.00	0.00	0.00	0.00
Bacteria;__Chloroflexi;__Chloroflexia;__Chloroflexiales;__OPB56	0.00	0.00	0.00	0.00	0.00	0.00	0.00	0.00	0.00	0.00	0.00	0.00	0.00	0.00	0.00	0.00	0.00	0.00
Bacteria;__Chloroflexi;__Chloroflexia;__Chloroflexiales;__SJA-28	0.00	0.00	0.00	0.00	0.00	0.00	0.00	0.00	0.01	0.00	0.00	0.00	0.00	0.00	0.00	0.00	0.00	0.00
Bacteria;__Chloroflexi;__Ignavibacteria;__Ignavibacteriales;Other	0.00	0.00	0.00	0.00	0.00	0.00	0.00	0.00	0.00	0.00	0.00	0.00	0.00	0.00	0.00	0.00	0.00	0.00
Bacteria;__Chloroflexi;__Ignavibacteria;__Ignavibacteriales;__BSV26	0.00	0.00	0.00	0.00	0.00	0.00	0.00	0.00	0.00	0.00	0.00	0.00	0.00	0.00	0.00	0.00	0.00	0.00
Bacteria;__Chloroflexi;__Ignavibacteria;__Ignavibacteriales;__Ignavibacteriaceae	0.00	0.00	0.00	0.00	0.00	0.00	0.00	0.00	0.00	0.00	0.00	0.00	0.00	0.00	0.00	0.00	0.00	0.00
Bacteria;__Chloroflexi;__Ignavibacteria;__Ignavibacteriales;__InsB3-7	0.00	0.00	0.00	0.00	0.00	0.00	0.00	0.00	0.00	0.00	0.00	0.00	0.00	0.00	0.00	0.00	0.00	0.00
Bacteria;__Chloroflexi;__Ignavibacteria;__Ignavibacteriales;__PHOS-HE36	0.00	0.00	0.00	0.00	0.00	0.00	0.00	0.00	0.00	0.00	0.00	0.00	0.00	0.00	0.00	0.00	0.00	0.00
Bacteria;__Chloroflexi;Other;Other;Other	0.00	0.01	0.01	0.01	0.01	0.01	0.01	0.01	0.02	0.00	0.01	0.00	0.00	0.00	0.00	0.00	0.00	0.00
Bacteria;__Chloroflexi;__Anaerolineae;__Anaerolineales;__Anaerolineaceae	0.06	0.07	0.07	0.07	0.08	0.09	0.08	0.09	0.08	0.09	0.11	0.01	0.04	0.02	0.07	0.01	0.00	0.07
Bacteria;__Chloroflexi;__Caldilineae;__Caldilineales;__Caldilineaceae	0.01	0.01	0.01	0.00	0.00	0.00	0.00	0.00	0.00	0.00	0.00	0.00	0.00	0.00	0.00	0.00	0.00	0.00
Bacteria;__Chloroflexi;__Dehalococcoidia;Other;Other	0.00	0.00	0.00	0.02	0.01	0.00	0.00	0.00	0.01	0.01	0.00	0.00	0.00	0.00	0.00	0.01	0.00	0.00
Bacteria;__Chloroflexi;__Dehalococcoidia;__FS117-23B-02;__f	0.00	0.00	0.00	0.00	0.00	0.00	0.00	0.00	0.00	0.00	0.00	0.00	0.00	0.00	0.00	0.00	0.00	0.00
Bacteria;__Chloroflexi;__Dehalococcoidia;__FW22;__f	0.00	0.00	0.00	0.00	0.00	0.00	0.00	0.00	0.00	0.00	0.00	0.00	0.00	0.00	0.00	0.00	0.00	0.00

Supplementary Table 2-2. Bacterial iTAG sequence data, page 2 of 4. All data is post-processed according to the details given in the methods section.

Bacteria;__Chloroflexi;__Dehalococcoidia;__GIF3;__f	0.00	0.00	0.00	0.00	0.00	0.00	0.00	0.00	0.00	0.00	0.00	0.00	0.00	0.00	0.00	0.00	0.00	0.00	0.00
Bacteria;__Chloroflexi;__Dehalococcoidia;__GIF9;__f	0.00	0.00	0.00	0.00	0.00	0.00	0.00	0.00	0.00	0.00	0.00	0.00	0.00	0.00	0.00	0.00	0.00	0.00	0.00
Bacteria;__Chloroflexi;__Dehalococcoidia;__MSBL5;__f	0.00	0.00	0.00	0.00	0.00	0.00	0.00	0.00	0.00	0.00	0.00	0.00	0.00	0.00	0.00	0.00	0.00	0.00	0.00
Bacteria;__Chloroflexi;__Dehalococcoidia;__Napoli-4B-65;__f	0.00	0.00	0.00	0.00	0.00	0.00	0.00	0.00	0.00	0.00	0.00	0.00	0.00	0.00	0.00	0.00	0.00	0.00	0.00
Bacteria;__Chloroflexi;__Dehalococcoidia;__Sh765B-AG-111;__f	0.00	0.00	0.00	0.00	0.00	0.00	0.00	0.00	0.00	0.00	0.00	0.00	0.00	0.00	0.00	0.00	0.00	0.00	0.00
Bacteria;__Chloroflexi;__Dehalococcoidia;__vadinBA26;__f	0.00	0.00	0.00	0.00	0.00	0.00	0.00	0.00	0.00	0.00	0.00	0.00	0.00	0.00	0.00	0.00	0.00	0.00	0.00
Bacteria;__Chloroflexi;__JG30-KF-CM66;__o:__f	0.00	0.00	0.00	0.00	0.00	0.00	0.00	0.00	0.00	0.00	0.00	0.00	0.00	0.00	0.00	0.00	0.00	0.00	0.00
Bacteria;__Chloroflexi;__KD4-96;__o:__f	0.00	0.00	0.00	0.00	0.00	0.00	0.00	0.00	0.00	0.00	0.00	0.00	0.00	0.00	0.01	0.00	0.00	0.00	0.00
Bacteria;__Chloroflexi;__S085;__o:__f	0.00	0.00	0.00	0.00	0.00	0.00	0.00	0.00	0.00	0.00	0.00	0.00	0.00	0.00	0.00	0.00	0.00	0.00	0.00
Bacteria;__Chloroflexi;__SAR202_clade;__o:__f	0.00	0.00	0.00	0.00	0.00	0.00	0.00	0.00	0.00	0.00	0.00	0.00	0.00	0.00	0.00	0.00	0.00	0.00	0.00
Bacteria;__Chloroflexi;__TK10;__o:__f	0.00	0.00	0.00	0.00	0.00	0.00	0.00	0.00	0.00	0.00	0.00	0.00	0.00	0.00	0.00	0.00	0.00	0.00	0.00
Bacteria;__Chloroflexi;__Thermomicrobia;__AKYG1722;__f	0.00	0.00	0.00	0.00	0.00	0.00	0.00	0.00	0.00	0.00	0.00	0.00	0.00	0.00	0.00	0.00	0.00	0.00	0.00
Bacteria;__Cyanobacteria;__4C0d-2;__o:__f	0.00	0.00	0.00	0.00	0.00	0.00	0.00	0.00	0.00	0.00	0.00	0.00	0.00	0.00	0.00	0.00	0.00	0.00	0.00
Bacteria;__Cyanobacteria;__Chloroplast;__o:__f	0.00	0.00	0.00	0.00	0.00	0.00	0.00	0.00	0.00	0.00	0.00	0.00	0.00	0.00	0.00	0.00	0.00	0.00	0.00
Bacteria;__Cyanobacteria;__Cyanobacteria;__Subsection0;__Family0	0.00	0.00	0.00	0.00	0.00	0.00	0.00	0.00	0.00	0.00	0.00	0.00	0.00	0.00	0.00	0.00	0.00	0.00	0.00
Bacteria;__Cyanobacteria;__ML633J-21;__o:__f	0.00	0.00	0.00	0.00	0.00	0.00	0.00	0.00	0.00	0.00	0.00	0.00	0.00	0.00	0.00	0.00	0.00	0.00	0.00
Bacteria;__Cyanobacteria;__SHA-109;__o:__f	0.00	0.00	0.00	0.00	0.00	0.00	0.00	0.00	0.00	0.00	0.00	0.00	0.00	0.00	0.00	0.00	0.00	0.00	0.00
Bacteria;__Deferribacteres;__Deferribacteres;__Deferribacteres;__Family_Incertae_Sedis	0.01	0.01	0.01	0.01	0.01	0.03	0.01	0.01	0.01	0.01	0.01	0.00	0.01	0.00	0.01	0.00	0.00	0.01	0.00
Bacteria;__Deferribacteres;__Deferribacteres;__Deferribacteriales;__LCP-89	0.00	0.00	0.00	0.00	0.00	0.00	0.00	0.00	0.00	0.00	0.00	0.00	0.00	0.00	0.00	0.00	0.00	0.00	0.00
Bacteria;__Deferribacteres;__Deferribacteres;__Deferribacteriales;__PAUC34f	0.00	0.00	0.00	0.00	0.00	0.00	0.00	0.00	0.00	0.00	0.00	0.00	0.00	0.00	0.00	0.00	0.00	0.00	0.00
Bacteria;__Deferribacteres;__Deferribacteres;__Deferribacteriales;__SAR406_clade(Marine_group_A)	0.00	0.00	0.00	0.00	0.00	0.00	0.00	0.00	0.00	0.00	0.00	0.00	0.00	0.00	0.00	0.00	0.00	0.00	0.01
Bacteria;__Deinococcus-Thermus;__Deinococci;__KD3-62;__f	0.00	0.00	0.00	0.00	0.00	0.00	0.00	0.00	0.00	0.00	0.00	0.00	0.00	0.00	0.00	0.00	0.00	0.00	0.00
Bacteria;__Elusimicrobia;__Elusimicrobia;Other;Other	0.00	0.00	0.00	0.00	0.00	0.00	0.00	0.00	0.00	0.00	0.00	0.00	0.00	0.00	0.00	0.00	0.00	0.00	0.00
Bacteria;__Elusimicrobia;__Elusimicrobia;__Lineage_IIa;__f	0.00	0.00	0.00	0.00	0.00	0.00	0.00	0.00	0.00	0.00	0.00	0.00	0.00	0.00	0.00	0.00	0.00	0.00	0.00
Bacteria;__Elusimicrobia;__Elusimicrobia;__Lineage_IIb;__f	0.00	0.00	0.00	0.00	0.00	0.00	0.00	0.00	0.00	0.00	0.00	0.00	0.00	0.00	0.00	0.00	0.00	0.00	0.00
Bacteria;__Elusimicrobia;__Elusimicrobia;__Lineage_IIc;__f	0.00	0.00	0.00	0.00	0.00	0.00	0.00	0.00	0.00	0.00	0.00	0.00	0.00	0.00	0.00	0.00	0.00	0.00	0.00
Bacteria;__Elusimicrobia;__Elusimicrobia;__Lineage_IV;__f	0.00	0.00	0.00	0.00	0.00	0.00	0.00	0.00	0.00	0.00	0.00	0.00	0.00	0.00	0.00	0.00	0.00	0.00	0.00
Bacteria;__Elusimicrobia;__Elusimicrobia;__Lineage_I_(Endomicrobia);__f	0.00	0.00	0.00	0.00	0.00	0.00	0.00	0.00	0.00	0.00	0.00	0.00	0.00	0.00	0.00	0.00	0.00	0.00	0.00
Bacteria;__Elusimicrobia;__Elusimicrobia;__MD2894-B20;__f	0.00	0.00	0.00	0.00	0.00	0.00	0.00	0.00	0.00	0.00	0.00	0.00	0.00	0.00	0.00	0.00	0.00	0.00	0.00
Bacteria;__Elusimicrobia;__Elusimicrobia;__MVP-88;__f	0.00	0.00	0.00	0.00	0.00	0.00	0.00	0.00	0.00	0.00	0.00	0.00	0.00	0.00	0.00	0.00	0.00	0.00	0.00
Bacteria;__Elusimicrobia;__Elusimicrobia;__Rs-M47;__f	0.00	0.00	0.00	0.00	0.00	0.00	0.00	0.00	0.00	0.00	0.00	0.00	0.00	0.00	0.00	0.00	0.00	0.00	0.00
Bacteria;__Elusimicrobia;__Elusimicrobia;__o:__f	0.00	0.00	0.00	0.00	0.00	0.00	0.00	0.00	0.00	0.00	0.00	0.00	0.00	0.00	0.00	0.00	0.00	0.00	0.00
Bacteria;__Fibrobacteres;__Fibrobacteria;__Fibrobacterales;Other	0.00	0.00	0.00	0.00	0.00	0.00	0.00	0.00	0.00	0.00	0.00	0.00	0.00	0.00	0.00	0.00	0.00	0.00	0.00
Bacteria;__Fibrobacteres;__Fibrobacteria;__Fibrobacterales;__Fibrobacteraceae	0.00	0.00	0.00	0.00	0.00	0.00	0.00	0.00	0.00	0.00	0.00	0.00	0.00	0.00	0.00	0.00	0.00	0.00	0.00
Bacteria;__Fibrobacteres;__Fibrobacteria;__Fibrobacterales;__MAT-CR-H6-H10	0.00	0.00	0.00	0.00	0.00	0.00	0.00	0.00	0.00	0.00	0.00	0.00	0.00	0.00	0.00	0.00	0.00	0.00	0.00
Bacteria;__Fibrobacteres;__Fibrobacteria;__Order_Incertae_Sedis;__Family_Incertae_Sedis	0.00	0.00	0.00	0.00	0.00	0.00	0.00	0.00	0.00	0.00	0.00	0.00	0.00	0.00	0.00	0.00	0.00	0.00	0.00
Bacteria;__Fibrobacteres;__Fibrobacteria;__possible_order_07;__f	0.00	0.00	0.00	0.00	0.00	0.00	0.00	0.00	0.00	0.00	0.00	0.00	0.00	0.00	0.00	0.00	0.00	0.00	0.00
Bacteria;__Firmicutes;__Bacilli;__Bacillales;__Alicyclobacillaceae	0.00	0.00	0.00	0.00	0.00	0.00	0.00	0.00	0.00	0.00	0.00	0.00	0.00	0.00	0.00	0.00	0.00	0.00	0.00
Bacteria;__Firmicutes;__Bacilli;__Bacillales;__Bacillaceae	0.00	0.00	0.00	0.00	0.00	0.00	0.00	0.00	0.00	0.00	0.00	0.00	0.00	0.00	0.00	0.00	0.00	0.00	0.00
Bacteria;__Firmicutes;__Bacilli;__Bacillales;__Paenibacillaceae	0.00	0.00	0.00	0.00	0.00	0.00	0.00	0.00	0.00	0.00	0.00	0.00	0.00	0.00	0.00	0.00	0.00	0.00	0.00
Bacteria;__Firmicutes;__Bacilli;__Bacillales;__Staphylococcaceae	0.00	0.00	0.00	0.00	0.00	0.00	0.00	0.00	0.00	0.00	0.00	0.00	0.00	0.00	0.00	0.00	0.00	0.00	0.00
Bacteria;__Firmicutes;__Bacilli;__Lactobacillales;__Carnobacteriaceae	0.00	0.00	0.00	0.00	0.00	0.00	0.00	0.00	0.00	0.00	0.00	0.00	0.00	0.00	0.00	0.00	0.00	0.00	0.00
Bacteria;__Firmicutes;__Bacilli;__Lactobacillales;__Enterococcaceae	0.00	0.00	0.00	0.00	0.00	0.00	0.00	0.00	0.00	0.00	0.00	0.00	0.00	0.00	0.00	0.00	0.00	0.00	0.00
Bacteria;__Firmicutes;__Clostridia;__Clostridiales;Other	0.00	0.00	0.00	0.00	0.00	0.00	0.00	0.00	0.00	0.00	0.00	0.00	0.00	0.00	0.00	0.00	0.00	0.00	0.00
Bacteria;__Firmicutes;__Clostridia;__Clostridiales;__Christensenellaceae	0.00	0.00	0.00	0.00	0.00	0.00	0.00	0.00	0.00	0.00	0.00	0.00	0.00	0.00	0.00	0.00	0.00	0.00	0.00
Bacteria;__Firmicutes;__Clostridia;__Clostridiales;__Clostridiaceae	0.00	0.00	0.00	0.00	0.00	0.00	0.00	0.00	0.00	0.00	0.00	0.00	0.00	0.00	0.00	0.00	0.00	0.00	0.00
Bacteria;__Firmicutes;__Clostridia;__Clostridiales;__Eubacteriaceae	0.00	0.00	0.00	0.00	0.00	0.00	0.00	0.00	0.00	0.00	0.00	0.00	0.00	0.00	0.00	0.00	0.00	0.00	0.00
Bacteria;__Firmicutes;__Clostridia;__Clostridiales;__Family_Incertae_Sedis	0.00	0.00	0.00	0.00	0.00	0.00	0.00	0.00	0.00	0.00	0.00	0.00	0.00	0.00	0.00	0.00	0.00	0.00	0.00
Bacteria;__Firmicutes;__Clostridia;__Clostridiales;__Family_XIII_Incertae_Sedis	0.00	0.00	0.00	0.00	0.00	0.00	0.00	0.00	0.00	0.00	0.00	0.00	0.00	0.00	0.00	0.00	0.00	0.00	0.00
Bacteria;__Firmicutes;__Clostridia;__Clostridiales;__Family_XII_Incertae_Sedis	0.00	0.00	0.00	0.00	0.00	0.00	0.00	0.00	0.00	0.00	0.00	0.00	0.00	0.00	0.00	0.00	0.00	0.00	0.00
Bacteria;__Firmicutes;__Clostridia;__Clostridiales;__Lachnospiraceae	0.00	0.00	0.00	0.00	0.00	0.00	0.00	0.00	0.00	0.00	0.00	0.00	0.00	0.00	0.00	0.00	0.00	0.00	0.00
Bacteria;__Firmicutes;__Clostridia;__Clostridiales;__Peptococcaceae	0.00	0.00	0.00	0.00	0.00	0.00	0.00	0.00	0.00	0.00	0.00	0.00	0.00	0.00	0.00	0.00	0.00	0.00	0.00
Bacteria;__Firmicutes;__Clostridia;__Clostridiales;__Peptostreptococcaceae	0.00	0.00	0.00	0.00	0.00	0.00	0.00	0.00	0.00	0.00	0.00	0.00	0.00	0.00	0.00	0.00	0.00	0.00	0.00
Bacteria;__Firmicutes;__Clostridia;__Clostridiales;__Ruminococcaceae	0.00	0.00	0.00	0.00	0.00	0.00	0.00	0.00	0.00	0.00	0.00	0.00	0.00	0.00	0.00	0.00	0.00	0.00	0.00
Bacteria;__Firmicutes;__Clostridia;__Clostridiales;__Syntrophomonadaceae	0.00	0.00	0.00	0.00	0.00	0.00	0.00	0.00	0.00	0.00	0.00	0.00	0.00	0.00	0.00	0.00	0.00	0.00	0.00
Bacteria;__Firmicutes;__Clostridia;__Clostridiales;__vadinBB60	0.00	0.00	0.00	0.00	0.00	0.00	0.00	0.00	0.00	0.00	0.00	0.00	0.00	0.00	0.00	0.00	0.00	0.00	0.00
Bacteria;__Firmicutes;__Clostridia;__Halanaerobiales;__SHA2	0.00	0.00	0.00	0.00	0.00	0.00	0.00	0.00	0.00	0.00	0.00	0.00	0.00	0.00	0.00	0.00	0.00	0.00	0.00
Bacteria;__Fusobacteria;__Fusobacteriia;__Fusobacteriales;__Fusobacteriaceae	0.00	0.00	0.00	0.00	0.00	0.00	0.00	0.00	0.00	0.00	0.00	0.00	0.00	0.00	0.00	0.00	0.00	0.00	0.00
Bacteria;__Fusobacteria;__Fusobacteriia;__MSBL6;__f	0.00	0.00	0.00	0.00	0.00	0.00	0.00	0.00	0.00	0.00	0.00	0.00	0.00	0.01	0.00	0.01	0.00	0.00	0.00
Bacteria;__GOUTA4;__c:__o:__f	0.00	0.00	0.00	0.00	0.00	0.00	0.00	0.00	0.00	0.00	0.00	0.00	0.00	0.00	0.00	0.00	0.00	0.00	0.00
Bacteria;__Gemmatimonadetes;__Gemmatimonadetes;__BD2-11_terrestrial_group;__f	0.00	0.00	0.00	0.00	0.00	0.00	0.00	0.00	0.00	0.00	0.00	0.00	0.00	0.00	0.00	0.00	0.00	0.00	0.00
Bacteria;__Gemmatimonadetes;__Gemmatimonadetes;__Gemmatimonadales;__Gemmatimonadaceae	0.00	0.00	0.00	0.00	0.00	0.00	0.00	0.00	0.00	0.00	0.00	0.00	0.00	0.00	0.00	0.00	0.00	0.00	0.00
Bacteria;__Gemmatimonadetes;__Gemmatimonadetes;__PAUC43f_marine_benthic_group;__f	0.00	0.00	0.00	0.00	0.00	0.00	0.00	0.00	0.00	0.00	0.00	0.00	0.00	0.00	0.00	0.00	0.00	0.00	0.00
Bacteria;__Hyd24-12;__c:__o:__f	0.00	0.00	0.00	0.00	0.00	0.01	0.00	0.01	0.01	0.01	0.00	0.00	0.00	0.00	0.00	0.00	0.00	0.00	0.01
Bacteria;__JL-ETNP-Z39;__c:__o:__f	0.00	0.00	0.00	0.00	0.00	0.00	0.00	0.00	0.00	0.00	0.00	0.00	0.00	0.00	0.00	0.00	0.00	0.00	0.00
Bacteria;__Kazan-3B-28;__c:__o:__f	0.00	0.00	0.00	0.00	0.00	0.00	0.00	0.00	0.00	0.00	0.00	0.00	0.00	0.00	0.00	0.00	0.00	0.00	0.00
Bacteria;__Lentisphaerae;__Lentisphaeria;Other;Other	0.00	0.00	0.00	0.00	0.00	0.00	0.00	0.00	0.00	0.00	0.00	0.00	0.00	0.01	0.00	0.00	0.00	0.00	0.00
Bacteria;__Lentisphaerae;__Lentisphaeria;__113B434;__f	0.00	0.00	0.00	0.00	0.00	0.00	0.00	0.00	0.00	0.00	0.00	0.00	0.00	0.00	0.00	0.00	0.00	0.00	0.00
Bacteria;__Lentisphaerae;__Lentisphaeria;__BS5;__f	0.00	0.00	0.00	0.00	0.00	0.00	0.00	0.00	0.00	0.00	0.00	0.00	0.00	0.00	0.00	0.00	0.00	0.00	0.00
Bacteria;__Lentisphaerae;__Lentisphaeria;__LD1-PB3;__f	0.00	0.00	0.00	0.00	0.00	0.00	0.00	0.00	0.00	0.00	0.00	0.00	0.00	0.00	0.00	0.00	0.00	0.00	0.00
Bacteria;__Lentisphaerae;__Lentisphaeria;__Lentisphaerales;__Lentisphaeraceae	0.00	0.00	0.00	0.00	0.00	0.00	0.00	0.00	0.00	0.00	0.00	0.00	0.00	0.00	0.00	0.00	0.00	0.00	0.00
Bacteria;__Lentisphaerae;__Lentisphaeria;__MSBL3;__f	0.00	0.00	0.00	0.00	0.00	0.00	0.00	0.00	0.00	0.00	0.00	0.00	0.00	0.00	0.00	0.00	0.00	0.00	0.00
Bacteria;__Lentisphaerae;__Lentisphaeria;__R76-B128;__f	0.00	0.00	0.00	0.00	0.00	0.00	0.00	0.00	0.00	0.00	0.00	0.00	0.00	0.00	0.00	0.00	0.00	0.00	0.00
Bacteria;__Lentisphaerae;__Lentisphaeria;__RFP12_gut_group;__f	0.00	0.00	0.00	0.00	0.00	0.00	0.00	0.00	0.00	0.00	0.00	0.00	0.00	0.00	0.00	0.00	0.00	0.00	0.00
Bacteria;__Lentisphaerae;__Lentisphaeria;__Victivallales;__Victivallaceae	0.00	0.00	0.00	0.00	0.00	0.00	0.00	0.00	0.00	0.00	0.00	0.00	0.00	0.01	0.00	0.00	0.00	0.00	0.00
Bacteria;__Lentisphaerae;__Lentisphaeria;__WCHB1-41;__f	0.00	0.00	0.00	0.00	0.00	0.00	0.00	0.00	0.00	0.00	0.00	0.00	0.00	0.00	0.00	0.00	0.00	0.00	0.00
Bacteria;__MVP-21;__c:__o:__f	0.00	0.00	0.00	0.00	0.00	0.00	0.00	0.00	0.00	0.00	0.00	0.00	0.00	0.00	0.00	0.00	0.00	0.00	0.00
Bacteria;__NPL-UPA2;__c:__o:__f	0.00	0.00	0.00	0.00	0.00	0.00	0.00	0.00	0.00	0.00	0.00	0.00	0.00	0.00	0.00	0.00	0.00	0.00	0.00
Bacteria;__Nitrospirae;__Nitrospira;__Nitrospirales;__40296	0.00	0.00	0.01	0.00	0.00	0.00	0.00	0.00	0.00	0.00	0.00	0.00	0.00	0.00	0.02	0.00	0.01	0.00	0.00
Bacteria;__Nitrospirae;__Nitrospira;__Nitrospirales;__Nitrospiraceae	0.00	0.00	0.00	0.00	0.00	0.00	0.00	0.00	0.00	0.00	0.00	0.00	0.00	0.00	0.02	0.00	0.03	0.00	0.00
Bacteria;__Planctomycetes;__028H05-P-BN-P5;__o:__f	0.00	0.00	0.00	0.00	0.00	0.00	0.00	0.00	0.00	0.00	0.00	0.00	0.00	0.00	0.00	0.00	0.00	0.00	0.00
Bacteria;__Planctomycetes;__BD7-11;__o:__f	0.00	0.00	0.00	0.00	0.00	0.00	0.00	0.00	0.00	0.00	0.00	0.00	0.00	0.00	0.00	0.00	0.00	0.00	0.00
Bacteria;__Planctomycetes;__MBMPE71;__o:__f	0.00	0.00	0.00	0.00	0.00	0.00	0.00	0.00	0.00	0.00	0.00	0.00	0.00	0.00	0.00	0.00	0.00	0.00	0.00
Bacteria;__Planctomycetes;__MD2896-B258;__o:__f	0.00	0.00	0.00	0.00	0.00	0.00	0.00	0.00	0.00	0.00	0.00	0.00	0.00	0.00	0.00	0.00	0.00	0.00	0.00
Bacteria;__Planctomycetes;__OM190;__o:__f	0.00	0.00	0.00	0.00	0.00	0.00	0.00	0.00	0.00	0.00	0.00	0.00	0.00	0.01	0.00	0.00	0.00	0.00	0.00
Bacteria;__Planctomycetes;__Phycisphaerae;Other;Other	0.00	0.00	0.00	0.00	0.00	0.00	0.00	0.00	0.00	0.00	0.00	0.00	0.00	0.00	0.00	0.00	0.00	0.00	0.00
Bacteria;__Planctomycetes;__Phycisphaerae;__062D293_hypersaline_microbial_mat_group;__f	0.00	0.00	0.00	0.00	0.00	0.00	0.00	0.00	0.00	0.00	0.00	0.00	0.00	0.00	0.00	0.00	0.00	0.00	0.00
Bacteria;__Planctomycetes;__Phycisphaerae;__Amsterdam-1B-07;__f	0.00	0.00	0.00	0.00	0.00	0.00	0.00	0.00	0.00	0.00	0.00	0.00	0.00	0.00	0.00	0.00	0.00	0.00	0.00
Bacteria;__Planctomycetes;__Phycisphaerae;__C86;__f	0.00	0.00	0.00	0.00	0.00	0.00	0.00	0.00	0.00	0.00	0.00	0.00	0.00	0.00	0.00	0.00	0.00	0.00	0.00
Bacteria;__Planctomycetes;__Phycisphaerae;__CCM11a;__f	0.00	0.00	0.00	0.00	0.00	0.00	0.00	0.00	0.00	0.00	0.00	0.00	0.00	0.00	0.00	0.00	0.00	0.00	0.00
Bacteria;__Planctomycetes;__Phycisphaerae;__ML-A-10;__f	0.00	0.00	0.00	0.00	0.00	0.00	0.00	0.00	0.00	0.00	0.00	0.00	0.00	0.00	0.00	0.00	0.00	0.00	0.00
Bacteria;__Planctomycetes;__Phycisphaerae;__MSB-3A7_sediment_group;__f	0.00	0.00	0.00	0.00	0.00	0.00	0.00	0.00	0.00	0.00	0.00	0.00	0.00	0.00	0.00	0.00	0.00	0.00	0.00
Bacteria;__Planctomycetes;__Phycisphaerae;__MSBL9;__f	0.00	0.00	0.00	0.01	0.01	0.00	0.00	0.00	0.01	0.00	0.00	0.00	0.00	0.00	0.00	0.00	0.00	0.00	0.00
Bacteria;__Planctomycetes;__Phycisphaerae;__Phycisphaerales;Other	0.00	0.00	0.00	0.00	0.00	0.01	0.00	0.01	0.01	0.00	0.00	0.00	0.00	0.00	0.00	0.00	0.00	0.00	0.00
Bacteria;__Planctomycetes;__Phycisphaerae;__Phycisphaerales;__0BD2Z94_hypersaline_microbial_mat_group	0.00	0.00	0.00	0.00	0.00	0.00	0.00	0.00	0.00	0.00	0.00	0.00	0.00	0.00	0.00	0.00	0.00	0.00	0.00
Bacteria;__Planctomycetes;__Phycisphaerae;__Phycisphaerales;__AKAU3564_sediment_group	0.00	0.00	0.00	0.00	0.00	0.00	0.00	0.00	0.00	0.00	0.00	0.00	0.00	0.00	0.00	0.00	0.00	0.00	0.00
Bacteria;__Planctomycetes;__Phycisphaerae;__Phycisphaerales;__ODP1230B30.02_sediment_group	0.00	0.00	0.00	0.00	0.00	0.00	0.00	0.00	0.00	0.00	0.00	0.00	0.00	0.00	0.00	0.00	0.00	0.00	0.00
Bacteria;__Planctomycetes;__Phycisphaerae;__Phycisphaerales;__Phycisphaeraceae	0.00	0.00	0.00	0.00	0.00	0.00	0.00	0.00	0.00	0.00	0.00	0.00	0.00	0.00	0.00	0.00	0.00	0.00	0.00
Bacteria;__Planctomycetes;__Phycisphaerae;__Phycisphaerales;__SBY2-984	0.00	0.00	0.00	0.00	0.00	0.00	0.00	0.00	0.00	0.00	0.00	0.00	0.00	0.00	0.00	0.00	0.00	0.00	0.00
Bacteria;__Planctomycetes;__Phycisphaerae;__Pla1_lineage;__f	0.00	0.00	0.00	0.00	0.00	0.00	0.00	0.00	0.00	0.00	0.00	0.00	0.00	0.00	0.00	0.00	0.00	0.00	0.00
Bacteria;__Planctomycetes;__Phycisphaerae;__SHA-43;__f	0.00	0.00	0.00	0.00	0.00	0.00	0.00	0.00	0.00	0.00	0.00	0.00	0.00	0.00	0.00	0.00	0.00	0.00	0.00
Bacteria;__Planctomycetes;__Phycisphaerae;__mle1-8;__f	0.00	0.00	0.00	0.00	0.00	0.01	0.00	0.00	0.00	0.00	0.00	0.00	0.00	0.00	0.00	0.00	0.00	0.00	0.00
Bacteria;__Planctomycetes;__Pla3_lineage;__o:__f	0.00	0.00	0.00	0.00	0.00	0.00	0.00	0.00	0.00	0.00	0.00	0.00	0.00	0.00	0.00	0.00	0.00	0.00

Supplementary Table 2-3. Bacterial iTAG sequence data, page 3 of 4. All data is post-processed according to the details given in the methods section.

Bacteria;__Planctomycetes;__Pla4_lineage;__o;__f	0.00	0.00	0.00	0.00	0.00	0.00	0.00	0.00	0.00	0.00	0.00	0.00	0.00	0.00	0.00	0.00	0.00	0.00
Bacteria;__Planctomycetes;__Planctomycetacia;__Brocadiales;__Brocadiaceae	0.00	0.00	0.00	0.00	0.00	0.00	0.00	0.00	0.00	0.00	0.00	0.00	0.00	0.00	0.03	0.00	0.00	0.00
Bacteria;__Planctomycetes;__Planctomycetacia;__Planctomycetales;__Planctomycetaceae	0.01	0.01	0.00	0.00	0.00	0.00	0.00	0.00	0.00	0.00	0.00	0.01	0.00	0.01	0.00	0.01	0.00	0.00
Bacteria;__Planctomycetes;__SGST604;__o;__f	0.00	0.00	0.00	0.00	0.00	0.00	0.00	0.00	0.00	0.00	0.00	0.00	0.00	0.00	0.00	0.00	0.00	0.00
Bacteria;__Planctomycetes;__vadinHA49;__o;__f	0.00	0.00	0.00	0.00	0.00	0.00	0.00	0.00	0.00	0.00	0.00	0.00	0.00	0.00	0.00	0.00	0.00	0.00
Bacteria;__Proteobacteria;Other;Other;Other	0.00	0.00	0.00	0.00	0.00	0.00	0.00	0.00	0.00	0.00	0.00	0.00	0.00	0.00	0.00	0.00	0.02	0.01
Bacteria;__Proteobacteria;__AEGEAN-245;__o;__f	0.00	0.00	0.00	0.00	0.00	0.00	0.00	0.00	0.00	0.00	0.00	0.00	0.00	0.00	0.00	0.00	0.00	0.00
Bacteria;__Proteobacteria;__Alphaproteobacteria;Other;Other	0.00	0.00	0.00	0.00	0.00	0.00	0.00	0.00	0.00	0.00	0.00	0.00	0.00	0.02	0.00	0.00	0.03	0.01
Bacteria;__Proteobacteria;__Alphaproteobacteria;__Caulobacterales;__Hyphomonadaceae	0.00	0.00	0.00	0.00	0.00	0.00	0.00	0.00	0.00	0.00	0.00	0.00	0.00	0.00	0.00	0.00	0.00	0.00
Bacteria;__Proteobacteria;__Alphaproteobacteria;__DB1-14;__f	0.00	0.00	0.00	0.00	0.00	0.00	0.00	0.00	0.00	0.00	0.00	0.00	0.00	0.00	0.00	0.00	0.00	0.00
Bacteria;__Proteobacteria;__Alphaproteobacteria;__OCS116_clade;__f	0.00	0.00	0.00	0.00	0.00	0.00	0.00	0.00	0.00	0.00	0.00	0.00	0.00	0.00	0.00	0.00	0.00	0.00
Bacteria;__Proteobacteria;__Alphaproteobacteria;__Parvularculales;__Parvularculaceae	0.00	0.00	0.00	0.00	0.00	0.00	0.00	0.00	0.00	0.00	0.00	0.00	0.00	0.00	0.00	0.00	0.00	0.00
Bacteria;__Proteobacteria;__Alphaproteobacteria;__Rhizobiales;Other	0.00	0.00	0.00	0.00	0.00	0.00	0.00	0.00	0.00	0.00	0.00	0.00	0.00	0.00	0.00	0.00	0.01	0.00
Bacteria;__Proteobacteria;__Alphaproteobacteria;__Rhizobiales;__Bradyrhizobiaceae	0.00	0.00	0.00	0.00	0.00	0.00	0.00	0.00	0.00	0.00	0.00	0.00	0.00	0.00	0.00	0.00	0.00	0.00
Bacteria;__Proteobacteria;__Alphaproteobacteria;__Rhizobiales;__Brucellaceae	0.00	0.00	0.00	0.00	0.00	0.00	0.00	0.00	0.00	0.00	0.00	0.00	0.00	0.00	0.00	0.00	0.00	0.00
Bacteria;__Proteobacteria;__Alphaproteobacteria;__Rhizobiales;__Hyphomicrobiaceae	0.00	0.00	0.00	0.00	0.00	0.00	0.00	0.00	0.00	0.00	0.00	0.00	0.00	0.00	0.00	0.00	0.00	0.00
Bacteria;__Proteobacteria;__Alphaproteobacteria;__Rhizobiales;__Phyllobacteriaceae	0.00	0.00	0.00	0.00	0.00	0.00	0.00	0.00	0.00	0.00	0.00	0.00	0.01	0.00	0.01	0.00	0.01	0.00
Bacteria;__Proteobacteria;__Alphaproteobacteria;__Rhizobiales;__Rhizobiaceae	0.00	0.00	0.00	0.00	0.00	0.00	0.00	0.00	0.00	0.00	0.00	0.00	0.00	0.00	0.00	0.00	0.00	0.00
Bacteria;__Proteobacteria;__Alphaproteobacteria;__Rhizobiales;__Rhodobiaceae	0.00	0.00	0.00	0.00	0.00	0.00	0.00	0.00	0.00	0.00	0.00	0.00	0.00	0.01	0.00	0.00	0.00	0.00
Bacteria;__Proteobacteria;__Alphaproteobacteria;__Rhizobiales;__Xanthobacteraceae	0.00	0.00	0.00	0.00	0.00	0.00	0.00	0.00	0.00	0.00	0.00	0.00	0.00	0.00	0.00	0.00	0.00	0.00
Bacteria;__Proteobacteria;__Alphaproteobacteria;__Rhizobiales;__uncultured	0.00	0.00	0.00	0.00	0.00	0.00	0.00	0.00	0.00	0.00	0.00	0.00	0.00	0.00	0.00	0.00	0.00	0.00
Bacteria;__Proteobacteria;__Alphaproteobacteria;__Rhodobacterales;__Rhodobacteraceae	0.00	0.00	0.00	0.00	0.00	0.00	0.00	0.00	0.00	0.00	0.00	0.01	0.00	0.01	0.00	0.01	0.02	0.00
Bacteria;__Proteobacteria;__Alphaproteobacteria;__Rhodospirillales;Other	0.00	0.00	0.00	0.00	0.00	0.00	0.00	0.00	0.00	0.00	0.00	0.00	0.00	0.00	0.00	0.00	0.00	0.00
Bacteria;__Proteobacteria;__Alphaproteobacteria;__Rhodospirillales;__AT-s3-44	0.00	0.00	0.00	0.00	0.00	0.00	0.00	0.00	0.00	0.00	0.00	0.00	0.00	0.00	0.00	0.00	0.00	0.00
Bacteria;__Proteobacteria;__Alphaproteobacteria;__Rhodospirillales;__Acetobacteraceae	0.00	0.00	0.00	0.00	0.00	0.00	0.00	0.00	0.00	0.00	0.00	0.00	0.00	0.00	0.00	0.00	0.00	0.00
Bacteria;__Proteobacteria;__Alphaproteobacteria;__Rhodospirillales;__Rhodospirillaceae	0.00	0.00	0.00	0.00	0.00	0.01	0.00	0.00	0.00	0.00	0.00	0.00	0.00	0.04	0.00	0.04	0.00	0.00
Bacteria;__Proteobacteria;__Alphaproteobacteria;__Rickettsiales;Other	0.00	0.00	0.00	0.00	0.00	0.00	0.00	0.00	0.00	0.00	0.00	0.00	0.00	0.00	0.00	0.00	0.00	0.00
Bacteria;__Proteobacteria;__Alphaproteobacteria;__Rickettsiales;__Family_Incertae_Sedis	0.00	0.00	0.00	0.00	0.00	0.00	0.00	0.00	0.00	0.00	0.00	0.00	0.00	0.00	0.00	0.00	0.00	0.00
Bacteria;__Proteobacteria;__Alphaproteobacteria;__Rickettsiales;__Rickettsiaceae	0.00	0.00	0.00	0.00	0.00	0.00	0.00	0.00	0.00	0.00	0.00	0.00	0.00	0.00	0.00	0.01	0.00	0.00
Bacteria;__Proteobacteria;__Alphaproteobacteria;__Rickettsiales;__S25-593	0.00	0.00	0.00	0.00	0.00	0.00	0.00	0.00	0.00	0.00	0.00	0.00	0.00	0.00	0.00	0.00	0.00	0.00
Bacteria;__Proteobacteria;__Alphaproteobacteria;__Rickettsiales;__TK34	0.00	0.00	0.00	0.00	0.00	0.00	0.00	0.00	0.00	0.00	0.00	0.00	0.00	0.01	0.00	0.04	0.00	0.00
Bacteria;__Proteobacteria;__Alphaproteobacteria;__Rickettsiales;__mitochondria	0.00	0.00	0.00	0.00	0.00	0.00	0.00	0.00	0.00	0.00	0.00	0.00	0.00	0.00	0.00	0.00	0.00	0.00
Bacteria;__Proteobacteria;__Alphaproteobacteria;__SB1-18;__f	0.00	0.00	0.00	0.00	0.00	0.00	0.00	0.00	0.00	0.00	0.00	0.00	0.00	0.00	0.00	0.00	0.00	0.00
Bacteria;__Proteobacteria;__Alphaproteobacteria;__Sphingomonadales;__Erythrobacteraceae	0.00	0.00	0.00	0.00	0.00	0.00	0.00	0.00	0.00	0.00	0.00	0.00	0.00	0.00	0.00	0.00	0.00	0.00
Bacteria;__Proteobacteria;__Alphaproteobacteria;__Sphingomonadales;__Sphingomonadaceae	0.00	0.00	0.00	0.00	0.00	0.00	0.00	0.00	0.00	0.00	0.00	0.00	0.00	0.00	0.00	0.00	0.00	0.00
Bacteria;__Proteobacteria;__Betaproteobacteria;__Burkholderiales;__Burkholderiaceae	0.00	0.00	0.00	0.00	0.00	0.00	0.00	0.00	0.00	0.00	0.00	0.00	0.00	0.00	0.00	0.00	0.00	0.00
Bacteria;__Proteobacteria;__Betaproteobacteria;__Burkholderiales;__Comamonadaceae	0.00	0.00	0.00	0.00	0.00	0.00	0.00	0.00	0.00	0.00	0.00	0.00	0.00	0.00	0.00	0.00	0.00	0.00
Bacteria;__Proteobacteria;__Betaproteobacteria;__Burkholderiales;__Oxalobacteraceae	0.00	0.00	0.00	0.00	0.00	0.00	0.00	0.00	0.00	0.00	0.00	0.00	0.00	0.00	0.00	0.01	0.00	0.00
Bacteria;__Proteobacteria;__Betaproteobacteria;__Hydrogenophilales;__Hydrogenophilaceae	0.00	0.00	0.00	0.00	0.00	0.00	0.00	0.00	0.00	0.00	0.00	0.00	0.00	0.00	0.00	0.00	0.00	0.00
Bacteria;__Proteobacteria;__Betaproteobacteria;__Nitrosomonadales;__Nitrosomonadaceae	0.00	0.00	0.00	0.00	0.00	0.00	0.00	0.00	0.00	0.00	0.00	0.00	0.00	0.00	0.00	0.00	0.00	0.00
Bacteria;__Proteobacteria;__Deltaproteobacteria;Other;Other	0.00	0.00	0.00	0.00	0.00	0.00	0.00	0.00	0.00	0.00	0.00	0.00	0.00	0.00	0.00	0.00	0.01	0.00
Bacteria;__Proteobacteria;__Deltaproteobacteria;__43F-1404R;__f	0.00	0.00	0.00	0.00	0.00	0.00	0.00	0.00	0.00	0.00	0.00	0.00	0.00	0.00	0.00	0.00	0.00	0.00
Bacteria;__Proteobacteria;__Deltaproteobacteria;__Bdellovibrionales;__Bacteriovoracaceae	0.00	0.00	0.00	0.00	0.00	0.00	0.00	0.00	0.00	0.00	0.00	0.01	0.00	0.00	0.00	0.00	0.00	0.00
Bacteria;__Proteobacteria;__Deltaproteobacteria;__Bdellovibrionales;__Bdellovibrionaceae	0.00	0.00	0.00	0.00	0.00	0.00	0.00	0.00	0.00	0.00	0.00	0.00	0.00	0.00	0.00	0.00	0.00	0.00
Bacteria;__Proteobacteria;__Deltaproteobacteria;__DTB120;__f	0.00	0.00	0.00	0.00	0.00	0.00	0.00	0.00	0.00	0.00	0.00	0.00	0.00	0.01	0.00	0.00	0.02	0.00
Bacteria;__Proteobacteria;__Deltaproteobacteria;__Desulfarculales;__Desulfarculaceae	0.03	0.03	0.03	0.03	0.04	0.06	0.05	0.03	0.03	0.03	0.03	0.01	0.02	0.01	0.03	0.00	0.00	0.02
Bacteria;__Proteobacteria;__Deltaproteobacteria;__Desulfobacterales;Other	0.00	0.00	0.00	0.00	0.00	0.00	0.00	0.00	0.00	0.00	0.00	0.00	0.00	0.00	0.00	0.00	0.00	0.00
Bacteria;__Proteobacteria;__Deltaproteobacteria;__Desulfobacterales;__Desulfobacteraceae	0.08	0.10	0.15	0.19	0.20	0.15	0.23	0.23	0.28	0.34	0.17	0.40	0.11	0.44	0.10	0.54	0.03	0.15
Bacteria;__Proteobacteria;__Deltaproteobacteria;__Desulfobacterales;__Desulfobulbaceae	0.08	0.08	0.10	0.09	0.12	0.19	0.14	0.10	0.06	0.08	0.15	0.05	0.10	0.02	0.18	0.02	0.03	0.19
Bacteria;__Proteobacteria;__Deltaproteobacteria;__Nitrospinaceae	0.00	0.00	0.01	0.00	0.00	0.01	0.01	0.00	0.00	0.00	0.00	0.00	0.00	0.00	0.00	0.00	0.00	0.00
Bacteria;__Proteobacteria;__Deltaproteobacteria;__Desulfovibrionales;Other	0.00	0.00	0.00	0.00	0.00	0.00	0.00	0.00	0.00	0.00	0.00	0.00	0.00	0.00	0.00	0.00	0.00	0.00
Bacteria;__Proteobacteria;__Deltaproteobacteria;__Desulfovibrionales;__Desulfovibrionaceae	0.00	0.00	0.00	0.00	0.00	0.00	0.00	0.00	0.00	0.00	0.00	0.00	0.00	0.00	0.00	0.00	0.00	0.00
Bacteria;__Proteobacteria;__Deltaproteobacteria;__Desulfurellales;__Desulfurellaceae	0.00	0.00	0.00	0.00	0.00	0.00	0.00	0.00	0.01	0.00	0.00	0.00	0.00	0.00	0.00	0.00	0.00	0.00
Bacteria;__Proteobacteria;__Deltaproteobacteria;__Desulfuromonadales;Other	0.00	0.00	0.00	0.00	0.00	0.00	0.00	0.00	0.00	0.00	0.00	0.00	0.00	0.00	0.00	0.00	0.00	0.00
Bacteria;__Proteobacteria;__Deltaproteobacteria;__Desulfuromonadales;__Desulfuromonadaceae	0.00	0.00	0.00	0.00	0.00	0.00	0.00	0.00	0.00	0.00	0.00	0.00	0.00	0.00	0.00	0.00	0.00	0.00
Bacteria;__Proteobacteria;__Deltaproteobacteria;__Desulfuromonadales;__GR-WP33-58	0.00	0.00	0.00	0.00	0.00	0.00	0.00	0.00	0.00	0.00	0.00	0.00	0.00	0.00	0.00	0.00	0.00	0.00
Bacteria;__Proteobacteria;__Deltaproteobacteria;__Desulfuromonadales;__Geobacteraceae	0.00	0.00	0.00	0.00	0.00	0.00	0.00	0.00	0.00	0.00	0.00	0.00	0.00	0.00	0.00	0.00	0.00	0.00
Bacteria;__Proteobacteria;__Deltaproteobacteria;__Desulfuromonadales;__Sva1033	0.00	0.00	0.00	0.00	0.00	0.00	0.00	0.00	0.00	0.00	0.00	0.01	0.00	0.00	0.00	0.00	0.00	0.00
Bacteria;__Proteobacteria;__Deltaproteobacteria;__f	0.00	0.00	0.00	0.00	0.00	0.00	0.00	0.00	0.00	0.00	0.00	0.00	0.00	0.00	0.00	0.00	0.00	0.00
Bacteria;__Proteobacteria;__Deltaproteobacteria;__FW113;__f	0.00	0.00	0.00	0.00	0.00	0.00	0.00	0.00	0.00	0.00	0.00	0.00	0.00	0.00	0.00	0.00	0.00	0.00
Bacteria;__Proteobacteria;__Deltaproteobacteria;__GR-WP33-30;__f	0.00	0.00	0.00	0.00	0.00	0.00	0.00	0.00	0.00	0.00	0.00	0.00	0.00	0.00	0.00	0.00	0.00	0.00
Bacteria;__Proteobacteria;__Deltaproteobacteria;__Myxococcales;Other	0.00	0.00	0.00	0.00	0.00	0.00	0.00	0.00	0.00	0.00	0.00	0.01	0.00	0.00	0.00	0.00	0.00	0.00
Bacteria;__Proteobacteria;__Deltaproteobacteria;__Myxococcales;__0319-6G20	0.00	0.00	0.00	0.00	0.00	0.00	0.00	0.00	0.00	0.00	0.00	0.00	0.00	0.00	0.00	0.00	0.00	0.00
Bacteria;__Proteobacteria;__Deltaproteobacteria;__Myxococcales;__Haliangiaceae	0.00	0.00	0.00	0.00	0.00	0.00	0.00	0.00	0.00	0.00	0.00	0.00	0.00	0.00	0.00	0.00	0.01	0.00
Bacteria;__Proteobacteria;__Deltaproteobacteria;__Myxococcales;__Nannocystaceae	0.00	0.00	0.00	0.00	0.00	0.00	0.00	0.00	0.00	0.00	0.00	0.00	0.00	0.00	0.00	0.00	0.00	0.00
Bacteria;__Proteobacteria;__Deltaproteobacteria;__Myxococcales;__Phaselicystidaceae	0.00	0.00	0.00	0.00	0.00	0.00	0.00	0.00	0.00	0.00	0.00	0.00	0.00	0.00	0.00	0.00	0.00	0.00
Bacteria;__Proteobacteria;__Deltaproteobacteria;__Myxococcales;__Polyangiaceae	0.00	0.00	0.00	0.00	0.00	0.00	0.00	0.00	0.00	0.00	0.00	0.00	0.00	0.00	0.00	0.00	0.00	0.00
Bacteria;__Proteobacteria;__Deltaproteobacteria;__Myxococcales;__Sandaracinaceae	0.00	0.00	0.00	0.00	0.00	0.00	0.00	0.00	0.00	0.00	0.01	0.00	0.02	0.00	0.00	0.00	0.01	0.00
Bacteria;__Proteobacteria;__Deltaproteobacteria;__Myxococcales;__VHS-B3-70	0.00	0.00	0.00	0.00	0.00	0.00	0.00	0.00	0.00	0.00	0.00	0.00	0.00	0.00	0.00	0.00	0.00	0.00
Bacteria;__Proteobacteria;__Deltaproteobacteria;__uncultured	0.00	0.00	0.00	0.00	0.00	0.00	0.00	0.00	0.00	0.00	0.00	0.00	0.00	0.00	0.00	0.00	0.01	0.01
Bacteria;__Proteobacteria;__Deltaproteobacteria;__SAR324_clade(Marine_group_B);__f	0.00	0.00	0.00	0.00	0.00	0.00	0.00	0.00	0.00	0.00	0.00	0.00	0.00	0.00	0.00	0.00	0.01	0.00
Bacteria;__Proteobacteria;__Deltaproteobacteria;__Sh765B-TzT-29;__f	0.00	0.00	0.00	0.00	0.00	0.00	0.00	0.00	0.00	0.00	0.00	0.02	0.00	0.00	0.00	0.00	0.01	0.00
Bacteria;__Proteobacteria;__Deltaproteobacteria;__Sva0485;__f	0.00	0.00	0.00	0.00	0.00	0.00	0.00	0.00	0.00	0.00	0.00	0.01	0.00	0.00	0.00	0.00	0.00	0.00
Bacteria;__Proteobacteria;__Deltaproteobacteria;__Syntrophobacterales;Other	0.00	0.00	0.00	0.00	0.00	0.00	0.00	0.00	0.00	0.00	0.00	0.00	0.00	0.00	0.00	0.00	0.00	0.00
Bacteria;__Proteobacteria;__Deltaproteobacteria;__Syntrophobacterales;__Syntrophaceae	0.00	0.00	0.00	0.01	0.01	0.00	0.00	0.00	0.01	0.01	0.00	0.00	0.00	0.01	0.00	0.00	0.00	0.00
Bacteria;__Proteobacteria;__Deltaproteobacteria;__Syntrophobacterales;__Syntrophobacteraceae	0.00	0.00	0.00	0.00	0.00	0.00	0.00	0.00	0.00	0.00	0.00	0.00	0.00	0.01	0.00	0.00	0.00	0.00
Bacteria;__Proteobacteria;__Epsilonproteobacteria;__Campylobacterales;Other	0.00	0.00	0.00	0.00	0.00	0.00	0.00	0.00	0.00	0.00	0.00	0.00	0.00	0.00	0.00	0.00	0.00	0.00
Bacteria;__Proteobacteria;__Epsilonproteobacteria;__Campylobacterales;__Campylobacteraceae	0.00	0.00	0.00	0.00	0.00	0.00	0.00	0.00	0.00	0.00	0.01	0.00	0.00	0.00	0.00	0.00	0.00	0.02
Bacteria;__Proteobacteria;__Epsilonproteobacteria;__Campylobacterales;__Helicobacteraceae	0.29	0.21	0.18	0.10	0.10	0.02	0.03	0.07	0.01	0.01	0.13	0.03	0.22	0.01	0.02	0.01	0.01	0.17
Bacteria;__Proteobacteria;__Gammaproteobacteria;__Alteromonadales;__Alteromonadaceae	0.00	0.00	0.00	0.00	0.00	0.00	0.00	0.00	0.00	0.00	0.00	0.01	0.00	0.00	0.00	0.00	0.00	0.00
Bacteria;__Proteobacteria;__Gammaproteobacteria;__Alteromonadales;__Colwelliaceae	0.00	0.00	0.00	0.00	0.00	0.00	0.00	0.00	0.00	0.00	0.00	0.00	0.00	0.00	0.00	0.00	0.00	0.00
Bacteria;__Proteobacteria;__Gammaproteobacteria;__Alteromonadales;__Idiomarinaceae	0.00	0.00	0.00	0.00	0.00	0.00	0.00	0.00	0.00	0.00	0.00	0.00	0.00	0.00	0.00	0.00	0.00	0.00
Bacteria;__Proteobacteria;__Gammaproteobacteria;__Alteromonadales;__Pseudoalteromonadaceae	0.00	0.00	0.00	0.00	0.00	0.00	0.00	0.00	0.00	0.00	0.00	0.00	0.00	0.00	0.00	0.00	0.00	0.00
Bacteria;__Proteobacteria;__Gammaproteobacteria;__Alteromonadales;__Psychromonadaceae	0.00	0.00	0.00	0.00	0.00	0.00	0.00	0.00	0.00	0.00	0.00	0.00	0.00	0.00	0.00	0.00	0.00	0.00
Bacteria;__Proteobacteria;__Gammaproteobacteria;__Alteromonadales;__Shewanellaceae	0.00	0.00	0.00	0.00	0.00	0.00	0.00	0.00	0.00	0.00	0.00	0.00	0.00	0.00	0.00	0.00	0.00	0.00
Bacteria;__Proteobacteria;__Gammaproteobacteria;__BD7-8_marine_group;__f	0.00	0.00	0.00	0.00	0.00	0.00	0.00	0.00	0.00	0.00	0.00	0.01	0.00	0.00	0.00	0.00	0.00	0.00
Bacteria;__Proteobacteria;__Gammaproteobacteria;__CS-B046;__f	0.01	0.01	0.01	0.00	0.00	0.00	0.00	0.00	0.00	0.00	0.00	0.00	0.00	0.00	0.00	0.00	0.00	0.00
Bacteria;__Proteobacteria;__Gammaproteobacteria;__Chromatiales;__Chromatiaceae	0.00	0.00	0.00	0.00	0.00	0.00	0.00	0.00	0.00	0.00	0.00	0.00	0.00	0.00	0.00	0.00	0.00	0.00
Bacteria;__Proteobacteria;__Gammaproteobacteria;__Chromatiales;__Chromatiaceae	0.00	0.00	0.00	0.00	0.00	0.00	0.00	0.00	0.00	0.00	0.00	0.00	0.00	0.00	0.00	0.00	0.00	0.00
Bacteria;__Proteobacteria;__Gammaproteobacteria;__Chromatiales;__Ectothiorhodospiraceae	0.01	0.00	0.00	0.00	0.00	0.00	0.00	0.00	0.00	0.00	0.00	0.00	0.00	0.00	0.00	0.00	0.00	0.00
Bacteria;__Proteobacteria;__Gammaproteobacteria;__E01-9C-26_marine_group;__f	0.00	0.00	0.00	0.00	0.00	0.00	0.00	0.00	0.00	0.00	0.00	0.00	0.00	0.00	0.00	0.00	0.00	0.00
Bacteria;__Proteobacteria;__Gammaproteobacteria;__EC3;__f	0.00	0.00	0.00	0.00	0.00	0.00	0.00	0.00	0.00	0.00	0.00	0.00	0.00	0.00	0.00	0.00	0.00	0.00
Bacteria;__Proteobacteria;__Gammaproteobacteria;__HOC36;__f	0.00	0.00	0.00	0.00	0.00	0.00	0.00	0.00	0.00	0.00	0.00	0.00	0.00	0.00	0.00	0.00	0.00	0.00
Bacteria;__Proteobacteria;__Gammaproteobacteria;__KB5A_clade;__f	0.00	0.00	0.00	0.00	0.00	0.00	0.00	0.00	0.00	0.00	0.00	0.00	0.00	0.00	0.00	0.00	0.00	0.00
Bacteria;__Proteobacteria;__Gammaproteobacteria;__Legionellales;__Coxiellaceae	0.00	0.00	0.00	0.00	0.00	0.00	0.00	0.00	0.00	0.00	0.00	0.00	0.00	0.00	0.00	0.00	0.00	0.00
Bacteria;__Proteobacteria;__Gammaproteobacteria;__Methylococcales;Other	0.00	0.00	0.00	0.00	0.00	0.00	0.00	0.00	0.00	0.00	0.00	0.01	0.00	0.00	0.00	0.05	0.00	0.00
Bacteria;__Proteobacteria;__Gammaproteobacteria;__Methylococcales;__Marine_Methylotrophic_Group_1	0.00	0.00	0.00	0.00	0.00	0.00	0.00	0.00	0.00	0.00	0.00	0.00	0.00	0.00	0.00	0.00	0.00	0.00
Bacteria;__Proteobacteria;__Gammaproteobacteria;__Methylococcales;__Marine_Methylotrophic_Group_2	0.00	0.00	0.00	0.00	0.00	0.00	0.00	0.00	0.00	0.00	0.00	0.00	0.00	0.02	0.00	0.05	0.00	0.00
Bacteria;__Proteobacteria;__Gammaproteobacteria;__Methylococcales;__Methylococcaceae	0.00	0.00	0.00	0.00	0.00	0.00	0.00	0.00	0.00	0.00	0.00	0.00	0.00	0.00	0.00	0.00	0.00	0.00
Bacteria;__Proteobacteria;__Gammaproteobacteria;__NKB5;__f	0.00	0.00	0.00	0.00	0.00	0.00	0.00	0.00	0.00	0.00	0.00	0.00	0.00	0.00	0.00	0.00	0.00	0.00
Bacteria;__Proteobacteria;__Gammaproteobacteria;__Oceanospirillales;Other	0.00	0.00	0.00	0.00	0.00	0.00	0.00	0.00	0.00	0.00	0.00	0.00	0.00	0.00	0.00	0.00	0.00	0.00
Bacteria;__Proteobacteria;__Gammaproteobacteria;__Oceanospirillales;__Alcanivoracaceae	0.00	0.00	0.00	0.00	0.00	0.00	0.00	0.00	0.00	0.00	0.00	0.00	0.00	0.00	0.00	0.00	0.00	0.00
Bacteria;__Proteobacteria;__Gammaproteobacteria;__Oceanospirillales;__MBAE14	0.00	0.00	0.00	0.00	0.00	0.00	0.00	0.00	0.00	0.00	0.00	0.00	0.00	0.00	0.00	0.00	0.00	0.00

Supplementary Table 2-4. Bacterial iTAG sequence data, page 4 of 4. All data is post-processed according to the details given in the methods section.

Bacteria;__Proteobacteria;__Gammaproteobacteria;__Oceanospirillales;__OM182_clade	0.00	0.00	0.00	0.00	0.00	0.00	0.00	0.00	0.00	0.00	0.00	0.00	0.00	0.00	0.00	0.00	0.00	0.00
Bacteria;__Proteobacteria;__Gammaproteobacteria;__Oceanospirillales;__Oceanospirillaceae	0.00	0.00	0.00	0.00	0.00	0.00	0.00	0.00	0.00	0.00	0.00	0.00	0.00	0.00	0.00	0.00	0.00	0.00
Bacteria;__Proteobacteria;__Gammaproteobacteria;__Oceanospirillales;__SUP05_cluster	0.00	0.00	0.00	0.00	0.00	0.00	0.00	0.00	0.00	0.00	0.00	0.00	0.00	0.00	0.00	0.00	0.00	0.00
Bacteria;__Proteobacteria;__Gammaproteobacteria;__Order_Incertae_Sedis;__Family_Incertae_Sedis	0.01	0.01	0.01	0.00	0.00	0.01	0.00	0.00	0.00	0.00	0.01	0.00	0.03	0.00	0.24	0.00	0.28	0.01
Bacteria;__Proteobacteria;__Gammaproteobacteria;__Pseudomonadales;__Moraxellaceae	0.00	0.00	0.00	0.00	0.00	0.00	0.00	0.00	0.00	0.00	0.00	0.00	0.00	0.00	0.00	0.00	0.00	0.00
Bacteria;__Proteobacteria;__Gammaproteobacteria;__Sva0071;__f	0.01	0.01	0.00	0.00	0.00	0.00	0.00	0.00	0.00	0.00	0.00	0.00	0.01	0.00	0.00	0.00	0.00	0.00
Bacteria;__Proteobacteria;__Gammaproteobacteria;__Thiotrichales;__Piscirickettsiaceae	0.01	0.01	0.00	0.00	0.00	0.00	0.00	0.00	0.00	0.00	0.00	0.00	0.01	0.00	0.01	0.00	0.01	0.01
Bacteria;__Proteobacteria;__Gammaproteobacteria;__Thiotrichales;__Thiotrichaceae	0.01	0.02	0.01	0.00	0.01	0.00	0.00	0.00	0.00	0.00	0.00	0.01	0.01	0.00	0.01	0.00	0.07	0.00
Bacteria;__Proteobacteria;__Gammaproteobacteria;__Vibrionales;__Vibrionaceae	0.00	0.00	0.00	0.00	0.00	0.00	0.00	0.00	0.00	0.00	0.00	0.00	0.00	0.00	0.00	0.00	0.00	0.00
Bacteria;__Proteobacteria;__Gammaproteobacteria;__Xanthomonadales;Other	0.00	0.00	0.00	0.00	0.00	0.00	0.00	0.00	0.00	0.00	0.00	0.00	0.00	0.00	0.00	0.00	0.00	0.00
Bacteria;__Proteobacteria;__Gammaproteobacteria;__Xanthomonadales;__JTB255_marine_benthic_group	0.00	0.00	0.00	0.00	0.00	0.00	0.00	0.00	0.00	0.00	0.00	0.00	0.02	0.00	0.01	0.00	0.03	0.00
Bacteria;__Proteobacteria;__Gammaproteobacteria;__Xanthomonadales;__uncultured	0.00	0.00	0.00	0.00	0.00	0.00	0.00	0.00	0.00	0.00	0.00	0.00	0.00	0.00	0.00	0.00	0.00	0.00
Bacteria;__Proteobacteria;__JTB23;__o;__f	0.00	0.00	0.00	0.00	0.00	0.00	0.00	0.00	0.00	0.00	0.00	0.00	0.00	0.00	0.00	0.00	0.00	0.00
Bacteria;__Proteobacteria;__Milano-WF1B-44;__o;__f	0.08	0.07	0.04	0.01	0.01	0.00	0.00	0.01	0.00	0.00	0.00	0.00	0.00	0.00	0.00	0.00	0.00	0.00
Bacteria;__Proteobacteria;__TA18;__o;__f	0.00	0.00	0.00	0.00	0.00	0.00	0.00	0.00	0.00	0.00	0.00	0.00	0.00	0.00	0.00	0.00	0.00	0.00
Bacteria;__Proteobacteria;__Zetaproteobacteria;__Mariprofundales;__Mariprofundaceae	0.00	0.00	0.00	0.00	0.00	0.00	0.00	0.00	0.00	0.00	0.00	0.00	0.00	0.00	0.00	0.00	0.00	0.00
Bacteria;__Proteobacteria;__pltb-vmat-80;__o;__f	0.00	0.00	0.00	0.00	0.00	0.00	0.00	0.00	0.00	0.00	0.00	0.00	0.00	0.00	0.00	0.00	0.00	0.00
Bacteria;__RF3;__c;__o;__f	0.00	0.00	0.00	0.00	0.00	0.00	0.00	0.00	0.00	0.00	0.00	0.00	0.00	0.00	0.00	0.00	0.00	0.00
Bacteria;__Spirochaetae;__Spirochaetes;__Kazan-3B-09;__f	0.00	0.00	0.00	0.00	0.00	0.00	0.00	0.00	0.00	0.00	0.00	0.00	0.00	0.00	0.00	0.00	0.00	0.00
Bacteria;__Spirochaetae;__Spirochaetes;__MSBL2;__f	0.00	0.00	0.00	0.00	0.00	0.00	0.00	0.00	0.01	0.00	0.00	0.00	0.00	0.00	0.00	0.00	0.00	0.00
Bacteria;__Spirochaetae;__Spirochaetes;__Spirochaetales;__Brevinemataceae	0.00	0.00	0.00	0.00	0.00	0.00	0.00	0.00	0.00	0.00	0.00	0.00	0.00	0.00	0.00	0.00	0.00	0.00
Bacteria;__Spirochaetae;__Spirochaetes;__Spirochaetales;__LNH41	0.00	0.00	0.00	0.00	0.00	0.00	0.00	0.00	0.00	0.00	0.00	0.00	0.00	0.00	0.00	0.00	0.00	0.00
Bacteria;__Spirochaetae;__Spirochaetes;__Spirochaetales;__Leptospiraceae	0.00	0.00	0.00	0.00	0.00	0.00	0.00	0.00	0.00	0.00	0.00	0.00	0.00	0.00	0.00	0.00	0.00	0.00
Bacteria;__Spirochaetae;__Spirochaetes;__Spirochaetales;__PL-11B10	0.00	0.00	0.00	0.00	0.00	0.00	0.00	0.00	0.00	0.00	0.00	0.00	0.00	0.00	0.00	0.00	0.00	0.00
Bacteria;__Spirochaetae;__Spirochaetes;__Spirochaetales;__Spirochaetaceae	0.01	0.01	0.02	0.02	0.02	0.02	0.01	0.02	0.02	0.01	0.03	0.02	0.01	0.01	0.02	0.02	0.05	0.02
Bacteria;__Spirochaetae;__Spirochaetes;__Spirochaetales;__V2072-189E03	0.00	0.00	0.00	0.00	0.00	0.00	0.00	0.00	0.00	0.00	0.00	0.00	0.00	0.00	0.00	0.00	0.00	0.00
Bacteria;__TA06;__c;__o;__f	0.01	0.01	0.01	0.02	0.02	0.03	0.03	0.04	0.02	0.02	0.01	0.03	0.00	0.02	0.01	0.02	0.00	0.01
Bacteria;__TM6;__c;__o;__f	0.00	0.00	0.00	0.01	0.00	0.00	0.00	0.00	0.01	0.00	0.00	0.01	0.00	0.01	0.01	0.01	0.00	0.00
Bacteria;__Verrucomicrobia;__OPB35_soil_group;__o;__f	0.00	0.00	0.00	0.00	0.00	0.00	0.00	0.00	0.00	0.00	0.00	0.00	0.00	0.00	0.00	0.00	0.00	0.00
Bacteria;__Verrucomicrobia;__Opitutae;Other;Other	0.00	0.00	0.00	0.00	0.00	0.00	0.00	0.00	0.00	0.00	0.00	0.00	0.00	0.00	0.00	0.00	0.00	0.00
Bacteria;__Verrucomicrobia;__Opitutae;__Opitutales;__Opitutaceae	0.00	0.00	0.00	0.00	0.00	0.00	0.00	0.00	0.00	0.00	0.00	0.00	0.00	0.00	0.00	0.00	0.00	0.00
Bacteria;__Verrucomicrobia;__Opitutae;__Puniceicoccales;__Puniceicoccaceae	0.00	0.00	0.00	0.00	0.00	0.00	0.00	0.00	0.00	0.00	0.00	0.00	0.00	0.00	0.00	0.00	0.00	0.00
Bacteria;__Verrucomicrobia;__Verrucomicrobiae;__Verrucomicrobiales;Other	0.00	0.00	0.00	0.00	0.00	0.00	0.00	0.00	0.00	0.00	0.00	0.00	0.00	0.00	0.00	0.00	0.00	0.00
Bacteria;__Verrucomicrobia;__Verrucomicrobiae;__Verrucomicrobiales;__DEV007	0.00	0.00	0.00	0.00	0.00	0.00	0.00	0.00	0.00	0.00	0.00	0.00	0.00	0.00	0.00	0.00	0.00	0.00
Bacteria;__Verrucomicrobia;__Verrucomicrobiae;__Verrucomicrobiales;__Rubritaleaceae	0.00	0.00	0.00	0.00	0.00	0.00	0.00	0.00	0.00	0.00	0.00	0.00	0.00	0.00	0.00	0.00	0.00	0.00
Bacteria;__Verrucomicrobia;__Verrucomicrobiae;__Verrucomicrobiales;__Verrucomicrobiaceae	0.00	0.00	0.00	0.00	0.00	0.00	0.00	0.00	0.00	0.00	0.00	0.00	0.00	0.00	0.00	0.00	0.00	0.00
Bacteria;__WCHB1-60;__c;__o;__f	0.00	0.00	0.00	0.00	0.00	0.00	0.00	0.00	0.00	0.00	0.00	0.00	0.00	0.00	0.00	0.00	0.00	0.00

1.11 SUPPLEMENTAL MATERIAL: FIGURES

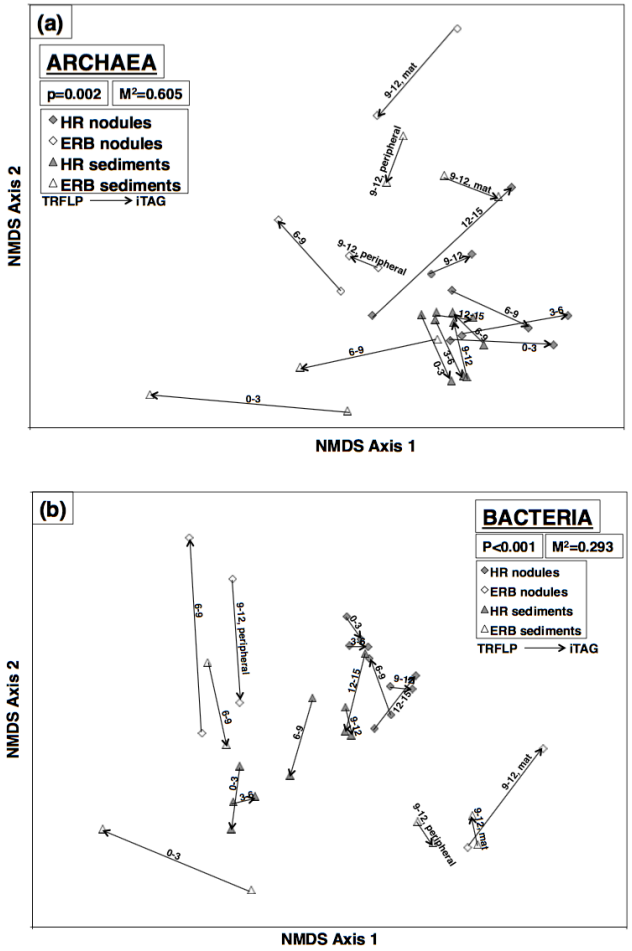

Supplementary Figure 1. Procrustes comparison of sample relationships between the iTAG and TRFLP datasets, for (a) archaea and (b) bacteria. iTAG ordination coordinates (see Figure 2 in main text) were used as the reference, against which TRFLP coordinates were transformed by translation, rotation, reflection, and/or scaling to minimize distance to the iTAG datapoints. The purpose was to test the closeness of fit between the two sets of datapoints, and therefore infer whether the biological similarity trends in iTAG and TRFLP data support one another. The analysis was completed 1,000 times and the resulting M^2 and p-values are given on the plot. Lower M^2 values indicate better closeness of fit between the datasets, and range from a possible value of 0 to 1. Lower p-values indicate stronger statistical support as determined through repeated iterations. Among the bacterial dataset, the p- and M^2-values indicate decent closeness of fit between the overall iTAG and TRFLP datasets. Among the archaeal dataset, the M^2 value is not particularly good, but NMDS biological patterns nonetheless appear to be largely maintained. As seen in the plots, some samples clearly fit more closely than others (that is, two points connected by a shorter arrow). Arrows are meant to help the reader connect iTAG and TRFLP ordination points from the same sample, to determine whether iTAG and TRFLP datasets demonstrate similar biological similarity trends. Arrows always point from the TRFLP to the iTAG point, since TRFLP coordinates were transformed to minimize distance to iTAG points. One archaeal sample (ERB clam core 0-3 cmbsf nodule) was excluded from analysis because it was substantially different than all other samples and skewed the ordination beyond possible interpretation.

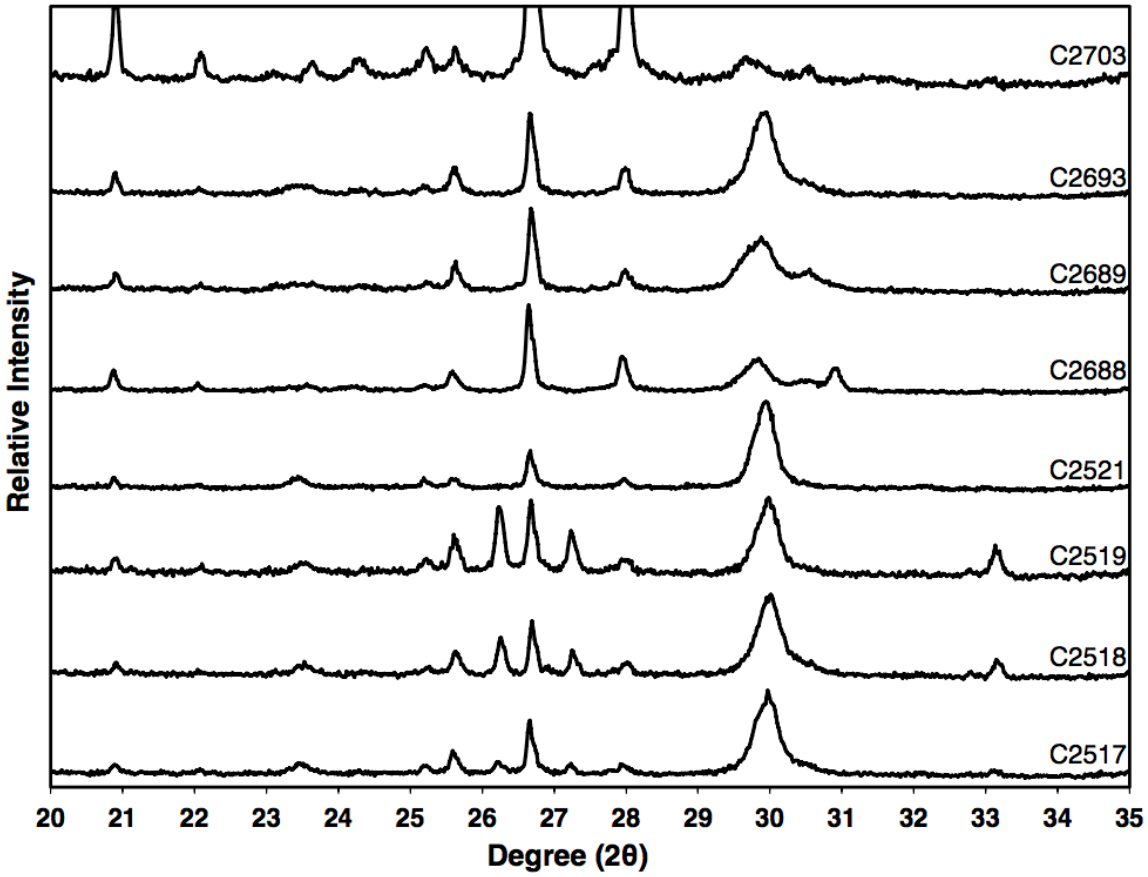

Supplementary Figure 2. XRD spectra from nodules in this study. Mineralogical assignments were made based on the (104) peak heights of calcite, Mg-calcite and dolomite, and the (111) peak height of aragonite. Nodule C2520 was not measured due to lack of material. For display in this figure, data from C2703 was amplified 5*x* in order to more clearly display the carbonate peaks at circa 30˚ 2θ.

1.12 REFERENCES

Aloisi, G., I. Bouloubassi, S. K. Heijs, R. D. Pancost, C. Pierre, J. S. Sinninghe Damsté, J. C. Gottschal, L. J. Forney, and J.-M. Rouchy. 2002. CH4-consuming microorganisms and the formation of carbonate crusts at cold seeps. Earth and Planetary Science Letters **203**: 195–203.

Aronesty, E. 2011. ea-utils: Command-line tools for processing biological sequencing data.

Ashelford, K. E., N. A. Chuzhanova, J. C. Fry, A. J. Jones, and A. J. Weightman. 2005. At Least 1 in 20 16S rRNA Sequence Records Currently Held in Public Repositories Is Estimated To Contain Substantial Anomalies. Applied and Environmental Microbiology **71**: 7724–7736.

Ashelford, K. E., N. A. Chuzhanova, J. C. Fry, A. J. Jones, and A. J. Weightman. 2006. New Screening Software Shows that Most Recent Large 16S rRNA Gene Clone Libraries Contain Chimeras. Applied and Environmental Microbiology **72**: 5734–5741.

Bailey, J. V., T. D. Raub, A. N. Meckler, B. K. Harrison, T. M. D. Raub, A. M. Green, and V. J. Orphan. 2010. Pseudofossils in relict methane seep carbonates resemble endemic microbial consortia. Palaeogeography, Palaeoclimatology, Palaeoecology **285**: 131–142.

Barry, J. P., H. Gary Greene, D. L. Orange, C. H. Baxter, B. H. Robison, R. E. Kochevar, J. W. Nybakken, D. L. R, and C. M. McHugh. 1996. Biologic and geologic characteristics of cold seeps in Monterey Bay, California. Deep Sea Research Part I: Oceanographic Research Papers **43**: 1739–1762.

Barry, J. P., R. E. Kochevar, and C. H. Baxter. 1997. The influence of pore-water chemistry and physiology on the distribution of vesicomyid clams at cold seeps in Monterey Bay: Implications for patterns of chemosynthetic community organization. Limnology and Oceanography **42**: 318–328.

Bayon, G., S. Dupré, E. Ponzevera, J. Etoubleau, S. Chéron, C. Pierre, J. Mascle, A. Boetius, and G. J. de Lange. 2013. Formation of carbonate chimneys in the Mediterranean Sea linked to deep-water oxygen depletion. Nature Geoscience **6**: 1–6.

Berry, D., K. Ben Mahfoudh, M. Wagner, and A. Loy. 2011. Barcoded Primers Used in Multiplex Amplicon Pyrosequencing Bias Amplification. Applied and Environmental Microbiology **77**: 7846–7849.

Birgel, D., M. Elvert, X. Han, and J. Peckmann. 2008a. ^{13}C-depleted biphytanic diacids as tracers of past anaerobic oxidation of methane. Organic geochemistry **39**: 152–156.

Birgel, D., T. Himmler, A. Freiwald, and J. Peckmann. 2008b. A new constraint on the antiquity of anaerobic oxidation of methane: Late Pennsylvanian seep limestones from southern Namibia. Geology **36**: 543–546.

Boetius, A., and E. Suess. 2004. Hydrate Ridge: a natural laboratory for the study of microbial life fueled by methane from near-surface gas hydrates. Chemical Geology **205**: 291–310.

Boetius, A., K. Ravenschlag, C. J. Schubert, D. Rickert, F. Widdel, A. Gieseke, R. Amann, B. B. Jørgensen, U. Witte, and O. Pfannkuche. 2000. A marine microbial consortium apparently mediating anaerobic oxidation of methane. Nature **407**: 623–626.

Bohrmann, G., J. Greinert, E. Suess, and M. Torres. 1998. Authigenic carbonates from the Cascadia subduction zone and their relation to gas hydrate stability. Geology **26**: 647.

Campbell, K. A., C. S. Nelson, A. C. Alfaro, S. Boyd, J. Greinert, S. Nyman, E. Grosjean, G. A. Logan, M. R. Gregory, S. Cooke, P. Linke, S. Milloy, and I. Wallis. 2010. Geological imprint of methane seepage on the seabed and biota of the convergent Hikurangi Margin, New Zealand: Box core and grab carbonate results. Marine Geology **272**: 285–306.

Caporaso, J. G., C. L. Lauber, W. A. Walters, D. Berg-Lyons, C. A. Lozupone, P. J. Turnbaugh, N. Fierer, and R. Knight. 2011. Global patterns of 16S rRNA diversity at a depth of millions of sequences per sample. Proceedings of the National Academy of Sciences **108**: 4516–4522.

Caporaso, J. G., C. L. Lauber, W. A. Walters, D. Berg-Lyons, J. Huntley, N. Fierer, S. M.

Owens, J. Betley, L. Fraser, M. Bauer, N. Gormley, J. A. Gilbert, G. Smith, and R. Knight. 2012. Ultra-high-throughput microbial community analysis on the Illumina HiSeq and MiSeq platforms. The ISME Journal **6**: 1621–1624.

Caporaso, J. G., J. Kuczynski, J. Stombaugh, K. Bittinger, F. D. Bushman, E. K. Costello, N. Fierer, A. G. Peña, J. K. Goodrich, J. I. Gordon, G. A. Huttley, S. T. Kelley, D. Knights, J. E. Koenig, R. E. Ley, C. A. Lozupone, D. McDonald, B. D. Muegge, M. Pirrung, J. Reeder, J. R. Sevinsky, P. J. Turnbaugh, W. A. Walters, J. Widmann, T. Yatsunenko, J. Zaneveld, and R. Knight. 2010. QIIME allows analysis of high-throughput community sequencing data. Nature Methods **7**: 335–336.

Chen, Z., W. Yan, M. Chen, S. Wang, J. Lu, F. Zhang, R. Xiang, S. Xiao, P. Yan, and S. Gu. 2006. Discovery of seep carbonate nodules as new evidence for gas venting on the northern continental slope of South China Sea. Chinese Science Bulletin **51**: 1228–1237.

Clarke, K. R., and R. M. Warwick. 2001. Change in Marine Communities, 2nd ed. PRIMER-E Ltd.

Edgar, R. C. 2010. Search and clustering orders of magnitude faster than BLAST. Bioinformatics **26**: 2460–2461.

Edgar, R. C., B. J. Haas, J. C. Clemente, C. Quince, and R. Knight. 2011. UCHIME improves sensitivity and speed of chimera detection. Bioinformatics **27**: 2194–2200.

Fischer, D., H. Sahling, K. Nöthen, G. Bohrmann, and S. Kasten. 2012. Interaction between hydrocarbon seepage, chemosynthetic communities, and bottom water redox at cold seeps of the Makran accretionary prism: insights from habitat-specific pore water sampling and modeling. Biogeosciences **9**: 2013–2031.

Gieskes, J. M., T. Gamo, and H. Brumsack. 1991. Chemical methods for interstitial water analysis aboard JOIDES Resolution. Ocean Drilling Program Texas A&M University.

Gieskes, J., C. Mahn, S. Day, J. Martin, J. Greinert, T. Rathburn, and B. McAdoo. 2005. A study of the chemistry of pore fluids and authigenic carbonates in methane seep environments: Kodiak Trench, Hydrate Ridge, Monterey Bay, and Eel River Basin. Chemical Geology **220**: 329–345.

Gilbert, J. A., F. Meyer, J. Jansson, J. Gordon, N. R. Pace, J. M. Tiedje, R. E. Ley, N. Fierer, D. Field, N. C. Kyrpides, F. O. Gloeckner, H. P. Klenk, K. E. Wommack, E. Glass, K. Docherty, R. Gallery, R. Stevens, and R. Knight. 2011. The Earth Microbiome Project: Meeting report of the "1st EMP meeting on sample selection and acquisition" at Argonne National Laboratory October 6th 2010. 1–5.

Goffredi, S. K., R. Wilpiszeski, R. Lee, and V. J. Orphan. 2008. Temporal evolution of methane cycling and phylogenetic diversity of archaea in sediments from a deep-sea whale-fall in Monterey Canyon, California. The ISME Journal **2**: 204–220.

Green-Saxena, A., A. E. Dekas, N. F. Dalleska, and V. J. Orphan. 2014. Nitrate-based niche differentiation by distinct sulfate-reducing bacteria involved in the anaerobic oxidation of methane. The ISME Journal **8**: 150–163.

Greinert, J., G. Bohrmann, and E. Suess. 2001. Gas Hydrate-Associated Carbonates and Methane-Venting at Hydrate Ridge: Classification, Distribution, and Origin of Authigenic Lithologies, p. 99–113. *In* C.K. Paull and W.P. Dillon [eds.], Natural Gas Hydrates. American Geophysical Union.

Griffiths, R. P., B. A. Caldwell, J. D. Cline, W. A. Broich, and R. Y. Morita. 1982. Field Observations of Methane Concentrations and Oxidation Rates in the Southeastern Bering Sea. Applied and Environmental Microbiology **44**: 435–446.

Guan, H., Y. Sun, X. Zhu, S. Mao, D. Feng, N. Wu, and D. Chen. 2013. Factors controlling the types of microbial consortia in cold-seep environments: A molecular and isotopic investigation of authigenic carbonates from the South China Sea. Chemical Geology **354**: 55–64.

Gulin, S. B., G. G. Polikarpov, and V. N. Egorov. 2003. The age of microbial carbonate

structures grown at methane seeps in the Black Sea with an implication of dating of the seeping methane. Marine Chemistry **84**: 67–72.

Haas, A., J. Peckmann, M. Elvert, H. Sahling, and G. Bohrmann. 2010. Patterns of carbonate authigenesis at the Kouilou pockmarks on the Congo deep-sea fan. Marine Geology **268**: 129–136.

Heijs, S. K., G. Aloisi, I. Bouloubassi, R. D. Pancost, C. Pierre, J. S. Sinninghe Damsté, J. C. Gottschal, J. D. Elsas, and L. J. Forney. 2006. Microbial Community Structure in Three Deep-Sea Carbonate Crusts. Microbial Ecology **52**: 451–462.

Heijs, S. K., J. S. Sinninghe Damsté, and L. J. Forney. 2005. Characterization of a deep-sea microbial mat from an active cold seep at the Milano mud volcano in the Eastern Mediterranean Sea. FEMS Microbiology Ecology **54**: 47–56.

Hoehler, T. M., M. J. Alperin, D. B. Albert, and C. S. Martens. 1994. Field and laboratory studies of methane oxidation in an anoxic marine sediment: Evidence for a methanogen-sulfate reducer consortium. Global Biogeochemical Cycles **8**: 451.

Hovland, M., M. R. Talbot, H. Qvale, S. Olaussen, and L. Aasberg. 1987. Methane-related Carbonate Cements in Pockmarks of the North Sea. Journal of Sedimentary Petrology **57**: 881–892.

Ijiri, A., U. Tsunogai, T. Gamo, F. Nakagawa, T. Sakamoto, and S. Saito. 2009. Enrichment of adsorbed methane in authigenic carbonate concretions of the Japan Trench. Geo-Marine Letters **29**: 301–308.

Inagaki, F., K. Takai, H. Kobayashi, K. H. Nealson, and K. Horikoshi. 2003. Sulfurimonas autotrophica gen. nov., sp. nov., a novel sulfur-oxidizing ε-proteobacterium isolated from hydrothermal sediments in the Mid-Okinawa Trough. Int J Syst Evol Microbiol **53**: 1801–1805.

Inagaki, F., K. Takai, K. H. Nealson, and K. Horikoshi. 2004. Sulfurovum lithotrophicum gen. nov., sp. nov., a novel sulfur-oxidizing chemolithoautotroph within the ε-Proteobacteria isolated from Okinawa Trough hydrothermal sediments. Int J Syst Evol Microbiol **54**: 1477–1482.

Jørgensen, N. O. 1989. Holocene methane-derived, dolomite-cemented sandstone pillars from the Kattegat, Denmark. Marine Geology **88**: 71–81.

Jørgensen, N. O. 1992. Methane-derived carbonate cementation of marine sediments from the Kattegat, Denmark: Geochemical and geological evidence. Marine Geology **103**: 1–13.

Kendall, M. M., G. D. Wardlaw, C. F. Tang, A. S. Bonin, Y. Liu, and D. L. Valentine. 2007. Diversity of Archaea in Marine Sediments from Skan Bay, Alaska, Including Cultivated Methanogens, and Description of Methanogenium boonei sp. nov. Applied and Environmental Microbiology **73**: 407–414.

Knittel, K., T. Lösekann, A. Boetius, R. Kort, and R. Amann. 2005. Diversity and Distribution of Methanotrophic Archaea at Cold Seeps. Applied and Environmental Microbiology **71**: 467–479.

Kodama, Y., and K. Watanabe. 2003. Isolation and Characterization of a Sulfur-Oxidizing Chemolithotroph Growing on Crude Oil under Anaerobic Conditions. Applied and Environmental Microbiology **69**: 107–112.

Krause, S., V. Liebetrau, S. Gorb, M. Sanchez-Roman, J. A. McKenzie, and T. Treude. 2012. Microbial nucleation of Mg-rich dolomite in exopolymeric substances under anoxic modern seawater salinity: New insight into an old enigma. Geology **40**: 587–590.

Kutterolf, S., V. Liebetrau, T. Mörz, A. Freundt, T. Hammerich, and D. Garbe-Schönberg. 2008. Lifetime and cyclicity of fluid venting at forearc mound structures determined by tephrostratigraphy and radiometric dating of authigenic carbonates. Geology **36**: 707–710.

Lein, A. 2004. Authigenic carbonate formation in the ocean. Lithology and Mineral Resources **39**: 1–30.

Levin, L. A. 2005. Ecology of cold seep sediments: Interactions of fauna with flow, chemistry, and

microbes. Oceanography and Marine Biology: An Annual Review **43**: 1–46.

Liebetrau, V., A. Eisenhauer, and P. Linke. 2010. Cold seep carbonates and associated cold-water corals at the Hikurangi Margin, New Zealand: New insights into fluid pathways, growth structures and geochronology. Marine Geology **272**: 307–318.

Lloyd, K. G., D. B. Albert, J. F. Biddle, J. P. Chanton, O. Pizarro, and A. Teske. 2010. Spatial Structure and Activity of Sedimentary Microbial Communities Underlying a Beggiatoa spp. Mat in a Gulf of Mexico Hydrocarbon Seep. PLoS ONE **5**: e8738.

Ludwig, W., O. Strunk, R. Westram, L. Richter, H. Meier, Yadhukumar, A. Buchner, T. Lai, S. Steppi, G. Jobb, W. Förster, I. Brettske, S. Gerber, A. W. Ginhart, O. Gross, S. Grumann, S. Hermann, R. Jost, A. König, T. Liss, R. Lüßmann, M. May, B. Nonhoff, B. Reichel, R. Strehlow, A. Stamatakis, N. Stuckmann, A. Vilbig, M. Lenke, T. Ludwig, A. Bode, and K.-H. Schleifer. 2004. ARB: a software environment for sequence data. Nucl. Acids Res. **32**: 1363–1371.

Luff, R., and K. Wallmann. 2003. Fluid flow, methane fluxes, carbonate precipitation and biogeochemical turnover in gas hydrate-bearing sediments at Hydrate Ridge, Cascadia Margin: numerical modeling and mass balances. Geochimica et Cosmochimica Acta **67**: 3403–3421.

Luff, R., K. Wallmann, and G. Aloisi. 2004. Numerical modeling of carbonate crust formation at cold vent sites: significance for fluid and methane budgets and chemosynthetic biological communities. Earth and Planetary Science Letters **221**: 337–353.

Marlow, J. J., J. A. Steele, W. Ziebis, A. R. Thurber, L. A. Levin, and V. J. Orphan. 2014a. Carbonate-hosted methanotrophy represents an unrecognized methane sink in the deep sea. Nature Communications **5**: 1–12.

Marlow, J., J. A. Steele, D. Case, S. A. Connon, L. A. Levin, and V. J. Orphan. 2014b. Microbial abundance and diversity patterns associated with sediments and carbonates from the methane seep environments of Hydrate Ridge, OR. Frontiers in Marine Science **1**: 1–16.

McCune, B., J. B. Grace, and D. L. Urban. 2002. Analysis of ecological communities, MjM Software Design.

Michaelis, W., R. Seifert, K. Nauhaus, T. Treude, V. Thiel, M. Blumenberg, K. Knittel, A. Gieseke, K. Peterknecht, T. Pape, A. Boetius, R. Amann, B. B. Jørgensen, F. Widdel, J. Peckmann, N. V. Pimenov, and M. B. Gulin. 2002. Microbial Reefs in the Black Sea Fueled by Anaerobic Oxidation of Methane. Science **297**: 1013–1015.

Naehr, T. H., D. Birgel, G. Bohrmann, I. R. MacDonald, and S. Kasten. 2009. Biogeochemical controls on authigenic carbonate formation at the Chapopote "asphalt volcano," Bay of Campeche. Chemical Geology **266**: 390–402.

Naehr, T. H., N. M. Rodriguez, G. Bohrmann, C. K. Paull, and R. Botz. 2000. Methane-derived authigenic carbonates associated with gas hydrate decomposition and fluid venting above the Blake Ridge Diapir. Proceedings of the Proceedings of the Ocean Drilling Program **164**: 285-300.

Naehr, T. H., P. Eichhubl, V. J. Orphan, M. Hovland, C. K. Paull, W. Ussler, T. D. Lorenson, and H. G. Greene. 2007. Authigenic carbonate formation at hydrocarbon seeps in continental margin sediments: a comparative study. Deep Sea Research Part II **54**: 1268–1291.

Niemann, H., P. Linke, K. Knittel, E. MacPherson, A. Boetius, W. Brückmann, G. Larvik, K. Wallmann, U. Schacht, E. Omoregie, D. Hilton, K. Brown, and G. Rehder. 2013. Methane-Carbon Flow into the Benthic Food Web at Cold Seeps – A Case Study from the Costa Rica Subduction Zone. PLoS ONE **8**: e74894.

Nunoura, T., Y. Takaki, H. Kazama, M. Hirai, J. Ashi, H. Imachi, and K. Takai. 2012. Microbial Diversity in Deep-sea Methane Seep Sediments Presented by SSU rRNA Gene Tag Sequencing. Microbes and Environments **27**: 382–390.

Orphan, V. J., Hinrichs, W. Ussler, C. K. Paull, L. T. Taylor, S. P. Sylva, J. M. Hayes, and E. F.

Delong. 2001a. Comparative Analysis of Methane-Oxidizing Archaea and Sulfate-Reducing Bacteria in Anoxic Marine Sediments. Applied and Environmental Microbiology **67**: 1922–1934.

Orphan, V., C. House, Hinrichs, K. McKeegan, and E. DeLong. 2001b. Methane-Consuming Archaea Revealed by Directly Coupled Isotopic and Phylogenetic Analysis. Science **293**: 484–487.

Orphan, V., W. Ussler, T. H. Naehr, C. H. House, Hinrichs, and C. K. Paull. 2004. Geological, geochemical, and microbiological heterogeneity of the seafloor around methane vents in the Eel River Basin, offshore California. Chemical Geology **205**: 265–289.

Paull, C. K., J. P. Chanton, A. C. Neumann, J. A. Coston, C. S. Martens, and W. Showers. 1992. Indicators of Methane-Derived Carbonates and Chemosynthetic Organic Carbon Deposits: Examples from the Florida Escarpment. Palaios **7**: 361.

Peckmann, J., A. Reimer, C. Luth, C. Luth, B. T. Hansen, C. Heinicke, J. Hoefs, and J. Reitner. 2001. Methane-derived carbonates and authigenic pyrite from the northwestern Black Sea. Marine Geology **177**: 129–150.

Peckmann, J., and V. Thiel. 2004. Carbon cycling at ancient methane-seeps. Chemical Geology **205**: 443–467.

Peckmann, J., V. Thiel, W. Michaelis, P. Clari, C. Gaillard, L. Martire, and J. Reitner. 1999. Cold seep deposits of Beauvoisin (Oxfordian; southeastern France) and Marmorito (Miocene; northern Italy): microbially induced authigenic carbonates. Int J Earth Sci (Geol Rundsch) **88**: 60–75.

Pernthaler, A., A. E. Dekas, C. T. Brown, S. K. Goffredi, T. Embaye, and V. J. Orphan. 2008. Diverse syntrophic partnerships from deep-sea methane vents revealed by direct cell capture and metagenomics. Proceedings of the National Academy of Sciences **105**: 7052–7057.

Quast, C., E. Pruesse, P. Yilmaz, J. Gerken, T. Schweer, P. Yarza, J. Peplies, and F. O. Glöckner. 2012. The SILVA ribosomal RNA gene database project: improved data processing and web-based tools. Nucl. Acids Res. 1-7.

Reeburgh, W. S. 2007. Oceanic Methane Biogeochemistry. Chemical Reviews **107**: 486–513.

Roalkvam, I., S. L. Jørgensen, Y. Chen, R. Stokke, H. Dahle, W. P. Hocking, A. Lanzén, H. Haflidason, and I. H. Steen. 2011. New insight into stratification of anaerobic methanotrophs in cold seep sediments. FEMS Microbiology Ecology **78**: 233–243.

Sahling, H., D. Rickert, R. W. Lee, P. Linke, and E. Suess. 2002. Macrofaunal community structure and sulfide flux at gas hydrate deposits from the Cascadia convergent margin, NE Pacific. Marine Ecology Progress Series **231**: 121–138.

Salter, S., M. Cox, E. Turek, S. Calus, W. Cookson, M. Moffatt, P. Turner, J. Parkhill, N. Loman, and A. Walker. 2014. Reagent and laboratory contamination can critically impact sequence-based microbiome analyses. BMC Biology **12**: 1–12.

Stadnitskaia, A., D. Nadezhkin, B. Abbas, V. Blinova, M. K. Ivanov, and J. S. Sinninghe Damsté. 2008. Carbonate formation by anaerobic oxidation of methane: Evidence from lipid biomarker and fossil 16S rDNA. Geochimica et Cosmochimica Acta **72**: 1824–1836.

Stadnitskaia, A., G. Muyzer, B. Abbas, M. J. L. Coolen, E. C. Hopmans, M. Baas, T. C. E. van Weering, M. K. Ivanov, E. Poludetkina, and J. S. Sinninghe Damsté. 2005. Biomarker and 16S rDNA evidence for anaerobic oxidation of methane and related carbonate precipitation in deep-sea mud volcanoes of the Sorokin Trough, Black Sea. Marine Geology **217**: 67–96.

Suess, E., M. E. Torres, G. Bohrmann, R. W. Collier, D. Rickert, C. Goldfinger, P. Linke, A. Heuser, H. Sahling, K. Heeschen, C. Jung, K. Nakamura, J. Greinert, O. Pfannkuche, A. Trehu, G. Klinkhammer, M. J. Whiticar, A. Eisenhauer, B. Teichert, and M. Elvert. 2001. Sea Floor Methane Hydrates at Hydrate Ridge, Cascadia Margin, p. 87–98. *In* C.K. Paull and W.P. Dillon [eds.], Natural Gas Hydrates. American Geophysical Union.

Suess, E., M. E. Torres, G. Bohrmann, R. W. Collier, J. Greinert, P. Linke, G. Rehder, A. Trehu, K. Wallmann, G. Winckler, and E. Zuleger. 1999. Gas hydrate destabilization: enhanced

dewatering, benthic material turnover and large methane plumes at the Cascadia convergent margin. Earth and Planetary Science Letters **170**: 1–15.

Takai, K., and K. Horikoshi. 1999. Genetic Diversity of Archaea in Deep-Sea Hydrothermal Vent Environments. Genetics **152**: 1285–1297.

Teichert, B., A. Eisenhauer, G. Bohrmann, A. Haase-Schramm, B. Bock, and P. Linke. 2003. U/Th systematics and ages of authigenic carbonates from Hydrate Ridge, Cascadia Margin: Recorders of fluid flow variations. Geochimica et Cosmochimica Acta **67**: 3845–3857.

Teichert, B., G. Bohrmann, and E. Suess. 2005. Chemoherms on Hydrate Ridge--Unique microbially-mediated carbonate build-ups growing into the water column. Palaeogeography, Palaeoclimatology, Palaeoecology **227**: 67–85.

Teske, A., and K. B. Sorensen. 2008. Uncultured archaea in deep marine subsurface sediments: have we caught them all? The ISME Journal **2**: 3–18.

Thiel, V., J. Peckmann, H. H. Richnow, U. Luth, J. Reitner, and W. Michaelis. 2001. Molecular signals for anaerobic methane oxidation in Black Sea seep carbonates and a microbial mat. Marine Chemistry **73**: 97–112.

Thurber, A. R., L. A. Levin, V. J. Orphan, and J. J. Marlow. 2012. Archaea in metazoan diets: implications for food webs and biogeochemical cycling. The ISME Journal **6**: 1602–1612.

Torres, M., J. McManus, D. Hammond, M. De Angelis, K. U. Heeschen, S. L. Colbert, M. D. Tryon, K. M. Brown, and E. Suess. 2002. Fluid and chemical fluxes in and out of sediments hosting methane hydrate deposits on Hydrate Ridge, OR, I: Hydrological provinces. **201**: 525–540.

Treude, T., A. Boetius, K. Knittel, K. Wallmann, and B. B. Jørgensen. 2003. Anaerobic oxidation of methane above gas hydrates at Hydrate Ridge, NE Pacific Ocean. Marine Ecology Progress Series **264**: 1–14.

Ussler, W., III, and C. K. Paull. 2008. Rates of anaerobic oxidation of methane and authigenic carbonate mineralization in methane-rich deep-sea sediments inferred from models and geochemical profiles. Earth and Planetary Science Letters **266**: 271–287.

Vasconcelos, C., J. A. Mckenzie, R. Warthmann, and S. M. Bernasconi. 2005. Calibration of the δ18O paleothermometer for dolomite precipitated in microbial cultures and natural environments. Geology **33**: 317–320.

Vasconcelos, C., J. A. Mckenzie, S. Bernasconi, D. Grujic, and A. J. Tiens. 1995. Microbial mediation as a possible mechanism for natural dolomite formation at low temperatures. Nature **377**: 220–222.

Wang, Q., G. M. Garrity, J. M. Tiedje, and J. R. Cole. 2007. Naïve Bayesian Classifier for Rapid Assignment of rRNA Sequences into the New Bacterial Taxonomy. Applied and Environmental Microbiology **73**: 5261–5267.

Watanabe, Y., S. Nakai, A. Hiruta, R. Matsumoto, and K. Yoshida. 2008. U–Th dating of carbonate nodules from methane seeps off Joetsu, Eastern Margin of Japan Sea. Earth and Planetary Science Letters **272**: 89–96.